

H3K4 Methylation Controls Vascular Smooth Muscle Cell Lineage Identity and Function

by

Mingjun Liu

Bachelor of Engineering, Chongqing University (China), 2015

Master of Science, Northwestern University, 2017

Submitted to the Graduate Faculty of the
School of Medicine in partial fulfillment
of the requirements for the degree of
Doctor of Philosophy

University of Pittsburgh

2022

UNIVERSITY OF PITTSBURGH
SCHOOL OF MEDICINE

This dissertation was presented

by

Mingjun Liu

It was defended on

June 15, 2022

and approved by

Dr. Wendy Mars, Associate Professor, Department of Pathology

Dr. Adam Straub, Associate Professor, Department of Pharmacology & Chemical Biology

Dr. Beth Roman, Associate Professor, Department of Human Genetics

Dr. Stephen Y. Chan, Professor of Medicine, Department of Medicine, Division of Cardiology

Dissertation Director: Dr. Delphine Gomez, Assistant Professor, Department of Medicine,
Division of Cardiology

Copyright © by Mingjun Liu

2022

H3K4 Methylation Controls Vascular Smooth Muscle Cell Lineage Identity and Function

Mingjun Liu, PhD

University of Pittsburgh, 2022

Vascular smooth muscle cells (SMC) are contractile cells regulating blood pressure and vascular homeostasis. Despite the highly specialized functions, SMC retain the plasticity for reversible phenotypic modulation between the contractile state and the “dedifferentiated” state, where SMC lose the expression of specialized contractile genes but acquire enhanced capabilities for proliferation, migration, and synthesis of extracellular matrix. The dynamic phenotypic modulation of SMC has been associated with both adaptive and maladaptive vascular remodeling, depending on whether SMC can efficiently reverse the phenotype back to the contractile state. However, the mechanisms required for SMC to retain its lineage identity during the phenotypic modulation remain unclear. We hypothesized the stable enrichment of H3K4 di-methylation (H3K4me2) on SMC-specific genes functions as an “epigenetic memory” mechanism in maintaining SMC lineage identity and restraining phenotypic plasticity. To study the roles of H3K4me2 enriched on SMC-specific genes, we developed a gene locus-specific H3K4me2 editing tool for selective demethylation of H3K4me2 located on SMC-specific genes without affecting the global H3K4me2 level. By performing selective H3K4me2 editing, we discovered that H3K4me2 is required for SMC contractility, retaining the lineage identity, and restraining plasticity. H3K4me2 is retained during the phenotypic modulation to function as the lineage-specific docking sites to recruit Tet Methylcytosine Dioxygenase 2 (TET2), a master regulator of SMC differentiation by oxidizing methylated DNA on SMC-specific genes. Surprisingly, H3K4me2 is also required for SMC participation in vascular remodeling upon the carotid artery injury through

the mechanism of maintaining a low level of miR145, an SMC-specific microRNA, to degrade migration inhibitory genes. Besides, H3K4me2 editing specifically in perivascular cells (SMC and pericytes, SMC-P) reduced SMC-P investment in neo-vessels and impaired microvascular remodeling in response to acute hindlimb ischemia. Loss of H3K4me2 disrupted the SMC-endothelial cell (EC) interaction and permitted SMC acquisition of EC-like morphology in a pro-angiogenesis environment, associated with loss of Notch receptors (Notch1 and Notch2) and downstream transcription factor Hey2. In conclusion, we discovered the stable H3K4me2 enrichment on SMC-specific genes functions as a central epigenetic memory mechanism to maintain the SMC lineage identity and function.

Table of Contents

Preface.....	xiv
Acknowledgements	xv
1.0 Introduction.....	1
1.1 Smooth muscle cell phenotypic diversity: at the crossroads of lineage tracing and single-cell transcriptomics	4
1.1.1 Summary	4
1.1.2 Introduction.....	5
1.1.3 Lessons learned from lineage tracing studies	6
1.1.4 SMC clonal expansion during cardiovascular disease.....	8
1.1.5 SMC phenotypic heterogeneity in the healthy media	16
1.1.6 SMC phenotypic characterization in the era of single-cell profiling: opportunities and challenges	17
1.1.7 Conclusion.....	20
1.1.8 Acknowledgements.....	20
1.2 Molecular regulators of vascular smooth muscle cell phenotypic modulation.....	21
1.2.1 Myocardin: a principal mediator of SMC differentiation	22
1.2.2 Transcription repressors of SMC differentiation	24
1.2.3 Epigenetic mechanisms of SMC phenotypic modulation	25
1.2.3.1 Histone Modifications.....	26
1.2.3.2 DNA Methylation.....	32
1.2.3.3 Non-coding RNA	35

1.3 Epigenetic memory – the encoding of lineage information	38
1.3.1 Lineage specification during embryonic development	38
1.3.2 Epigenetic memory mechanisms in mature cells – H3K4 di-methylation	41
1.4 Summary and Hypothesis.....	43
2.0 H3K4 di-methylation Governs Smooth Muscle Lineage Identity and Promotes	
Vascular Homeostasis by Restraining Plasticity.....	45
2.1 Summary	46
2.2 Introduction	47
2.3 Results.....	51
2.3.1 Selective demethylation of H3K4me2 on Myocardin-regulated genes.....	51
2.3.2 H3K4me2 editing impairs SMC contractile function	55
2.3.3 H3K4me2 mediates TET2 recruitment on myocardin-regulated contractile	
genes.....	60
2.3.4 H3K4me2 editing induces profound transcriptomic changes consistent with	
loss of SMC lineage identity.....	64
2.3.5 H3K4me2 editing exacerbates SMC phenotypic plasticity	67
2.3.6 H3K4me2 editing impairs SMC participation in adaptive vascular	
remodeling.....	70
2.3.7 H3K4me2/TET2 complex impairment leads to miR145 repression and loss of	
miR145-dependent cytoskeleton dynamics	72
2.4 Discussion	75
2.4.1 Limitations of the study	79
2.5 Acknowledgement.....	79

2.6 Source of funding.....	80
2.7 Methods	80
2.7.1 Myocd-LSD1 cloning and expression.....	80
2.7.2 Mice	81
2.7.3 Cell culture.....	82
2.7.4 Chromatin Immunoprecipitation	83
2.7.5 CUT & Tag sequencing and data analysis.....	84
2.7.6 Methylated/Hydroxymethylated DNA Immunoprecipitation (MeDIP/hMeDIP)	85
2.7.7 hMeDIP Sequencing and Data Processing.....	86
2.7.8 Real-time Quantitative PCR (RT-qPCR)	87
2.7.9 RNA extraction from FFPE sections.....	87
2.7.10 RNA-sequencing and Data Analysis.....	88
2.7.11 MicroRNA Isolation and Quantification	89
2.7.12 MicroRNA Transfection.....	89
2.7.13 Western Blot	89
2.7.14 Ex-vivo Myography.....	90
2.7.15 Immunofluorescent Staining.....	91
2.7.16 Collagen Contraction Assay.....	92
2.7.17 Proximity Ligation Assay	92
2.7.18 Peptide Binding Assay	93
2.7.19 Plasticity Assays	94
2.7.20 Cell Viability Assay.....	95

2.7.21 Transwell Assay.....	95
2.7.22 Luciferase Assay.....	96
2.7.23 Quantification and Statistical Analysis.....	96
3.0 H3K4me2 regulates perivascular cell participation in microvascular remodeling	
in mouse hindlimb ischemia model	98
3.1 Summary	99
3.2 Introduction	100
3.3 Results.....	103
3.3.1 H3K4me2 editing in SMC-P was associated with an impaired microvascular remodeling in the murine hindlimb ischemia model.....	103
3.3.2 Defective microvascular remodeling was associated with a lack of SMC-P perivascular coverage in Myocd-LSD1 mice.	104
3.3.3 H3K4me2 editing in SMC disrupted tube formation and SMC-EC interaction.	107
3.3.4 H3K4me2 editing altered Notch signaling pathways in Myocd-LSD1 SMC	109
3.3.5 Reduction of H3K4me2 in perivascular cells was associated with peripheral artery disease	110
3.4 Conclusion and Future Directions	113
3.5 Methods	116
3.5.1 Mice model.....	116
3.5.2 Hindlimb ischemia model and laser doppler measurement.....	116
3.5.3 Cell culture.....	117

3.5.4 In vitro tube formation assay	117
3.5.5 Competition assay	118
3.5.6 Immunofluorescent staining.....	118
3.5.7 Immobilized Jagged-1 Fc stimulation	119
3.5.8 RNA-seq and CUT&Tag seq analysis	119
4.0 General Conclusion and Discussion	120
4.1 Epigenetic heterogeneity across vascular beds	122
4.2 Mechanisms regulating H3K4me2 deposition in SMC	124
4.3 Lesson learned from H3K4me2 editing.....	125
Appendix A Key Resources Table	129
Appendix B Supplementary Figures	135
Bibliography	149

List of Tables

Table 1 Epigenetic modifications and functions	29
Appendix Table 1 Key Resources Table	129

List of Figures

Figure 1 Phenotypic modulation of SMC within atherosclerotic lesions.....	5
Figure 2 Smooth muscle cell (SMC) clonal expansion vs SMC proliferative capacities: a review of experimental design and possible outcomes.....	11
Figure 3 Molecular regulators of SMC phenotypic modulation	22
Figure 4 Myocd-LSD1 selectively performs H3K4me2 demethylation on myocardin-regulated SMC gene repertoire	54
Figure 5 H3K4me2 editing induces loss of SMC contractility <i>in vitro</i>	57
Figure 6 H3K4me2 editing impairs SMC contractile gene expression <i>in vivo</i>	59
Figure 7 H3K4me2 interacts with TET2 and is required for its recruitment on the SMC contractile genes	63
Figure 8 H3K4me2 editing is associated with a profound loss of SMC lineage identity.....	66
Figure 9 Loss of H3K4me2 on myocardin-regulated genes exacerbates SMC plasticity.....	69
Figure 10 H3K4me2 editing inhibits SMC investment in the neointima after vascular injury.	71
Figure 11 H3K4me2/TET2 complex impairment leads to miR145 repression and loss of miR145-dependent cytoskeleton dynamics.....	74
Figure 12 Myocd-LSD1 mice exhibited impaired blood reperfusion in murine hindlimb ischemia model	104
Figure 13 Defective microvascular remodeling was associated with a lack of SMC contribution in Myocd-LSD1 mice	106
Figure 14 H3K4me2 editing in SMC disrupted angiogenesis and SMC-EC interaction ...	108

Figure 15 H3K4me2 editing altered Notch signaling pathways in Myocd-LSD1 SMC 110

Figure 16 Reduction of H3K4me2 in perivascular cells was associated with human PAD 112

**Appendix Figure 1 Myocd-LSD1 mediates loss of H3K4me2 on myocardin-regulated genes.
..... 135**

**Appendix Figure 2 H3K4me2 editing induces a defect in contractility without a major change
in chromatin state or disruption of the SRF/Myocardin complex. 137**

**Appendix Figure 3 Myocd-LSD1 transduction in mouse carotid arteries inhibits SMC
differentiated phenotype without altering cell viability, proliferation, and apoptosis
..... 139**

Appendix Figure 4 TET2 interacts with H3K4me2 in SMC..... 141

**Appendix Figure 5 RNAseq reveals marked differences in transcription profiles in Myocd-
LSD1 expressing SMC 143**

Appendix Figure 6 H3K4me2 editing exacerbates SMC phenotypic plasticity 144

**Appendix Figure 7 Myocd-LSD1 expression in ligated carotid artery induces impaired
vascular remodeling due to PDGF-BB signaling-independent defective migration 146**

**Appendix Figure 8 H3K4me2 editing is associated with the upregulation of multiple miR 145
target genes related to cell migration and motility inhibition..... 148**

Preface

Dedication

I am dedicating this dissertation to my grandma, Yueying.

I know you would have been proud if you are still with us. Thank you for everything!

Lots of love,

Your grandson, Mingjun

Acknowledgements

It is finally this moment when I start to summarize my adventure over my last five years at University of Pittsburgh. I am incredibly grateful to be admitted into Interdisciplinary Biomedical Graduate Program (IBGP) and Cellular and Molecular Pathology (CMP) track. The program is designed to support and train the next generation of scientists, and I am proud to become an alumnus of IBGP and CMP soon.

During my last five years, I would not have made it this far without all the help and guidance I received. First, I would like to thank my dissertation committee members, Drs Wendy Mars, Adam Straub, Stephen Chan, and Beth Roman, for your constant support and encouragement. Next, I'd like to thank the Vascular Medicine Institute for providing an excellent training environment for graduate students and organizing research seminars where I got the chance to meet and interact with leaders in cardiovascular research. University of Pittsburgh has also provided institutional support for graduate students. I would like to thank all the technical support from Health Science Library System (HSLs), especially Dr. Ansuman Chattopadhyay and Sri Chaprala, who guided me in the bioinformatic analysis; and Centre of Biomedical Imaging (CBI) for the training on the confocal microscope; Genomic Sequencing Core at Children's Hospital for their help with all the NGS experiments, and Center for Research Computing (CRC) for providing the detailed tutorials in learning command-line tools.

Next, I would like to thank all the current and past members of Gomez Lab. Thank you, Dr. Delphine Gomez, for offering me the chance to study in your lab. You have always been inspiring and supportive the entire time. You have shown me how to be a successful scientist, a collaborator, and a caring mentor. I'd like to appreciate all our conversations about science, career

development, and cats. Second, I would like to thank my dear colleague, Dr. Cristina Espinosa-Diez! You have brought so much laughter and a brighter atmosphere into the lab. Thank you for being my second mentor in the lab, brainstorming on my projects, getting coffee together, and sharing your experience with career development. Lastly, I'd like to thank Sidney Mahan for sharing your skills in animal surgery and tissue sectioning; Jianxin Wei, for your help on experiments and for keeping all the lab resources in order; Dr. Mingyuan Du, for being a fantastic lab mate and sharing all the joys; and all the past trainees in Gomez Lab, it is my great honor to work with you all.

My adventure in the States would not be the same without all the friends I am fortunate to have after landing in this different country alone. I'd like to thank all the friends I made during my short stay in Chicago, especially Dr. Yaqi Zhang, Yu-Chen (Theodore) Lee, Xiang Zhou, and many others from my master's program; Thank you, Drs Kai Ding, Ashu Elangovan, Namrata Kumar, Kien Tran, Sam Herron, Rick van der Geest and all my peers here at Pittsburgh. You have shared all my up and downs and I hope to keep this friendship for a lifetime. I would also like to thank all the mentors I am lucky to have during my entire career, including Drs. Shourong Wu, Hua Cassan-Wang, Teresa Woodruff and Shuo Xiao. I have learned so much from every one of you.

Finally, I'd like to thank my family, especially my parents, who have fully supported all my decisions. It has been five years since I saw them in person due to the COVID pandemic, but they have always been there with love and support whenever I feel down. I would like to thank my little family here in Pittsburgh, Vincent Xia, and our cat Lola (Dudu). Thank you for your constant love and support. It indeed has been a difficult journey exploring the edge of knowledge, but I truly enjoyed every moment along the way, accompanied by every one of you!

1.0 Introduction

Vascular smooth muscle cells (SMC) are specialized cells arranged circumferentially into layer(s) embedded between the elastin lamellae of large arteries (elastic and muscular arteries) or wrapping around smaller arterioles. The major functions of mature SMC in healthy vasculatures include (1) regulation of blood pressure and vascular tone through specialized contraction and relaxation; (2) providing mechanical support in response to hemodynamic changes; (3) maintenance of vascular homeostasis by participating in adaptive vascular remodeling and production of extracellular matrix (ECM). (reviewed in^{1,2}).

In response to environmental cues (e.g., differential blood pressure induced by pulsatile hemodynamics), arteries react via active contraction or relaxation of SMC within the artery walls. SMC contractility is achieved by the expression of an SMC-specific contractile apparatus, including α -smooth muscle actin (α SMA or ACTA2)³⁻⁵, SM-specific isoform of myosin heavy chain dimers (MHC or MYH11)^{6,7}, SM22- α (TAGLN)⁸ and etc. Specifically, SMC contraction is performed by the interaction of two major filaments, a thin filament composed of α SMA oligomerization and a thick filament composed of MHC and myosin light chain elements⁹. Contraction is triggered by an increase of intracellular calcium (Ca^{2+}) concentration induced by vasoconstriction agonists, such as norepinephrine, angiotensin II and endothelin, which binds to calmodulin that activates myosin light chain kinase (MLCK)^{10,11}. Activated MLCK phosphorylates the myosin regulatory light chains (RLCs), leading to activation of the MHC motor domain that drives movements between the filaments and develops contraction force.¹⁰ When

intracellular Ca^{2+} level drops in response to muscle relaxation signals, such as Nitric Oxide¹², Myosin light chain phosphatase (MLCP) dephosphorylates RLC and induces muscle relaxation¹⁰.

For decades, SMC-specific contractile proteins have been used as markers for the identification of SMC. However, unlike other muscle lineages (skeletal muscle cell or cardiomyocyte), mature SMC is not terminally differentiated and retains the ability to undergo extensive and reversible phenotypic modulations in response to external stimuli. Such phenotypic reprogramming was first reported in the 1970s by pioneers in the field of SMC biology. They observed SMCs changed their typical morphology and behaviors and gained “synthetic” features, such as the appearance of synthetic organelles and enhanced capacity of proliferation, in response to injury *in vivo* or under the *in vitro* culture condition¹³⁻¹⁵. Importantly, the reversibility of such phenotypic changes was reported in SMC using an *in vitro* culture model, where SMC could reversed their synthetic phenotypes back to contractile phenotype with the appearance of myofilaments¹⁶. Since then, a classic model, known as “phenotypic switching”, was established that differentiated SMC can temporarily turn off the expression of contractile gene repertoire and regain the ability of proliferation, migration, and synthesis of ECM².

It is widely accepted that the phenotypic plasticity of SMC is required for the proper vascular formation and maturation during embryonic development and vascular remodeling.^{17,18} Meanwhile, phenotypic switching of SMC was also believed to be involved in major cardiovascular diseases (CVDs), such as atherosclerosis, where SMC infiltrates through internal elastic lamina into the intima, proliferates, produces extracellular matrix, and contributes to fibrous cap formation.¹⁹ This central dogma was only supported by indirect evidence relying on immunostaining of SMC contractile markers (ATAC2, MYH11, TAGLN), which is not reliable in identifying SMC undergoing phenotyping modulation and losing expression of these contractile

markers. Besides, other cell types could acquire the expression of SMC contractile genes in the disease state. For example, studies using the bone-marrow transplantation model illustrated a proportion of ACTA2⁺ cells were derived from bone-marrow-derived myeloid cells in coronary atherosclerotic plaque.²⁰ To unambiguously characterize SMC behavior and contribution during disease progression, there is a need for a conditional and inducible cell fate mapping system to permanently label mature SMC and their progenies irrespective of their gene expression status. The development of a reliable SMC fate tracing model is a breakthrough in the field of SMC biology. Studies in the 2010s using the reliable SMC fate tracing animal model revealed that SMC contribution in CVDs has been largely underestimated and identified a broader spectrum of phenotypes SMC could acquire in CVDs.²¹⁻²⁸ However, the characterization of SMC-acquired phenotypes still heavily relies on immunostaining of markers of other lineages, such as SCA-1 for mesenchymal stem cells and LGALS3 for macrophages. Yet whether these gene markers truly represent the cell types or cell functions requires further investigation. Therefore, a more recent combination of SMC fate tracing and single-cell transcriptomics provided further evidence of the extensive phenotypic plasticity of SMC under pathological conditions, especially within the atherosclerotic lesion²⁹, moving the field to the next level with a high-resolution characterization of SMC-derived cells in CVDs.³⁰⁻³³ (reviewed in^{29,34})

1.1 Smooth muscle cell phenotypic diversity: at the crossroads of lineage tracing and single-cell transcriptomics

Mingjun Liu, MS^{1,2}; Delphine Gomez, PhD^{1,2}

¹Pittsburgh Heart, Lung, Blood, and Vascular Medicine Institute, University of Pittsburgh

²Division of Cardiology, University of Pittsburgh School of Medicine; Pittsburgh

Copyright, Arteriosclerosis, Thrombosis, and Vascular Biology, 2019

1.1.1 Summary

Vascular smooth muscle cells (SMC) play a critical role in controlling blood pressure and blood distribution, as well as maintaining the structural integrity of the blood vessel. SMC also participate in physiological and pathological vascular remodeling due to their remarkable ability to dynamically modulate their phenotype. During the past decade, the development of *in vivo* fate mapping systems for unbiased identification and tracking of SMC and their progeny has led to major discoveries as well as the reevaluation of well-established concepts regarding the contribution of vascular SMC in major vascular diseases including atherosclerosis. Lineage-tracing studies revealed that SMC undergo multiple phenotypic transitions characterized by the expression of markers of alternative cell types (e.g., macrophage-like, mesenchymal stem cell-like) and populate injured or diseased vessels by oligoclonal expansion of a limited number of medial SMC. With the development of high-throughput transcriptomics and single-cell RNA sequencing (scRNAseq), the field is moving forward towards in-depth SMC phenotypic characterization.

Herein, we review the major observations put forth by lineage and clonality tracing studies and as well as the evidence in support for SMC phenotypic diversity in healthy and diseased vascular tissue. We will also discuss the opportunities and remaining challenges of combining lineage tracing and single-cell transcriptomics technologies, as well as studying the functional relevance of SMC phenotypic transitions and identifying the mechanisms controlling them.

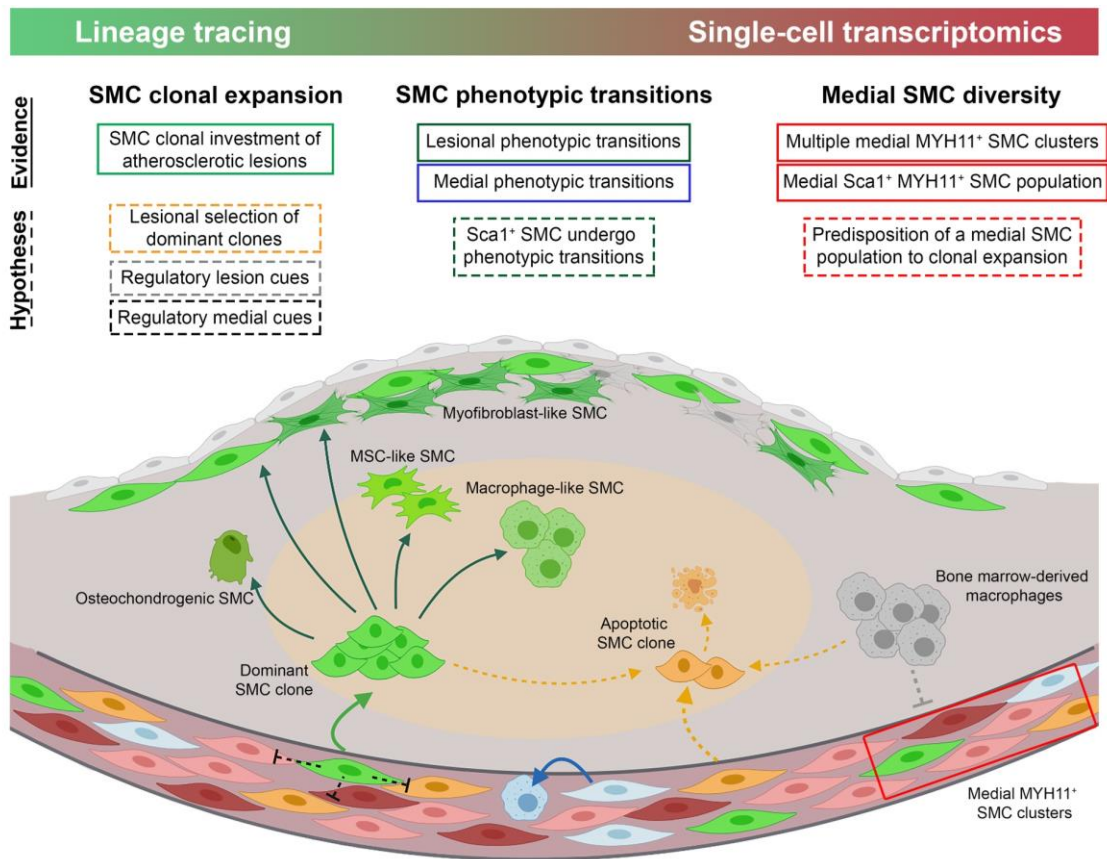


Figure 1 Phenotypic modulation of SMC within atherosclerotic lesions.

1.1.2 Introduction

The vascular smooth muscle cell (SMC) is a differentiated cell type located within the medial layer of arteries and veins and expressing a unique repertoire of proteins (e.g., MYH11,

ACTA2, TAGLN, MYOCD) required for their contractile function³⁵. Despite being highly specialized, SMC retains remarkable plasticity. The plastic nature of SMC has been extensively studied *in vitro* for the past 30 years^{36,37}. From these studies emerged the concept of SMC phenotypic switching, a model in which SMC shift between a differentiated, contractile phenotype and a dedifferentiated, “synthetic” phenotype, the latter characterized by the loss of SMC marker gene expression, the increase in extracellular matrix (ECM) component synthesis, and the increase in SMC proliferation and migration upon exposure to various stimuli and environmental cues. Yet, the rigorous assessment of the SMC contribution to vascular remodeling *in vivo* was virtually impossible due to the major limitation in their identification using traditional SMC marker genes, motivating the development of *in vivo* lineage-tracing and fate mapping systems³⁸.

1.1.3 Lessons learned from lineage tracing studies

The need for unambiguous and definitive tracking of SMC fate arose from the following observations³⁸: *First*, studies have demonstrated the loss of expression of SMC contractile genes and the repression of their promoters during atherosclerosis or vascular injury, challenging their identification^{39,40}. *Second*, the expression of some of the marker genes classically used for SMC identification is not restricted to the SMC lineage and can be expressed by other cell types. For example, ACTA2 is expressed by both SMC and myofibroblasts. TAGLN is transiently expressed by cardiomyocytes and skeletal muscle cells during embryonic development⁴¹. *Third*, cell types, which do not express SMC marker genes under physiological conditions, can transition to a SMC-like state in diseased or injured blood vessels (e.g., endothelial cells express SMC markers like ACTA2 during endothelial-to-mesenchymal transition)⁴². Consequently, fate mapping systems allowing reliable SMC tracking in healthy and disease tissue have been developed by

combining^{43,44}: (i) efficient and definitive labeling of SMC and their progeny with reporter systems (e.g., fluorescent proteins, LacZ); (ii) conditional expression of these reporters by Cre recombinases specifically expressed in the SMC lineage; and (iii) an inducible system permitting activation of the tracking system of mature SMC at a given time upon treatment with tamoxifen⁴⁵. These conditional and inducible Cre recombinase systems allow for the labeling of mature SMC prior to injury or the development of vascular disease and the ability to follow their fate independently of marker gene expression while critically avoiding the labeling of cells acquiring the expression of these marker genes during disease or injury. The first SMC-specific inducible lineage tracing mouse model was developed by the Robert Feil's group in the early 2000's⁴⁶⁻⁴⁸. They generated a tamoxifen-inducible *Tagln*-CreER^{T2} x *loxP*-STOP-*loxP*-reporter system⁴⁶ in which a series of tamoxifen injections induces the translocation of Cre recombinase from the cytoplasm to the nucleus and the excision of a floxed STOP codon localized upstream of a reporter gene in exclusively TAGLN⁺ cells. These studies were the first to provide rigorous evidence of the participation of SMC to atherosclerotic lesion formation^{23,47,48}. Thereafter, SMC-lineage tracing studies have employed tamoxifen-inducible *Myh11*-CreER^{T2} x *loxP*-STOP-*loxP*-reporter mouse models⁴⁹ to track the fate and phenotype of SMC expressing MYH11 at the time of tamoxifen treatment^{24,25,50-55}.

These studies have clearly demonstrated that a large fraction of cells present in the neointima or the atherosclerotic lesion originate from medial differentiated SMC. For example, Herring et al.⁵² found that 80% of the neointimal cells are of SMC origin after carotid ligation. In advanced atherosclerosis, SMC represent between 40 and 70% of plaque cells^{24,25}, yet, up to 80% of SMC-derived cells within atherosclerotic plaque do not express detectable levels of SMC markers including MYH11 and ACTA2^{24,51}. There is compelling evidence that SMC not only lose

the expression of their marker gene repertoire in injured or diseased vessels, but can undergo phenotypic transitions into other types of cells, including chondrocyte-like cells (SOX9⁺, Runx2/Cbfa1⁺), foam cells and macrophage-like cells (Oil Red O⁺, LGALS3⁺, Mac3⁺), mesenchymal stem cell (MSC)-like cells (Sca1⁺), myofibroblasts (PDGFβR⁺), or beige adipocyte-like cells (UCP1⁺)²¹⁻²⁸. Overall, development of conditional and inducible cell-lineage tracing systems has enabled the unbiased fate mapping of SMCs during the progression of cardiovascular diseases, and unveiled the contribution of SMC to vascular disease pathogenesis.

SMC lineage tracing models have also been used in conjunction with SMC-specific knockout of genes of interest and SMC fate mapping to identify key molecules and pathways regulating SMC participation in vascular disease. To name a few, studies have identified factors playing critical roles in regulating SMC phenotypes (e.g., KLF4^{24,27}), as well as their proliferative or migrative capacities during vascular remodeling (e.g., cGKI⁴⁷, TAGLN⁴⁸, PTEN⁵⁰, PDGFbR⁵⁶, OCT4⁵³, IL1R1⁵⁴).

1.1.4 SMC clonal expansion during cardiovascular disease

Since the 1970's, the mechanisms underlying SMC participation in intimal proliferation during atherosclerotic or after vascular injury have been a major focus of research. In 1973, Earl and John Benditt reported the first evidence of SMC clonality within atherosclerotic plaques by performing X-linked inactivation assays [**Figure 2A**]⁵⁷. Benditt^{57,58} and others⁵⁹⁻⁶¹ described that portions of atherosclerotic plaques were composed of cells with the same X-inactivation profile and concluded that atherosclerotic plaques form by clonal expansion of a few cells. However, this technique presents inherent limitations and a poor resolution that preclude a rigorous identification of single clones⁶². As X-chromosome inactivation occurs early during development (stage 8-cell

embryo in human)⁶³, the cells from a given lineage can originate from distinct precursors with high homogeneity in their X-chromosome inactivation profile. Illustrating this caveat, large patches of cells bearing the same X-chromosome inactivation profile have been found in the normal vessel. This makes impossible to ascertain whether SMC investment of atherosclerotic lesions occurs by the expansion of a limited number of clones or the involvement of multiple SMC with the same X-chromosome inactivation profile originating from a medial patch. Finally, the X-linked inactivation assay does not permit the clear identification of cell types responsible for the clonal expansion (SMC *vs* non-SMC).

The development of SMC lineage tracing systems has permitted to reevaluate these studies and determine more accurately the clonal profile of SMC within atherosclerotic lesions in mice. These studies leveraged the combinatorial use of multi-color reporter alleles (i.e., R26R-Confetti, R26R-Rainbow) and SMC-specific inducible Cre systems (i.e. *Tagln*-CreER^{T2}, *Myh11*-CreER^{T2}) systems described above to track the clonality of SMC-derived lesion cells by random labeling of SMC with one of the colors included in the reporter allele [**Figure 2B**]^{21,23,25,55}. These clonality tracking systems can be used at high and low recombination rates by varying the tamoxifen treatment dose and duration. A high recombination rate induces the labelling of all SMC and the robust quantification of SMC lesion investment and phenotypic transitions, whereas a low recombination rate allows the precise identification of single individual clones. Of note, the reliability of the cell-specific conditional and inducible tracking systems is particularly critical for clonality studies since the expansion of a very small number of cells makes qualitative and quantitative analysis vulnerable to inefficient or leaky Cre systems. Low recombination rate experiments provided new evidence of the clonal origin of SMC-derived lesion cells²³. Subsequently, Chappell et al.²⁵ reported that over 90% of the atherosclerotic plaques only

contained 1 or 2 colors. This key observation, confirmed by two other studies^{21,55}, strongly supports that a few mature medial MYH11⁺ SMC contribute to SMC investment and population of atherosclerotic lesions. However, consensus has not been achieved on how only a few out of all underlying medial SMCs contribute to atherogenesis and key questions have not been yet resolved [recently discussed in ⁶⁴⁻⁶⁶].

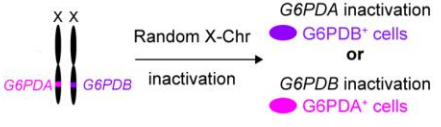
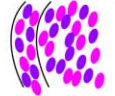
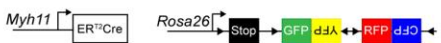
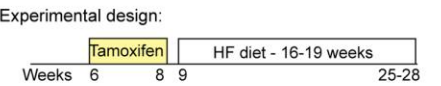
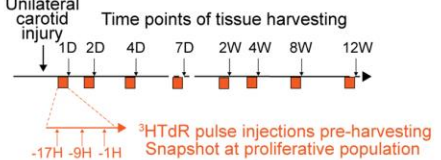
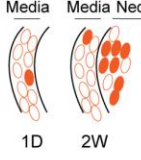
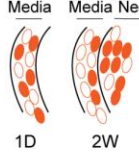
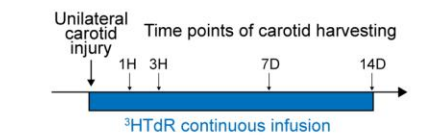
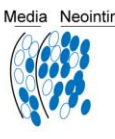
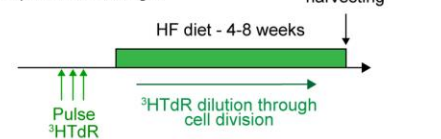
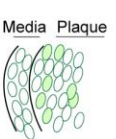
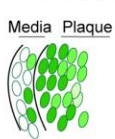
Methodology/experimental design	Hypothesis tested/Possible outcomes	Observations/Limitations
A - Benditt & Benditt, 1973: Atherosclerosis clonality by X-chromosome inactivation analysis		
<p>Species: Human - Heterozygous <i>G6DP</i> females</p>  <p>Random X-Chr inactivation → <i>G6PDA</i> inactivation → G6PDB⁺ cells or <i>G6PDB</i> inactivation → G6PDA⁺ cells</p>	<p>Monoclonal investment</p> <p>Media Plaque</p>  <p>Polyclonal investment</p> <p>Media Plaque</p>  <p>● G6PDA⁺ cells ● G6PDB⁺ cells</p>	<ul style="list-style-type: none"> - Plaques with dominant expression of one <i>G6PD</i> allele suggesting monoclonal investment. - Limited resolution and inability to ascertain intimal cell lineages.
B - Feil et al. 2014; Chappell et al., 2016: SMC clonality in atherosclerotic plaque using lineage and clonality tracing mouse		
<p>Species: Mouse - <i>Myh11-ER²Cre Rosa26-Confetti ApoE^{-/-}</i></p>  <p>Experimental design:</p>  <p>Weeks 6 8 9 16 19 25-28</p>	<p>Monoclonal investment</p> <p>Media Plaque</p>  <p>Polyclonal investment</p> <p>Media Plaque</p>  <p>● CFP⁺ SMC ● RFP⁺ SMC ● YFP⁺ SMC ● GFP⁺ SMC</p>	<ul style="list-style-type: none"> - Plaques composed of 1 or 2 SMC clones. - Limited understanding of mechanisms driving the monoclonal investment: clonal expansion vs clonal selection.
C - Clowes et al., 1983: Medial SMC proliferation after vascular injury		
<p>Species: Rat</p> <p>Experimental design:</p>  <p>Unilateral carotid injury</p> <p>Time points of tissue harvesting</p> <p>1D 2D 4D 7D 2W 4W 8W 12W</p> <p>-17H -9H -1H</p> <p>³HTdR pulse injections pre-harvesting Snapshot at proliferative population</p>	<p>Clonal expansion</p> <p>Media Neoint.</p>  <p>Proliferation of a large number of medial SMC</p> <p>Media Neoint.</p>  <p>● ³HTdR⁺ cells ○ ³HTdR⁻ cells</p> <p>1D 2W 1D 2W Time point post-injury</p>	<ul style="list-style-type: none"> - Large proportion (46%) of medial SMC proliferate after vascular injury. - Inability to ascertain intimal cell lineages. No tracking of proliferative cells over time.
D - Clowes et al., 1985: SMC growth fraction after vascular injury		
<p>Species: Rat</p> <p>Experimental design:</p>  <p>Unilateral carotid injury</p> <p>Time points of carotid harvesting</p> <p>1H 3H 7D 14D</p> <p>³HTdR continuous infusion</p>	<p>Investment of proliferative cells</p> <p>Media Neointima</p>  <p>Investment of proliferative & non-proliferative cells</p> <p>Media Neointima</p>  <p>● ³HTdR⁺ cells ○ ³HTdR⁻ cells</p>	<ul style="list-style-type: none"> - Small fraction of unlabelled cells within the neointima suggesting that medial SMC can invest the neointima irrespectively of their proliferative status. - Inability to ascertain intimal cell lineages and the origin of the non-proliferative cells.
E - Thomas et al., 1975: Clonality tracking by tritiated Thymidine labeling in atherosclerosis		
<p>Species: Swine</p> <p>Experimental design:</p>  <p>Atherosclerotic lesion harvesting</p> <p>HF diet - 4-8 weeks</p> <p>Pulse ³HTdR</p> <p>³HTdR dilution through cell division</p>	<p>Monoclonal investment</p> <p>Media Plaque</p>  <p>Polyclonal investment</p> <p>Media Plaque</p>  <p>³HTdR dilution</p> <p>● ³HTdR⁺ cells ○ ³HTdR⁻ cells</p>	<ul style="list-style-type: none"> - Large number of plaque cells labeled with ³HTdR suggesting polyclonal investment. - Inability to ascertain intimal cell lineages.

Figure 2 Smooth muscle cell (SMC) clonal expansion vs SMC proliferative capacities: a review of experimental design and possible outcomes.

This table summarizes the methodology and experimental design of seminal studies investigating: A, SMC clonality in human atherosclerotic lesions by X-chromosome (Chr) inactivation. B, SMC clonality in experimental

atherosclerosis in SMC lineage tracing mice by random labeling with GFP, YFP, RFP, or CFP (green, yellow, red, or cyan fluorescent protein, respectively). C, Medial SMC proliferative capacity after vascular injury by tritiated thymidine incorporation ($^3\text{HTdR}$). D, Medial and intimal SMC growth fraction after vascular injury. E, SMC proliferative profile within atherosclerotic lesion after tritiated thymidine pulse delivery. The table includes representations of the experimental designs and possible outcomes, as well as a summary of the main observations and limitations of these studies.

Is clonal expansion a common process during development, physiological and pathological remodeling? In addition to atherosclerosis, clonal expansion of SMC has been observed in carotid artery following vascular injury²⁵, distal pulmonary arterioles in a model of pulmonary arterial hypertension⁵⁶, and in dissecting aortic aneurysm⁶⁷. This suggests that SMC clonality is a conserved mechanism that might have evolved for retention of blood vessel structure and contractility during vascular remodeling. In contrast, SMC investment of forming arteries during embryonic development does not involve clonal expansion as demonstrated by the following observations: 1) medial SMC originate from multiple precursors; and 2) the progeny of a SMC precursor undergoes extensive migration and intermixing within developing arteries and does not form large patches of cells^{21,55,68}.

Are SMC clonally expanding the only medial SMC capable of proliferation? Studies by Clowes^{69,70} and Thomas⁷¹ based on tritiated thymidine ($^3\text{HTdR}$) incorporation and SMC growth fraction assessment provided evidence challenging the idea that proliferative capacity would be restricted to SMC undergoing clonal expansion. Analysis of the frequency and the intensity in $^3\text{HTdR}$ labeling, and its dilution through cell division showed that [**Figure 1C-E**]: 1) a large fraction (46%) of medial cells were labeled with $^3\text{HTdR}$ 48 hours post vascular injury⁶⁹; 2) both labeled (proliferative) and unlabeled (non-proliferative) cells contribute to the neointima formation, indicating that non-proliferative medial SMC could migrate and invest the neointima⁷⁰; and 3)

after pulse injection of $^3\text{HTdR}$ preceding high-fat diet in swine, tracking of tritiated thymidine dilution suggested that multiple SMC proliferate and undergo a limited number of cell cycles rather than the extensive proliferation of a single cell. Indeed, the clonal proliferation of a single cell would imply a large number of cell divisions and a greater dilution of tritiated thymidine than observed⁷¹. Although these studies faced similar limitations than Benditt's studies (i.e., inability to ascertain lesion cell lineages of proliferating and non-proliferating cells), these results imply that a large number of medial SMC have proliferative capacities. In accordance with this conclusion, SMC-clonality tracing studies demonstrated that alteration of the Integrin- β 3 pathway led to atherosclerotic lesion polyclonality suggesting that a large number of medial SMC retain proliferative capacity and that environmental cues might play a critical role in regulating SMC proliferation and clonal expansion⁵⁵.

Is there a subpopulation of SMC primed to undergo clonal expansion? Is there an environmental pressure selecting for the expansion of a limited number of SMC clones? The fact that a few SMC undergo clonal expansion despite having a large number of medial SMC exposed to similar environmental perturbations suggests that an upstream priming process might be required for these cells to become a dominant clone. Benditt postulated that, similar to neoplastic growth, atherosclerosis monoclonality may be caused by mutational events in SMC⁵⁷. Although the occurrence and clinical significance of somatic mutations in myeloid cells have been recently demonstrated^{72,73}, there is, yet, no evidence supporting or refuting the involvement of a similar process in medial SMC and whether it influences SMC proliferative and clonal capacities. The predisposition of a few SMC to clonally expand could also be due to the presence within the media of phenotypically distinct SMC subpopulations that display higher proliferation, migration and/or survival capacities, thus outcompeting other SMC populations.

Environmental cues, including cell-cell interaction, cell-extracellular matrix interaction, and juxtacrine and paracrine signaling, may also regulate positively or negatively the capacity of SMC to invest the atherosclerotic lesion and/or survive during lesion development. Here are a few examples of possible mechanisms. *First*, a medial SMC clone could inhibit the proliferation and/or the migration of surrounding cells. *Second*, lesion cells of other lineages (e.g. macrophages, endothelial cells) could influence the ability of medial SMC to undergo clonal expansion. A recent study provided supporting evidence that bone marrow-derived macrophages play an essential role in restricting multiple SMCs from migrating into atherosclerotic plaques through an integrin- β 3-dependent mechanism⁵⁵. Finally, another hypothesis postulates that the propensity of a SMC to invest the plaque may be dependent on its location within the forming atherosclerotic lesion. For example, it has been postulated that the proximity of the SMC to the endothelium at the shoulders of fatty streak-like lesions could influence their ability for clonal expansion^{21,55}. Similarly, it has been proposed that SMC in the vicinity of internal elastic lamina fenestration could preferentially migrate within the lesion^{21,74}. Since these processes are not mutually exclusive, it is likely that SMC clonal expansion and investment of atherosclerotic plaque are initiated and regulated by a combination of phenotypic priming and environmental selection.

Clonal expansion vs phenotypic modulation. Another key observation of the SMC clonality studies is that SMC within a lesion derived from a single clone can undergo multiple phenotypic transitions thus, a clone is not predisposed to any particular phenotypic transition^{21,25} (**Figure 2**). The progeny of a SMC clone displays an atheroprotective ACTA2⁺ phenotype within the fibrous cap as well as an atheropromoting phenotype of lipid-loaded foam cells and macrophage-like cells within the necrotic core^{21,25}. Importantly, there is clear evidence that SMC phenotypic modulation occurs within the inner layer of the media^{24,25,53}. The inner layer of the

media underlying the lesion is composed of a significant proportion of ACTA2⁻ SMC as well as LGALS3⁺ SMC. Importantly, these medial phenotypically modulated SMCs do not originate from a single SMC clone nor undergo clonal expansion within the intimal space, demonstrating that clonal expansion and phenotypic modulation are distinct and independent processes²⁵. In other words, SMC phenotypic modulation, proliferative and migratory processes are not necessarily interdependent and concomitant, and therefore might be regulated by different mechanisms^{24,53,54}. These findings are very important when considering and evaluating therapeutic strategies for treatment of atherosclerosis. Relevant strategies should likely consist of polarizing the phenotypic transitions of lesion SMC to atheroprotective phenotypes (e.g., ACTA2⁺) rather than inhibiting clonal expansion and SMC plaque investment. Indeed, there is clear evidence that inhibition of SMC investment within atherosclerotic lesions does not necessarily results in a reduction of the plaque size but rather lead to the formation of advanced and unstable plaques due to compensation of SMC absence by other cell types^{53,75}.

Interspecies differences in SMC investment mechanisms? The discrepancies in the observations and conclusions summarized above could be explained, at least partially, by differences in experimental designs and methodologies, but might also arise from fundamental interspecies differences. For example, unlike rodents, human and swine can develop “normal intimal proliferation” in large arteries^{66,71,76}. The “normal intima” is supposedly composed of medial SMC migrating in the intimal space in absence of lipid accumulation⁶⁶. However, the mechanisms of formation of the “normal intima”, including the clonal profile of intimal SMC, remain largely unknown. Moreover, although the PDAY study showed that vascular territories with “normal intima” are preferential sites for atherosclerosis, the impact of the “normal intima”

on lesion formation, cellular composition and SMC participation and clonality has not been yet determined^{66,77}.

1.1.5 SMC phenotypic heterogeneity in the healthy media

A potential explanation for SMC oligoclonal investment of atherosclerotic plaques is the predisposition of a distinct medial SMC subpopulation. Implicit in this postulate is the existence of SMC heterogeneity within the medial layer. While the regional- and developmental-associated phenotypic diversity has been extensively studied [see reviews by Majesky^{78,79}], there has been a limited investigation and characterization of the inherent SMC heterogeneity within the healthy media of a given vascular territory. *In vitro* studies have identified two phenotypically distinct populations of SMC within large arteries, classically characterized as “spindle-shaped contractile” and “rhomboid synthetic” SMC^{80,81}. These subpopulations, while expressing at least some SMC marker genes, had different morphological, proliferative, and migratory capacities when grown in culture or exposed to mitogens like PDGF-BB. *In vivo*, the variation in expression of the SMC marker genes in normal bovine pulmonary artery suggested the presence of SMC subpopulations in the healthy media⁸². However, this study did not consider the possibility of the presence of non-SMC cells which would not express the SMC gene repertoire. Moreover, the proliferative and migratory characteristics observed *in vitro* might not reflect of a diversity of SMC phenotypes and functions *in vivo* due to the major alterations occurring after tissue dissociation and during SMC culture and expansion³⁷. Nevertheless, these observations support two plausible hypothesis for medial SMC diversity^{83,84}: 1) the media is composed of two or more distinct and stable SMC phenotypes including a less differentiated and multifunctional population⁸⁵; or 2) one medial SMC population changes its phenotype transiently and reversibly within the healthy media between a

differentiated and a less differentiated state. A reasonable explanation for this hypothesis is that the dynamic transition of medial SMC phenotype would be driven by the need for continuous production of ECM components required for ECM turnover and maintenance^{86,87}.

A recent study by the Jorgensen group provided new insights into medial SMC diversity by combining SMC lineage tracing and scRNAseq⁸⁸ (**Figure 2**). Remarkably, it provided compelling evidence of SMC heterogeneity within the healthy media of a given vascular region. By performing scRNAseq on the whole aorta of *Myh11*-CreER^{T2} Confetti mice, seven distinct SMC clusters were identified and were distinct from endothelial and adventitial cells. Importantly, SMC in these seven clusters expressed SMC contractile genes including MYH11. Moreover, a small subset of medial MYH11⁺ SMC expressed the MSC marker *Sca1*. Interestingly, *Sca1* expression was not restricted to one of the seven SMC clusters but rather present in a very limited number of SMC in each cluster. These results are significant in that they demonstrate that differentiated MYH11⁺ SMC can express detectable, maybe transient, levels of the MSC marker *Sca1*. ScRNAseq performed on atherosclerotic lesion of SMC lineage tracing mice showed an expected phenotypic diversity of SMC-derived lesion cells, including macrophage-like and osteogenic phenotypes, as well as a cluster of SMC expressing *Sca1*, confirming previous studies^{22,24}. These studies gave an unprecedented depth to the characterization of the SMC phenotypic diversity in healthy and diseased blood vessels.

1.1.6 SMC phenotypic characterization in the era of single-cell profiling: opportunities and challenges

The use of scRNAseq provides a comprehensive and unbiased characterization of cell population phenotype and relative abundance within complex healthy or diseased tissues including

atherosclerosis⁸⁸⁻⁹¹. The combination of scRNAseq and lineage tracing gives the tremendous advantage to follow the phenotypic transitions of cell types during disease development and progression without relying on established lineage-specific markers or modeled transcriptomic profiles. The identification of lineage-traced cells for scRNAseq studies can be based on different approaches: the pre-sorting of reporter⁺ cells⁸⁸⁻⁹¹ or the detection of reporter transcripts post-sequencing^{92,93}. Yet, limitations and potential biases should be acknowledged and carefully considered when analyzing and interpreting scRNAseq datasets. *Firstly*, unlike bulk RNAseq, scRNAseq relies on obtaining single-cell suspension representative of all cell populations present within tissue samples which involves enzymatic and mechanical tissue disruption. This critical step can induce significant bias with respect to cell population abundance and transcript expression because it can differently impact the viability and the gene expression of various cell types and subpopulations^{94,95}. This potential bias can be partially controlled by comparing transcript expression profiles generated by scRNAseq and bulk RNA-seq, the latter utilizing undissociated frozen tissue. *Secondly*, scRNAseq lacks spatial information regarding the distribution of the different subpopulations within tissues. *Thirdly*, an ensemble of processes (i.e., gene activation burst, stochastic gene expression, RNA stability) can generate variations in transcript levels that might not reflect differences in protein levels or cellular functions and can artificially increase single-cell heterogeneity⁹⁶⁻⁹⁸. *Finally*, the lack of depth of scRNAseq (stochastic dropout) presents major limitations for investigation of low-expression genes. Although this might not be an issue in defining cell subpopulations and their relative abundance, it might limit the identification of key regulators of cell polarizations and phenotypic transitions.

With respect to SMC heterogeneity, the next challenge will be to determine the functional relevance of the SMC subpopulations identified by scRNAseq. Indeed, although very informative,

scRNAseq studies are descriptive by nature. For example, Dobnikar et al.⁸⁸ suggest that the medial Sca1⁺ SMC subpopulation might be predisposed for undergoing clonal expansion based on the fact that a subset of SMC-derived lesion cells express Sca1. However, the scRNAseq provides only correlative evidence supporting this conclusion and cannot preclude that medial Sca1⁻ SMC would start expressing Sca1 during lesion investment and phenotypic transition. Studying the fate and function of the different medial SMC subpopulations would require the development of dual inducible genetic tracing systems permitting the lineage tracing of the SMC lineage and the tracking of a defined subpopulation. While a first lineage tracing system would be used to track the SMC lineage in its globality (MYH11⁺ SMC), a second tracing system could be implemented to track a particular SMC medial subpopulation to assess precisely its fate in atherosclerosis and its contribution to the disease pathogenesis. For example, tracking the medial Sca1⁺ SMC subpopulation for rigorous assessment of the functional relevance of these cells would require such a dual lineage tracing/fate mapping system. Remarkably, alternatives to Cre-mediated recombination have been recently developed including *Dre-rox*⁹⁹ and *Nigri-nox* systems¹⁰⁰. The use of these new technologies in combination with traditional Cre systems allow for independent tracking of two populations or lineage¹⁰¹⁻¹⁰³ and give a glimpse of possible SMC subpopulations *in vivo*. However, to date, no study has employed a combination of two independent conditional and inducible models. Thus, two challenges remain: the development of multiple inducible systems for concomitant tracking of the SMC lineage and given medial SMC subpopulations and the selection of markers for precise and unambiguous identification of SMC subpopulations by promoter driven Cre systems.

1.1.7 Conclusion

The field has positioned itself at the crossroads of lineage tracing and single-cell transcriptomics to study phenotypic diversity and phenotypic evolution of SMC during vascular disease and remodeling. We are in an exciting era with advanced tools to perform robust and precise analysis at the single-cell resolution on systems allowing unbiased tracking of cell lineage and fate. Whereas we are gaining depth in the phenotypic characterization of the SMC lineage, future studies must focus on key remaining considerations including the full characterization of SMC heterogeneity at the epigenetic and genetic levels, the origin and environmental control of medial SMC heterogeneity, the functional relevance of SMC medial subpopulations during disease formation, the identification of mechanisms controlling SMC clonal expansion/SMC investment and phenotypic transitions, and the identification of therapeutic axes to bias SMC phenotypic transitions.

1.1.8 Acknowledgements

We would like to thank Sidney Mahan and Drs Cynthia St. Hilaire and Brittany Durgin for their help in editing the article. The graphic abstract was created with Biorender. This work is supported by the National Institute of Health R01HL146465 and the American Heart Association 15SDG25860021 grants (to D.G.). The authors have nothing to disclose.

1.2 Molecular regulators of vascular smooth muscle cell phenotypic modulation

Decades of efforts generate the current picture of the regulatory network that controls SMC phenotypes at multiple levels. When SMC is in the contractile state, the central regulator Myocardin/Serum Response Factor (SRF)/CArG box complex drives the expression of SMC-specific contractile genes. To facilitate this transcription activity, activating epigenetic programs (H3K4me3, H3K79me2, H3Ac, H4Ac, 5hmC, *etc.*) are presented on these gene loci. When SMC undergoes phenotypic modulation, diverse transcription repressors, such as KLF4, ELK-1, TCF21, *etc.*, block Myocardin activity and repress SMC contractile gene expression, with a simultaneous shifting of epigenetic landscape to a repressive state (H3K9me3, H3K27me3, 5mC, *etc.*).

Meanwhile, regulator RNAs (miRNAs and lncRNAs) add another network level by regulating transcription factors or epigenetic modifications. Of particular interest, a stable H3K4me2 is stably retained on SMC contractile genes regardless of transcription activities, suggesting a potential role as an intrinsic epigenetic memory mechanism to maintain the SMC lineage during the dynamic phenotypic modulation. This chapter will introduce several layers of important molecular regulators of SMC phenotypic modulation, including transcription factors, histone modifications, DNA methylation, and non-coding RNAs.

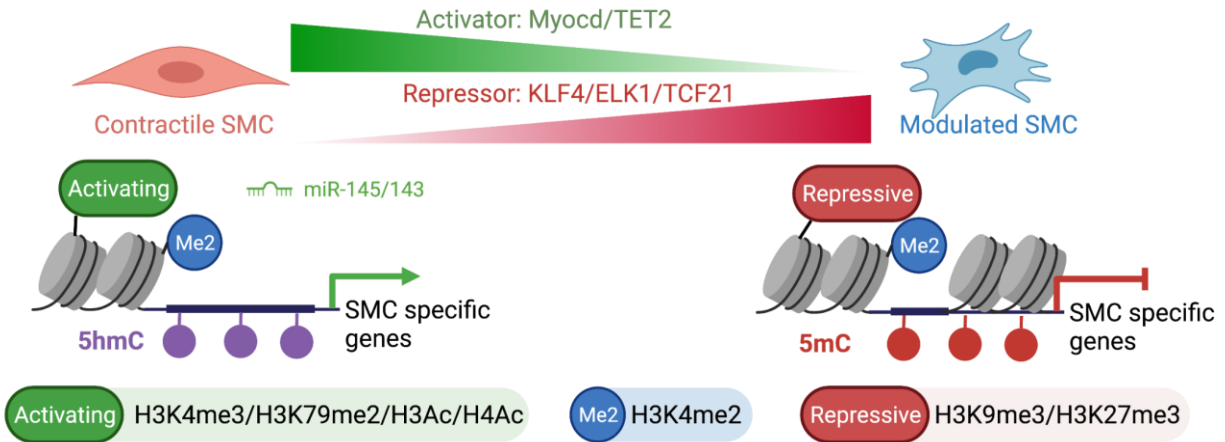


Figure 3 Molecular regulators of SMC phenotypic modulation

1.2.1 Myocardin: a principal mediator of SMC differentiation

One of the most pivotal transcription master regulators in mediating SMC differentiation is Myocardin (Myocd). Myocd is a highly conserved transcriptional activator exclusively expressed in cardiac muscle¹⁰⁴, mature gut, vascular SMC^{105,106} and early-stage SMC-lineage in embryonic aorta¹⁰⁷. Structure-function studies characterized the Myocd functional domains, including a non-consensus RPEL domain, which does not form a stable interaction with G-actin, allowing for the preferential nuclear translocation of Myocd without cytoplasmic sequestration¹⁰⁸; a conserved basic and glutamine-rich domain responsible for binding to serum response factor (SRF) and nuclear localization^{104,109}; an SAP (SAF-A/B, Acinus, PIAS) domain with unknown function, yet the deletion of SAP domain led to a variable transactivation activity on different genes, suggesting a potential role in mediating interaction with specific transcription factors¹⁰⁴; and a C-terminal transcriptional activation domain (TAD) responsible for the transactivation functions¹⁰⁴. Mechanistically, Myocd does not directly interact with DNA, but forms a ternary complex with SRF, which binds to CArG box [CC(A/T)₆GG], a DNA motif predominantly

enriched on the promoters of SMC-specific genes (e.g., *Acta2*, *Myh11*, *Tagln*)¹¹⁰, and activates SMC gene expression repertoire^{105,111,112}. *Myocd* mRNA level is reduced in phenotypically modulated SMC, suggesting its role in mediating SMC transient dedifferentiation.¹¹³ Ectopic expression of *Myocd* in non-SMC lines, such as myoblast or hepatocyte, could drive the expression of several SMC-specific contractile genes.^{113,114} Collectively, these elegant *in vitro* studies established that *Myocd* functions as a principal mediator of SMC contractile phenotype. Further animal studies using genetically modified mouse models confirmed the key roles of *Myocd* in mediating SMC differentiation program. Pan knockout of *Myocd* (*Myocardin*^{-/-}) in mouse embryo induced embryonic lethality associated with defects in SMC differentiation while endothelial cell patterning and cardiac morphology remained unperturbed.¹¹⁵ Conditional knockout of *Myocd* in SMC precursors (*Wnt1*-Cre, *Myocd*^{f/f}; *Pax3*-Cre, *Myocd*^{f/f}) resulted in postnatal death from arterial malformation (patent ductus arteriosus) and defects in SMC differentiation. SMC derived from these *Myocd*-deficient mice exhibited a dramatic reduction of contractile genes with “synthetic” ultrastructural features.¹¹⁶ More recently, the inducible SMC-specific deletion of *Myocd* (*Myh11*-Cre^{ERT2}, *Myocd*^{f/f}) demonstrated the postnatal loss of *Myocd* in SMC led to profound derangements in arteries and SMC-rich organs, including gastrointestinal and genitourinary tracts.¹¹⁷ Beside losing contractility in SMC, *Myocd* knockout SMC exhibited elevated endoplasmic reticulum (ER) stress, autophagy and activation of programmed cell death over time, suggesting an important role of *Myocd* in maintaining vascular and visceral homeostasis.¹¹⁷ *Myocd* also restrains SMC plasticity and represses developmental programs of other lineages by counteracting key transcriptional factors, such as Sox9-mediated chondrocyte differentiation¹¹⁸, and MEF2-MyoD-mediated skeletal muscle cell differentiation¹⁰⁷. In conclusion, *Myocd* is one of the most important discoveries unveiling the mechanisms governing SMC differentiation and contractile function.

1.2.2 Transcription repressors of SMC differentiation

Several repressive transcription factors are involved in the process of contractile gene repression, including Krüppel-Like Factor-4 (KLF4), ETS Like-1 protein (ELK1)^{106,119,120}, Transcription Factor 21 (TCF21)¹²¹. One common mechanism shared by these repressors is to disrupt the formation of Myocd/SRF/CArG box complex that is critical for contractile gene expression. Among these transcription repressors, KLF4 is the most studied factor in SMC.

KLF4 is a critical gene highly expressed in embryonic stem cells to maintain stem cell pluripotency.¹²² It is also known as one of the Yamanaka factors that drive somatic cell reprogramming to induced pluripotent stem cells (iPSCs).^{123,124} Of note, KLF4 is lowly expressed in contractile SMC to maintain the proper perivascular coverage on the microvasculature.¹²⁵ KLF4 expression can be activated in phenotypically modulated SMC in response to various dedifferentiation stimulations, such as platelet-derived growth factor-BB (PDGF-BB) treatment, high-fat diet-induced atherosclerosis, and vascular injury.¹²⁶⁻¹²⁹ Importantly, knockdown of KLF4 in SMC blocked PDGF-BB-induced repression of contractile genes, suggesting the major role of KLF4 in controlling SMC phenotypes.^{126,129} Upon activation, KLF4 mediates SMC phenotypic dedifferentiation through multiple mechanisms: *First*, KLF4 was shown to repress transcription of Myocd by directly binding to an Upstream Repressor Region (URR) within the Myocd promoter.¹²⁹ *Second*, KLF4 represses SMC-specific contractile genes by binding to the adjacent DNA motif (G/C-rich repressor elements) and disrupting Myocd/SRF/CArG-box complex formation.¹²⁶ *Third*, KLF4 mediates epigenetic silencing on SMC contractile genes via cooperation with histone deacetylases (HDAC2 and HDAC5).^{130,131}

A pioneering study using *ApoE* null SMC-specific knockout of KLF4 in the SMC fate tracing mouse model (*Myh11-Cre*^{ERT2}, *ROSA26-flox-STOP-YFP*, *Klf4*^{F/F}) demonstrated a

protective effect on atherosclerosis lesion by promoting SMC contractile phenotype for the formation of protective fibrous caps, and restraining SMC “trans-differentiation” into mesenchymal stem cell (MSC)-like or macrophage-like cells to reduce lesion inflammation burden and lesion size.¹³² In combination with SMC fate tracing mouse model and the recent blooming single-cell RNA sequencing (scRNA-seq) tool, the complex roles of KLF4 in modulating SMC phenotype are being further investigated at single-cell resolution. Indeed, SMC-specific knockout of KLF4 prevented SMC transition into an LGALS3+ transient pioneer state within atherosclerosis lesion induced by the high-fat diet.³¹ Although expressing a classic macrophage marker, LGALS3+ pioneer cells exhibited pro-inflammation, production of ECM and osteogenesis differentiation transcriptome profile.³¹ To summarize, KLF4 plays a pivotal role in regulating SMC phenotypic modulation, mediating dedifferentiation and determining the transition to a transient multipotent stage in the context of cardiovascular diseases.

1.2.3 Epigenetic mechanisms of SMC phenotypic modulation

Epigenetics, literally meaning “outside conventional genetics”, is defined as heritable alterations in gene expression and phenotypes without changing the DNA sequence.¹³³ Epigenetics controls genes through multiple mechanisms: post-translational modifications of histone tails^{134,135}; chemical modification of DNA cytosine bases¹³⁶⁻¹³⁸; non-coding RNAs, including microRNAs (miRNAs), long non-coding RNAs (lncRNAs) and recently identified circular RNAs (circRNAs)^{139,140}; and histone subunit variants¹⁴¹, e.g., H2A.Z¹⁴². All these diverse epigenetic programs have been identified in SMC that play key roles in regulating SMC differentiation, phenotypic modulation, and SMC behaviors under various physiological or pathological conditions. In this

section, I will discuss some of the major epigenetic programs that are pivotal in controlling SMC phenotypic modulations.

1.2.3.1 Histone Modifications

Genomic DNA is packaged into a condensed structure known as chromatin inside the nucleus.¹⁴³ Chromatin is not just a stable condensed structure storing DNA information but a dynamic scaffold that is continuously morphing and converting between diverse states in response to specific cues to regulate DNA accessibility to the cellular machinery. The fundamental unit of chromatin is the nucleosome, which is composed of 146 bp of DNA wrapping around a central histone octamer formed by two copies of H2A, H2B, H3 and H4. Each histone subunit contains an N-terminal tail that is freely exposed to the nuclear environment and can be decorated by a plethora of chemical modifications, including acetylation, methylation, phosphorylation, ubiquitination, and SUMOylation.¹⁴⁴ These modifications regulate chromatin structure and DNA accessibility for various cellular processes. Indeed, the combination of these post-translational modifications at different modification sites is referred to as the histone code, which conveys diverse messages regarding gene expression profiles.¹³⁴ The histone modification landscape is dynamically modulated by numerous signaling pathways, involving enzymes known as epigenetic modifiers, including writers (enzymes catalyze the formation of a specific modification), readers (proteins recognize and interact with a specific modification) and erasers (enzymes remove a modification).¹⁴⁵ Thus, by controlling the level and accessibility of these modifiers, cells could reshape their epigenetic program in adaptation to different environment.¹⁴⁴

Among all the forms of histone modifications, histone methylation and acetylation are the most studied forms with variable functions. Histone acetylation is regulated by two families of enzymes: histone acetyltransferases (HATs, e.g., CBP/p300) and histone deacetylase (HDACs).¹⁴⁶

Histone acetylation and deacetylation function as an “on-off” system controlling gene expression. Briefly, histone acetylation is associated with transcription activation. HATs utilize acetyl-CoA as a cofactor to transfer the acetyl group to histone lysine side chains, which weakens DNA-histone interaction by neutralizing the positive charge of lysine residues. DNA is released from the compact chromatin structure for the access of transcription machinery. Meanwhile, HDACs function oppositely by removing the acetyl group and restoring the positive charge of lysine residues to stabilize DNA-histone interactions and restrict DNA accessibility. (reviewed in¹⁴⁶)

Histone methylation, on the other hand, is a more complicated and context-dependent system, where its regulatory function is determined by both (1) the location of amino acid residue on histone tails and (2) the degree of methylation (me1, me2, or me3). For example, H3K4me3 is commonly associated with active promoters¹⁴⁷, while H3K4me1 is usually enriched on the enhancer regions and associated with enhancer functions¹⁴⁸. H3K27me3 is associated with a repressed chromatin structure.¹⁴⁸ Besides, histone methylation is not mutually exclusive on a specific gene locus, and the combination of variable histone modifications is related to complex gene regulatory networks. For example, a histone modification pattern, termed as a bivalent domain, with both activating H3K4me2/3 and repressive H3K27me3 decorated around the same region has been identified on key developmental genes in embryonic stem cells. The bivalent domains are associated with poised genes, but are required for efficient activation as a priming mechanism.¹⁴⁹

Histone methylations are dynamically regulated by several families of histone methyltransferases and demethylases. Histone methyltransferases include three families: the SET-domain-containing proteins¹⁵⁰, DOT1-like proteins¹⁵¹ and protein arginine N-methyltransferase (PRMT) family¹⁴⁶. Two families of histone demethylases have been identified: amine oxidases¹⁵²

and jumonji C (JmjC)-domain-containing iron-dependent dioxygenases¹⁵³⁻¹⁵⁵. These enzyme families cooperate to construct the histone methylation code, yet each enzyme preferentially catalyzes a subset of methylations. For example, Lysine-specific demethylase 1 (LSD1, also known as KDM1A, belonging to the amine oxidase family), was the first identified histone demethylase in mammalian cells, which specifically catalyzes demethylation of H3K4/K9 mono-/di-methyl (me1/2).¹⁵²

Table 1 Epigenetic modifications and functions

Modification Type	Role in transcription	Modification site	Writer	Eraser
Methylation	Activation	H3K4me1/2/3	SET1A; SET1B; MLL1; MLL2; MLL3; MLL4; SMYD1; SMYD2; SET7/9; PRDM9	LSD1; LSD2; NO66; JARID1A; JARID1B; JARID1C; JARID1D
		H3K79me2	DOT1L	
	Repression	H3K9me3	SUV39H; G9a; GLP; SETDB1; PRDMs	HP1 α/β ;
		H3K27me3	EZH1; EZH2	CBX7; EED; BAHD1; NSD2
Acetylation	Activation	H3K9Ac	HATs	HDACs
		H4Ac		
DNA methylation	Repression	5mC	DNMT1;	TET1;
	Activation	5hmC	DNMT3A; DNMT3B	TET2; TET3

Together, a cell develops an efficient system to precisely control its gene expression profile by coordinating histone modifications as a layer of the epigenetic regulatory network. Undoubtedly, histone modifications have been extensively studied in SMC. The first report describing the

epigenetic regulation of SMC differentiation was published by the Owens group in the early 2000s.¹⁵⁶ By using a retinoic acid (RA)-inducible SMC differentiation model using precursor cells (P19-derived A404 cells), they discovered that SRF, although highly expressed in undifferentiated A404 cells, was unable to bind to the CArG boxes of SMC-specific contractile genes within the intact chromatin. However, RA treatment induced recruitment of SRF to the CArG boxes of SMC gene repertoire, in association with hyperacetylation of histones H3 and H4.¹⁵⁶ This pioneer study suggested that SMC differentiation is controlled by not only the expression of key transcription factors, but also epigenetic-mediated modifications of chromatin structure and DNA accessibility.

Consistent with this discovery, the following studies further characterized the roles of histone acetylation in regulating SMC differentiation. *Pitx2*, a homeodomain transcription factor, was induced at an early stage during SMC differentiation from A404 and was required for SMC contractile gene expression by regulating histone acetylation balance by enhancing HAT (p300) recruitment over HDACs.¹⁵⁷ Induction of SMC contractile genes (e.g., *Tagln*) by transforming growth factor β (TGF- β) depends on histone acetylation around *Tagln* promoter region. Specifically, inhibition of HDACs with trichostatin A, TSA, or overexpression of HAT (CBP/p300), increased *Tagln* promoter activity and gene expression.^{158,159} On the contrary, inhibition of HATs activity or overexpression of HDACs suppressed *Tagln* expression and abolished TGF- β -induced pro-differentiation effect.^{158,159} Mechanistically, Cao *et al.* discovered that the central regulator *Myocd* directly interacted with p300 via the transcription activation domain, thus inducing SMC contractile gene expression partly through histone acetylation.¹⁶⁰

Histone deacetylation is also associated with SMC phenotypic modulation. Yoshida *et al.* reported the repression of SMC contractile genes induced by PDGF-BB or oxidized phospholipids was associated with H4 deacetylation, which depends on specific recruitment of HDAC2, HDAC4,

and HDAC5.^{119,120} Of particular interest, KLF4, the key repressor of SMC contractile genes, interacted with HDAC5 for its recruitment to SMC gene repertoire.¹²⁰ Interestingly, HDACs do not only interact with transcription repressors in SMC. Cao *et al.* discovered that Myocd could interact with both P300 and class II HDACs, suggesting Myocd functions as a central nexus for both positive and negative regulation of SMC gene repertoire via dynamic histone acetylation balance.¹⁶⁰

When SMC is in a contractile state, a unique combination of histone modifications has been observed to be enriched around SMC-specific gene promoters, which is associated with relaxed chromatin structure and gene activation, including H3K4me2, H3K4me3, H3K79me2, H3K9Ac, and H4Ac.^{114,161} During the phenotypic modulation, histone modifications on these genes transition from the activating, relaxed state to a repressive state marked by H3K9me3 and H3K27me3 that are associated with condensed chromatin structure and DNA inaccessibility.^{114,161} Unlike activating (H3K4me3, H3K79me2, H3K9Ac, and H4Ac) or repressive (H3K9me3 and H3K27me3) histone marks that are only present on SMC specific genes in one state, H3K4me2 is constantly retained on these gene loci disregard of transcription activities during the SMC phenotypic modulation.¹¹⁴ A novel molecular imaging method in a combination of In-Situ Hybridization and Proximity Ligation Assay (ISH-PLA) was designed to visualize the enrichment of a specific epigenetic modification on a specific genome locus.¹⁶² Using ISH-PLA, concrete evidence has been provided that the presence of H3K4me2 on *Myh11* promoter was restricted to SMC-lineage and persistently retained in phenotypically modulated SMC within the atherosclerotic lesion in both human and mouse tissues.¹⁶²⁻¹⁶⁴ Persistence of H3K4me2 on *Myh11* promoter has been used as the second SMC fate tracing method.^{27,165} However, it remains unclear if this stable H3K4me2 plays a functional role in modulating SMC behaviors and phenotypes.

In addition to SMC-specific genes, histone methylations have also been identified in regulating SMC inflammatory phenotype, which contributes to the development of major cardiovascular diseases, such as atherosclerosis. For example, the repressive histone mark H3K9me3 was significantly decreased on key inflammatory genes in SMC from obese *db/db* mice, associated with the pro-inflammatory phenotype of diabetic mice.¹⁶⁶ Similarly, Harman *et al.* recently reported a global reduction of the repressive mark H3K9me3 in SMC after vascular injury or induction of atherosclerosis, which was enriched on several pro-inflammatory genes, such as matrix metalloproteinases (MMPs) and interleukin-6 (IL-6).¹⁶⁷ Reduction of H3K9me3 by inhibiting H3K9 methyltransferase G9A/GLP significantly enhanced pro-inflammatory transcription factors binding and potentiated pro-inflammatory effects under pathological conditions.¹⁶⁷

1.2.3.2 DNA Methylation

DNA methylation is another aspect of epigenetic control of the transcription activity in mammalian cells. DNA methylation is commonly associated with gene repression and actively occurs on the fifth carbon of a cytosine through DNA methyltransferases DNMT1, DNMT3A, and DNMT3B.¹⁶⁸ DNMT3A and DNMT3B perform *de novo* methylation on unmodified DNA¹⁶⁹, while DNMT1 maintains methylation pattern from parental DNA strands to daughter strands during DNA replication.¹⁷⁰ DNA methylation has been widely implicated in lineage specification during embryonic development and is related to lineage-specific functions.¹⁷¹

DNA methylation used to be characterized as an irreversible process, except being alleviated during DNA replication, until the significant discovery of Ten-Eleven-Translocation 1 (TET1).¹⁷² TET1 has been shown to erase DNA methylation through an oxidation reaction.¹⁷² TET1, along with the other two identified members, TET2 and TET3, belongs to the TET family.

Each TET protein shares a similar protein structure, including a conserved double-stranded b-helix (DSBH) domain, a cysteine-rich domain, and binding sites for cofactors Fe (II) and 2-oxoglutarate (2-OG).¹⁷³ These domains form the core catalytic domain that is required for TETs performing DNA demethylation.¹⁷³ Intriguingly, only TET1 and TET3 contain an N-terminal zinc finger cysteine-X-X-cysteine (CXXC) domain which is known to recognize and bind to methylated CpGs, granting TET1 and TET3 the capability for direct DNA binding.¹⁷⁴⁻¹⁷⁷ On the other hand, TET2 does not contain the CXXC DNA binding domain, suggesting TET2 is recruited to the genome through a CXXC domain-independent mechanism, likely through interaction with protein or RNA partners.¹⁷⁸⁻¹⁸¹ Upon binding to methylated DNA, TETs oxidize methylated cytosine (5mC) into stepwise formats, including 5-hydroxymethylcytosine (5hmC), 5-formylcytosine (5fC), and 5-carboxylcytosine (5caC), which is further converted to unmodified cytosine via DNA repair pathways and thymine-DNA glycosylase (TDG).^{137,182-185} Both DNA methylation and demethylation have been implicated in regulating SMC phenotypes.

Alteration of DNA methylation patterns has also been investigated in SMC in the context of vascular diseases or vascular injury, yet whether DNA methylation plays a protective or detrimental role during disease development is context-dependent and remains to be further examined. Hiltunen *et al.* reported for the first time that global DNA hypomethylation was observed within atherosclerotic lesions (human and mouse) and proliferating neointimal SMC arteries undergoing balloon denudation, concomitant with a decreased DNA methyltransferases activity.¹⁸⁶ This study suggests a correlation between DNA hypomethylation and harmful phenotypic switching that contributes to vascular diseases. Consistent with this study, another early study identified DNA hypomethylation on extracellular superoxide dismutase (*ec-sod*) gene associated with the development of atherosclerosis.¹⁸⁷ On the other hand, DNA hypermethylation

has also been found in disease protective genes in SMC, such as atheroprotective genes, cell-cycle inhibitory genes, and pro-differentiation genes, in the context of atherosclerosis or vascular injury.¹⁸⁸⁻¹⁹⁰ Therefore, strategies targeting DNA methyltransferases to interfere with genome-wide DNA methylation patterns are controversial given the complex nature of DNA methylation system. For example, DNMT1 inhibitor 5-aza-2'-deoxycytidine (5-Aza) treatment in SMC induced hypomethylation on alkaline phosphatase promoter and facilitated mineralization *in vitro*, associated with detrimental vascular calcification.¹⁹¹ Meanwhile, 5-Aza treatment has also been shown to attenuate SMC dedifferentiation, proliferation, and migration regarding atherosclerosis progression and neointima formation by prohibiting hypermethylation on a master regulator of SMC differentiation.^{192,193} A limitation of global epigenetic intervention is the complexity and heterogeneity between cell types and between cell states of the same cell type.

TETs have been extensively studied in embryonic development and stem cell biology, yet their roles in regulating SMC phenotypes remain primordial. Liu *et al.* first reported the roles of TET2 in promoting SMC differentiation.¹⁶¹ Compared with other members of TET family, TET2 is highly expressed in differentiated SMC. At the same time, its expression can be reduced during SMC phenotypic modulation, suggesting a potential regulatory role of TET2 in controlling SMC phenotypes. Indeed, loss of TET2 inhibited expression of SMC contractile genes and pro-differentiation transcription factors, including *Myocd*, while increased expression of repressors, such as *KLF4*.¹⁶¹ Overexpression of TET2 strongly promoted SMC differentiation by performing DNA hydroxymethylation on the promoters of SMC master regulator *Myocd* and contractile gene repertoire, which was associated with enhanced active histone modification patterns (increased H3K4me3 and decreased H3K27me3).¹⁶¹ Interestingly, instead of being an intermediate product during DNA demethylation, TET2-mediated 5hmC persists in mature SMC within the medial

layers of aortas, implying 5hmC is actively maintained in SMC, and itself could serve a distinct function.¹⁶¹ Similarly, loss of 5hmC pattern in cells has been linked with oncogenesis associated with losing specific lineage identity.¹⁹⁴ Remarkably, overexpression or activation of TET2 by vitamin C prevented SMC apoptosis and synthetic phenotypes responsible for intimal thickening in vascular injury and coronary allograft vasculopathy^{161,195}, suggesting enhancing TET2 activity could be used as a potential therapeutic strategy in treating cardiovascular diseases contributed by SMC phenotypic modulation.

1.2.3.3 Non-coding RNA

With the advancement of sequencing techniques, research focusing on non-coding RNA is blooming in the field of vascular biology. Excitingly, previously uncharacterized RNAs, such as long non-coding RNAs (lncRNAs), and circular RNAs (circRNAs), join the realm of numerous microRNAs (miRNAs) as molecular regulators of SMC behavior and functions.

miRNAs are well-characterized non-coding RNAs in SMC, functioning as a major post-translational gene silencing mechanism. miRNAs are a class of small non-coding RNAs with a length of 21-25 nucleotides (nt). There are several steps in generating miRNAs in mammalian cells: miRNAs are first transcribed by RNA polymerase II as primary (pri)-miRNAs, long transcripts containing single or multiple miRNAs. Pri-miRNAs are further processed by an RNase III enzyme Droscha into 60-100 nt transcripts known as precursor miRNAs (pre-miRNAs) in the nucleus, which are followed by exporting into the cytoplasm and being processed by the RNase III enzyme Dicer into mature miRNAs. The mature miRNA is then incorporated into the RNA-induced silencing complex (RISC) that recognizes complementary mRNA sequences and induces mRNA targets degradation and gene silencing.¹⁹⁶

miRNA is a class of non-coding RNAs critical for vascular development, SMC differentiation, and phenotypic modulation. Of note, SMC-specific knockout of miRNA processor Dicer (*Tagln-Cre, Dicer^{fllox}*) induced severe embryonic lethality with abnormality in vessel formation and lack of SMC differentiation and contractility^{197,198} despite the fact that *Tagln* expression is not limited to SMC during development. This study highlights the essential roles of miRNA in controlling SMC differentiation. Until now, dozens of miRNAs have been identified in regulating diverse functions of SMC, among which the miR-143/145 miRNA cluster is one of the most characterized miRNAs specifically expressed in SMC.¹⁹⁹⁻²⁰² Like other SMC-specific genes, miR-143/145 is regulated by Myocd/SRF/CArG complex^{199,203}, as well as TET2 recruitment²⁰⁴. miR-143/145 overexpression strongly increased SMC contractile gene markers, such as ACTA2 and MYH11, which were decreased upon treatment with miR-145 inhibitor.^{199,202} Interestingly, ectopic overexpression of miR-145 was sufficient to induce neural crest cells, one of the embryonic origins of aortic SMC, to differentiate into SMC, or transdifferentiate fibroblasts into SMC.^{199,202} These pilot studies indicate that miR-143/145, specifically expressed in SMC and regulated by SMC-specific master regulators, indeed plays a pivotal role in promoting SMC differentiation and expression of SMC contractile genes. These observations were further validated by *in vivo* animal studies where miR-143/145 were knockout in a murine model.^{200,201,203} Showing no difference in viability and fertility, miR-143/145 is dispensable during development. However, miR-143/145 KO severely reduced the contractile SMC number while the increased percentage of SMC underwent phenotypic modulation in the aorta and femoral artery.²⁰¹ Likely due to lack of contractile SMC, miR-143/145 KO mice showed systemic arterial hypotension with reduced systolic and diastolic blood pressures under steady-state or anesthesia.^{201,203} Interestingly, miR-143/145 not only promotes SMC contractile phenotype, but is also required for cytoskeletal

arrangement required for SMC migration and participation in vascular remodeling in response to vascular injury.²⁰³ Overall, these *in vivo* functional studies further validated the essential roles of miR-143/145 in maintaining vascular structure, integrity and homeostasis.

Mechanistically, miRNAs control cellular functions by targeting a cohort of genes. For example, miR-143/145 enhances SMC contractile genes expression by targeting major transcription repressors, KLF4 and Ets Like Gene 1 (ELK1).¹⁹⁹ Meanwhile, miR-145 regulates SMC migration by repressing genes associated with actin dynamics and cytoskeleton rearrangement, such as Sling-shot 2 (Ssh2), Slit-Robo GTPase-activating protein 1 (Srgap1), Srgap2, etc.²⁰³ Intriguingly, miR-143/145 can regulate opposite cell behaviors, such as SMC differentiation and contractility versus migration, by targeting a different cohort of transcripts depending on the transcriptome profile in a context-dependent manner. Therefore, co-profiling both mRNA transcriptome and miRNA transcriptome can serve as a useful tool in interpreting miRNA functions upon various stimulations.²⁰⁵

Besides miRNAs that have been studied for decades, recently emerged lncRNAs and circRNAs have drawn large attention in the field of SMC biology, adding another layer to the complex epigenetic regulatory network. circRNAs are a newly discovered class of RNA forming a covalently closed loop through transcript back-splicing. Several circRNAs influence SMC phenotypes by sponging miRNAs or proteins, meaning sequestration of miRNAs or proteins from interacting with linear mRNAs (reviewed in²⁰⁶). For instance, circACTA2 has been identified by back splicing of the Acta2 transcript in SMC.²⁰⁷ CircACTA2 promotes ACTA2 expression by sponging miR-548f-5p, a miRNA targeting ACTA2 transcript.²⁰⁷ Meanwhile, circACTA2 has also been discovered to be upregulated in SMC from Angiotensin II-induced hypertensive SMC.²⁰⁸ Angiotensin II-induced circACTA2 prevented SMC senescence by competing with CDK4 for the

interaction with ILF4, which contributes to the degradation of CDK4, a factor promoting Angiotensin II-induced SMC senescence.²⁰⁸

LncRNAs are a class of non-coding RNAs with lengths longer than 200 nt. Several mechanisms of lncRNA regulation have been identified in both the nucleus and cytoplasm. For example, nucleus-localized lncRNAs can regulate gene expression by guiding or sequestering transcription factors or epigenetic modifiers. Cytoplasmic lncRNAs can serve as miRNA sponges, a regulator of mRNA stability or mediating protein-protein interaction (reviewed in²⁰⁹). Several lncRNAs have been identified in SMC that play functional roles in regulating SMC phenotype and behaviors. For example, CARMEN, a lncRNA located upstream of the miR-143/145 cluster, is also specifically expressed in SMC. CARMN maintains SMC contractile phenotype by directly binding to Myocd and facilitating its activity, and mediating the expression of miR-143/145. Consequently, loss of CARMN in SMC led to exacerbated atherosclerosis plaque formation and injury-induced neointima formation associated with excessive phenotypic modulation.^{200,201}

1.3 Epigenetic memory – the encoding of lineage information

1.3.1 Lineage specification during embryonic development

A fascinating topic in developmental biology remains how a single embryonic stem cell develops into a complex organism consisting of various cell types with lineage-specific gene expression patterns. Tissue-specific transcriptional factors are being continuously identified as the central driver of the differentiation process into specific lineages, such as heart-specific transcription factors GATA4, Mef2C and Tbx5 could induce trans-differentiation from fibroblasts

into cardiomyocytes.²¹⁰ Epigenetic programming functions to establish a more stable and heritable chromatin landscape, where naïve developmental programs are silenced while lineage-specific genes are accessible to the transcription machinery.²¹¹

Early observation using electron microscopy shows that embryonic stem cell (ESC) contains a loosely packaged homogenous chromatin structure compared with differentiated cells, where chromatin is more heterogeneously packaged into blocks of loose or condensed chromatin structure. These two types of chromatin are referred to as euchromatin and heterochromatin and are associated with gene activation and repression, respectively.²¹² Concomitantly, heterochromatin histone marker H3K9me2 is more enriched in the genome of differentiated cells than ESCs, while euchromatin markers H3K4me3, H3K9Ac and H3/H4 acetylation are reduced at genome level after differentiation.²¹³⁻²¹⁵ These initial studies provide a global depiction of the unique chromatin structure in ESC with great plasticity to rearrange euchromatin/heterochromatin distribution in response to different developmental cues.

Besides the global chromatin organization, ESC contains another epigenetic feature called bivalent chromatin domains. Both activating mark, H3K4me2 and H3K4me3, and silencing mark, H3K27me3, are decorated on transcriptionally poised developmental genes associated with lineage determination.¹⁴⁹ Bivalent domains are gradually resolved with lineage commitment when repressive H3K27me3 is converted into H3K27ac and activating H3K4me3 is retained, coinciding with activation of poised genes and cell fate determination.²¹⁶ Meanwhile, bivalent domains of other genes associated with other lineage commitment remain silenced with additional silencing histone marks, H3K27me3, H3K9me3 and DNA methylation.²¹⁷⁻²¹⁹ This balanced bivalent system permits the lineage plasticity of ESC to activate specific genes efficiently in response to certain developmental cues.

Chromatin immunoprecipitation sequencing (ChIP-seq) profiling and chromatin conformation and accessibility studies provide an unbiased description of the dynamic epigenetic programming during lineage specification. To simplify, the homogeneous chromatin structure and bivalent domains gradually switch into a more heterogeneous chromatin structure. The poised lineage-specific developmental program is activated and genes related to other lineages or naïve pluripotency are silenced with stable repressive epigenetic decorations, suggesting the epigenetic modifiers play essential roles in mediating the lineage development. Functional studies using genetic deletion or pharmacological inhibition provided solid evidence on the roles of diverse epigenetic modifiers during lineage specification. For example, global inhibition of histone deacetylase with Trichostatin A in ESC prevented heterochromatin reorganization and strongly inhibited ESC differentiation.²¹⁵ Genetic knockout of H3K4 methyltransferase MLL1 or MLL2 in ESC did not affect global H3K4 methylation or impair stem cell self-renewal but skewed and delayed ESC differentiation program.^{220,221} Similarly, depletion of Dpy30, a subunit of MLL complexes, in ESC did not affect self-renewal but significantly altered differentiation potential by reducing H3K4me3 within the bivalent domains.²²² H3K4 demethylase, lysine-specific demethylase 1 (LSD1) has been shown to demethylate H3K4me2 in bivalent domains. Deletion of LSD1 in ESC disrupted the pluripotency and activation of bivalent poised developmental genes, which led to precocious endoderm and mesoderm differentiation.²²³ Of particular interest, cardiac precursor deletion of H3K4me1/2 methyltransferase *Kmt2d* (*Mesp1-Cre, Kmt2d^{flox}*) disrupted cardiac development with defects on H3K4me2 enrichment on genes associated with cardiomyocyte-specific functions, further supporting a key role of H3K4me2 in activating lineage-specific genes during development.²²⁴

1.3.2 Epigenetic memory mechanisms in mature cells – H3K4 di-methylation

As described above, histone modification redistribution and chromatin structure reorganization are required processes for lineage determination during development. Yet, it remains less understood if similar mechanisms operate in mature cells to maintain their lineage identity and memory when their gene expression pattern is transiently altered upon changes in the environment. Fully differentiated SMC could transiently modulate its phenotype by turning off the expression of contractile genes and reversibly differentiate back to the contractile state according to external stimuli. How does SMC remember its original lineage identity during phenotypic “de-differentiation”? What mechanisms permit SMC to efficiently recover the expression of contractile genes upon stimulation?

There are observations suggesting H3K4me2 might function as an epigenetic mechanism for the determination and maintenance of cell lineage identity.. Comprehensive ChIP-seq studies have revealed that H3K4me2 is distributed across genes related to lineage-specific functions in various cell lines or tissues, including retina²²⁵, CD4+ T lymphocytes²²⁶, fibroblasts and hepatoma cell line HepG2²²⁷, breast and prostate cancer cell lines²²⁸, and neural tissue²²⁹. Similarly, such lineage specific H3K4me2 enrichment is also presented in SMC. There is evidence suggesting H3K4me2 might function as an epigenetic mechanism in maintaining lineage identity based on the following observations. *First*, H3K4me2 marks lineage-specific genes. Comprehensive ChIP-seq studies have revealed that H3K4me2 is distributed across genes related to lineage-specific functions in various cell lines or tissues, including retina²²⁵, CD4+ T lymphocytes²²⁶, fibroblasts and hepatoma cell line HepG2²²⁷, breast and prostate cancer cell lines²²⁸, and neural tissue²²⁹. Similarly, such lineage-specific H3K4me2 enrichment is also presented in SMC^{114,162}.

Second, H3K4me2 enrichment is independent of gene expression status and primes transcriptionally poised genes for further activation. In contrast with H3K4me3, which is strictly enriched on the transcription start site (TSS) and correlated with transcription activity, H3K4me2 enrichment can also be found outside TSS and may not correlate with transcription in a cell-type and cell-state-dependent manner.²²⁷ D'Urso A. *et al.* used a novel genetic model where H3 lysine 4 was substituted with arginine (H3K4R) or alanine (H3K4A) to study the epigenetic memory mechanism of H3K4me2. They demonstrated that H3K4me2 was stable during transient gene repression and was required to recruit poised RNA polymerase II (RNAPII) to enhance the repression of poised genes.²³⁰ Epigenetic programming on SMC-specific contractile genes exhibits a similar feature. While the level of activating histone modifications, H3K4me3 or H3/4 acetylation, is diminished upon contractile gene repression, H3K4me2 is stably retained on these gene loci regardless of gene silencing *in vitro*¹¹⁴ and *in vivo*^{27,162-164}. Importantly, H3K4me2 enrichment is independent of the proper formation of the activating transcription complex Myocd/SRF/CArG, as *Acta2* transgene containing mutant CArG remained at a similar level of H3K4me2 as endogenous *Acta2* loci.¹¹⁴

These previous studies indicated that H3K4me2 cannot be simply classified as an activating histone mark but may act to prime lineage-specific gene activation in response to trans-regulator elements. However, this concept needs more direct evidence and functional studies. The concept of epigenetic memory and the lineage-specific functional relevance of H3K4me2 has been challenging to study for the following reasons. *First*, ChIP-seq studies are by nature descriptive and can only provide correlative and indirect evidence regarding the transcription activity of a histone modification and its function during cell differentiation. *Second*, by far, the majority of functional studies utilized global manipulation of histone modifiers, such as genetic knockout or

overexpression, the substitution of global histone lysine residues, or pharmacologically inhibition of enzyme activities. These studies inspire and establish the foundation of functional epigenetics, yet it is difficult to exclude “off-target” secondary effects caused by global epigenome alteration. Therefore, innovative techniques and tools are needed in the future to elucidate the functions of a specific epigenetic modification on a specific genome locus.

1.4 Summary and Hypothesis

Vascular smooth muscle cells are highly specialized contractile cells within the vascular walls that can undergo extensive phenotypic modulation in response to various physiological or pathological stimulations, meaning mature SMC can transiently turn off its SMC-specific gene repertoire (e.g., contractile genes *Acta2/Myh11/Tagln* etc.) and acquire features of enhanced proliferation, migration, protein synthesis and extracellular matrix production. Under pathological conditions, mature SMC could even acquire features of other lineages, such as phagocytosis of cholesterol or osteochondrogenesis. Such phenotypic plasticity has been widely reported in recent studies using stringent SMC-lineage fate tracing animal models or single-cell transcriptomics. However, the key molecular mechanism controlling SMC phenotypic plasticity remains largely unclear. Several transcription “switches” responsible for contractile gene expression or repression have been identified, including key activators (*Myocd*), repressors (*KLF4*), or epigenetic programming associated with gene expression status. Yet, it is unknown how SMC retains its lineage identity during the reversible phenotypic modulation, and mechanisms restraining SMC plasticity and preventing SMC acquisition of other-lineage features.

Epigenetic mechanisms are involved in lineage specification and maintenance. Enrichment of H3K4me2 on SMC contractile gene repertoire is specific to SMC lineage and persistently retained in the transiently dedifferentiated SMC when contractile genes are temporarily silenced. Based on these properties, H3K4me2 on SMC-specific genes is characterized as the SMC-lineage epigenetic signature, yet whether H3K4me2 plays a functional role in mediating SMC phenotype is unknown. Here, we propose to test the central hypothesis that the histone modification H3K4me2 enriched on SMC-specific genes functions as the “epigenetic memory” mechanism controlling SMC lineage identity and function.

2.0 H3K4 di-methylation Governs Smooth Muscle Lineage Identity and Promotes Vascular Homeostasis by Restraining Plasticity

Mingjun Liu^{1,2}, Cristina Espinosa-Diez¹, Sidney Mahan¹, Mingyuan Du^{1,3}, Anh T. Nguyen⁴,
Scott Hahn¹, Raja Chakraborty^{5,6}, Adam C. Straub^{1,7,8}, Kathleen A. Martin^{5,6}, Gary K. Owens^{4,9},
Delphine Gomez^{1,2}

¹ Pittsburgh Heart, Lung, Blood, and Vascular Medicine Institute, University of Pittsburgh;
Pittsburgh, PA, USA

² Division of Cardiology, Department of Medicine, University of Pittsburgh; Pittsburgh, PA,
USA

³ Department of Vascular Surgery, The Second Xiangya Hospital of Central South University,
Changsha, China

⁴ Robert M. Berne Cardiovascular Research Center, University of Virginia; Charlottesville, VA,
USA

⁵ Internal Medicine, Cardiovascular Medicine Section, Yale Cardiovascular Research Center,
Yale University; New Haven, CT, USA

⁶ Department of Pharmacology, Yale University; New Haven, CT, USA

⁷ Department of Pharmacology & Chemical Biology, University of Pittsburgh School of
Medicine; Pittsburgh, PA, USA

⁸ Center for Microvascular Research, University of Pittsburgh School of Medicine; Pittsburgh,
PA, USA

⁹ Department of Molecular Physiology and Biological Physics, University of Virginia;
Charlottesville, VA, USA

Copyright to Elsevier, Developmental Cell, 2021

2.1 Summary

Epigenetic mechanisms contribute to the regulation of cell differentiation and function. Vascular smooth muscle cells (SMCs) are specialized contractile cells that retain phenotypic plasticity even after differentiation. Here, by performing selective demethylation of histone H3 lysine 4 di-methylation (H3K4me2) at SMC-specific genes, we uncovered that H3K4me2 governs SMC lineage identity. Removal of H3K4me2 via selective editing in cultured vascular SMCs and in murine arterial vasculature led to loss of differentiation and reduced contractility due to impaired recruitment of the DNA methylcytosine dioxygenase TET2. H3K4me2 editing altered SMC adaptative capacities during vascular remodeling due to loss of miR-145 expression. Finally, H3K4me2 editing induced a profound alteration of SMC lineage identity by redistributing H3K4me2 toward genes associated with stemness and developmental programs, thus exacerbating plasticity. Our studies identify the H3K4me2-TET2-miR145 axis as a central epigenetic memory mechanism controlling cell identity and function, whose alteration could contribute to various pathophysiological processes.

2.2 Introduction

Unlike adult cardiac and skeletal myocytes, which are terminally differentiated, adult SMCs retain remarkable plasticity in response to acute and chronic changes in their environment^{2,35}. Recent fate mapping and transcriptomic studies have provided compelling evidence of SMC phenotypic modulation and the complex fate of this cell type in vascular diseases. In the context of major vascular diseases including atherosclerosis^{31,231,232} and aortic aneurysm^{233,234}, SMCs profoundly alter their specialized phenotype by losing the expression of their contractile gene repertoire including smooth muscle α -actin (ACTA2) and smooth muscle myosin heavy chain (MYH11). Moreover, SMCs partition into multiple transcriptionally distinct subpopulations and can acquire the expression of genes associated with alternative cell types and functions like osteochondrogenic cells (RUNX2, SOX9), phagocytic cells (LGALS3, CD68), or mesenchymal stem cells (SCA1)^{88,163}. Although consensus regarding a definitive categorization of SMC populations has not been reached, these studies have markedly enhanced our understanding of SMC phenotypic diversity and plasticity²³⁵.

It is less appreciated that, besides its implication in vascular disease, SMC phenotypic modulation is an evolutionarily conserved mechanism under physiological conditions, which plays a key role in the efficient adaptation of SMCs to changes in environmental cues driving vascular network development, growth, and remodeling as well as maintenance of vascular homeostasis (e.g., extracellular matrix production in response to increased mechanical strain)^{2,86}. This adaptive vascular remodeling implies that: 1) SMCs transiently decrease the expression of contractile genes, 2) activate genes associated with cell proliferation, migration, or extracellular matrix synthesis, and 3) re-differentiate into contractile SMCs and re-express their SMC marker genes. This process of reversible dedifferentiation has been well characterized *in vitro*. SMCs transiently exposed to

Platelet Derived Growth Factor-BB (PDGF-BB), a potent inducer of SMC dedifferentiation, fully regain expression of the SMC contractile genes *Acta2* and *Myh11* upon removal of the growth factor¹¹⁴. *In vivo*, SMC-lineage tracing studies identified populations of SMCs with a differentiated phenotype (i.e., *ACTA2*⁺, *MYH11*⁺) after their investment in atherosclerotic lesions^{55,163}, or pulmonary capillaries^{56,236}, a process involving their dedifferentiation, proliferation, and migration. These studies support the concept of reversible dedifferentiation, reacquisition of SMC contractile gene expression, and retention of SMC lineage identity during vascular remodeling.

Such reversible modulation of SMC contractile gene expression requires tight yet dynamic regulation by master regulators responsible for gene activation or repression. It also implies the participation of stable lineage maintenance mechanisms granting retention of their lineage identity during transient dedifferentiation. Many transcriptional and epigenetic mechanisms have been implicated in the dynamic and specific regulation of the contractile gene repertoire in SMC²³⁷. The CArG box-SRF-myocardin complex has been identified as a central master regulator of the SMC contractile gene activation. Myocardin is a potent myogenic coactivator exclusively expressed in SMC and cardiomyocytes^{104,105,113}. Myocardin functions by forming a complex with SRF (Serum Response Factor) recruited to the *cis*-element CArG box CC(A/T)₆GG commonly present in SMC marker genes including *Acta2*, *Myh11*, *Tagln*, and *Cnn1*. Myocardin is required for proper SMC differentiation during vascular development as demonstrated by *in vivo* loss-of-function studies^{115,116}. Myocardin also restrains SMC phenotypic plasticity by counteracting transcription factors promoting differentiation into other lineages, including *Sox9* for chondrocyte differentiation¹¹⁸. Besides myocardin, the DNA methylcytosine dioxygenase TET2 promotes SMC differentiation by preventing DNA methylation at SMC contractile genes²³⁸. Although such transcriptional or epigenetic control of SMC-specific gene expression has been extensively studied,

factors responsible for upstream priming of these genes and maintenance of SMC lineage identity during reversible dedifferentiation have not been identified.

We have previously characterized the enrichment of Histone 3 Lysine 4 di-methylation (H3K4me2) on the CArG regions of myocardin-regulated SMC genes as a stable “epigenetic signature” of SMC lineage. This H3K4me2 epigenetic signature presents important characteristics^{114,162}. First, the enrichment of H3K4me2 on myocardin-regulated genes, including SMC gene markers *Acta2*, *Myh11*, and *Tagln*, is restricted to the SMC lineage. Second, the H3K4me2 epigenetic signature appears in SMC precursors during all trans retinoic acid (ATRA)-induced SMC differentiation. Third, H3K4me2 enrichment on the SMC contractile genes occurs independently of binding of the SRF-myocardin complex on CArG boxes. CArG box mutations in *Acta2* promoter-enhancer transgenes did not prevent enrichment of H3K4me2. Fourth, the H3K4me2 signature is stably retained on poised SMC marker genes during SMC transient phenotypic modulation *in vitro* and *in vivo*. Collectively, these observations suggest that the presence of H3K4me2 on the SMC gene repertoire is an SMC-lineage specific epigenetic signature present on these genomic loci irrespective of gene activation status. Given H3K4me2 signature lineage selectivity and stability, it appears that H3K4me2 does not act as a conventional activating histone modification but instead provides a mechanism for the maintenance of lineage identity during reversible dedifferentiation²³⁹.

Contemporary to the development of the “histone code” paradigm²⁴⁰, the concepts of epigenetic control of lineage determination and maintenance of lineage epigenetic memory have been proposed²⁴¹⁻²⁴³. In support of these concepts, several reports have shown that H3K4me2 is preferentially distributed on genes related to lineage identity and cell-specific functions in multiple cell types and tissues²⁴⁴⁻²⁴⁶. Cardiac-specific knockout (KO) of the H3K4 methyltransferase

KMT2D led to an average decrease in H3K4me2 levels at promoter regions and functional defects during cardiac development²⁴⁷. Together, these studies indicate that H3K4me2 might play a central role in cell differentiation and lineage-specific epigenetic programming. However, they also present experimental limitations precluding the direct and unambiguous investigation of H3K4me2 functions²³⁹. First, the comparison of genome-wide epigenetic landscape by ChIP sequencing is inherently descriptive and does not inform on the causality between histone modification enrichment, gene expression and cellular phenotype. Second, global genetic or pharmacologic inhibition of histone-modifying enzymes is often difficult to interpret due to the general lack of specificity of these enzymes for a single histone residue and their impact on a vast number of genomic loci. Thus, despite assumptions to the contrary, characterization of the role of H3K4me2 is lacking and there are critical unresolved questions: What is the role of H3K4me2 in regulating vascular SMC differentiated state? Does H3K4me2 serve as a mechanism for maintenance of SMC lineage identity? To address these questions, we performed gene-selective H3K4me2 loss-of-function studies by inducing demethylation of H3K4me2 selectively on myocardin-dependent genes in SMC. H3K4me2 editing on this gene repertoire led to a profound loss of SMC identity and contractile function *in vitro* and *in vivo*. Overall, our studies demonstrate a central role of H3K4me2 for maintenance of an epigenetically controlled lineage identity in adult cells.

2.3 Results

2.3.1 Selective demethylation of H3K4me2 on Myocardin-regulated genes

To assess the functional relevance of H3K4me2 in controlling SMC phenotype and function, we developed a targeted epigenome editing strategy consisting of gene-specific demethylation of H3K4me2 on the family of myocardin-dependent gene repertoire. We engineered a fusion protein linking the nuclear localization signals and the SRF binding domain of myocardin and the Lysine Specific Demethylase 1 (LSD1) to serve as recruitment and catalytic subunits, respectively (**Figure 4A**). The myocardin fragment excluded the Leucine zipper and transactivation domains. This design allows for the selective binding of Myocd-LSD1 to the large family of CARG/SRF/Myocardin-regulated genes characteristic of differentiated SMC while preventing cytoplasmic sequestration and myocardin-dependent transactivation²⁴⁸. To control for potential H3K4me2 demethylation-independent effects of Myocd-LSD1, we designed a non-functional editing system (Myocd-LSD1^{NF}) containing the catalytically inactive LSD1^{K661A} (**Figure 4A**)²⁴⁹. We generated rat aortic SMCs stably expressing Myocd-LSD1 and Myocd-LSD1^{NF} (**Appendix Figure 1A**). Myocd-LSD1 and Myocd-LSD1^{NF} were recruited to the CARG box regions of myocardin-regulated genes including the SMC contractile genes *Acta2*, *Tagln* and *Myh11* (**Figures 4B** and **Appendix Figure 1B**). We measured a significant decrease in H3K4me2 levels on these genes in SMCs expressing Myocd-LSD1 specifically while no noticeable effect was observed in SMCs expressing Myocd-LSD1^{NF}, demonstrating that Myocd-LSD1-induced H3K4me2 demethylation is dependent on LSD1 demethylase activity. Importantly, there was no Myocd-LSD1 recruitment or H3K4me2 alteration on CARG/SRF-dependent but myocardin-independent early response genes (**Figures 4B** and **Appendix Figure 1B**).

Genome-wide evaluation of H3K4me2 distribution and Myocd-LSD1 occupancy confirmed the concomitant binding of Myocd-LSD1 and the loss of H3K4me2 on myocardin-regulated contractile genes in Myocd-LSD1 SMC specifically, while no difference was observed on *cfos* or the myocardin-independent contractile gene *Smtn* (**Figures 4C** and **Appendix Figure 1C**). Importantly, H3K4me2 abundance was not altered in Myocd-LSD1 SMC compared to control and Myocd-LSD1^{NF} SMC (**Figures 4D** and **Appendix Figure 1D**). However, we identified subsets of genes with either statistically higher or lower H3K4me2 enrichment, demonstrating that Myocd-LSD1 induces a redistribution of H3K4me2 (**Figures 4E** and **4F**). Loci with lower H3K4me2 were located in gene promoters and 1st introns, consistent with CARG box location (**Appendix Figure 1G**)¹¹⁰. By comparing H3K4me2 and Myocd-LSD1 CUT&Tag sequencing, we found that more than 75% of the genes with lower H3K4me2 contained Myocd-LSD1 peaks (**Appendix Figure 1H**). Gene Ontology (GO) Pathway analysis revealed that genes with lower H3K4me2 abundance in Myocd-LSD1 SMC participate in biological processes related to vascular development, SMC differentiation and SMC function demonstrating the demethylation of H3K4me2 on key SMC gene repertoire by Myocd-LSD1 (**Figures 4E** and **Appendix Figure 1I**).

LSD1 induces demethylation of H3K4me2, as well as H3K4me1 and H3K9me. Expression of Myocd-LSD1 was not associated with differences in activating (H3K4me3, panH3ac) or repressive histone modifications (H3K9me3, H3K27me3), as well as expression of epigenetic modifiers (**Figures 4F**, **Appendix Figure 2A**, **2B**, and **2C**). We observed an increase in H3K4me1 in Myocd-LSD1 SMCs which can be due to the active H3K4me2 demethylation (**Figure 4F**). Expression of Myocd-LSD1 did not impact the expression, recruitment, or transcriptional activity of the endogenous SRF-myocardin complex (**Figures 4G**, **4H**, **Appendix Figure 2D**, and **2E**). Moreover, we found that more than 50% of genes with loss of H3K4me2 in Myocd-LSD1 SMC

were those with enrichment in SRF binding (**Appendix Figure 1J**)²⁵⁰. Analysis of these intersected genes was enriched in pathways associated with SMC differentiation and function (**Appendix Figure 1K**). Overall, these data demonstrate the specificity and efficiency of Myocd-LSD1 in performing targeted H3K4me2 demethylation on myocardin-regulated genes and validate our strategy to address the biological relevance of H3K4me2 in SMC.

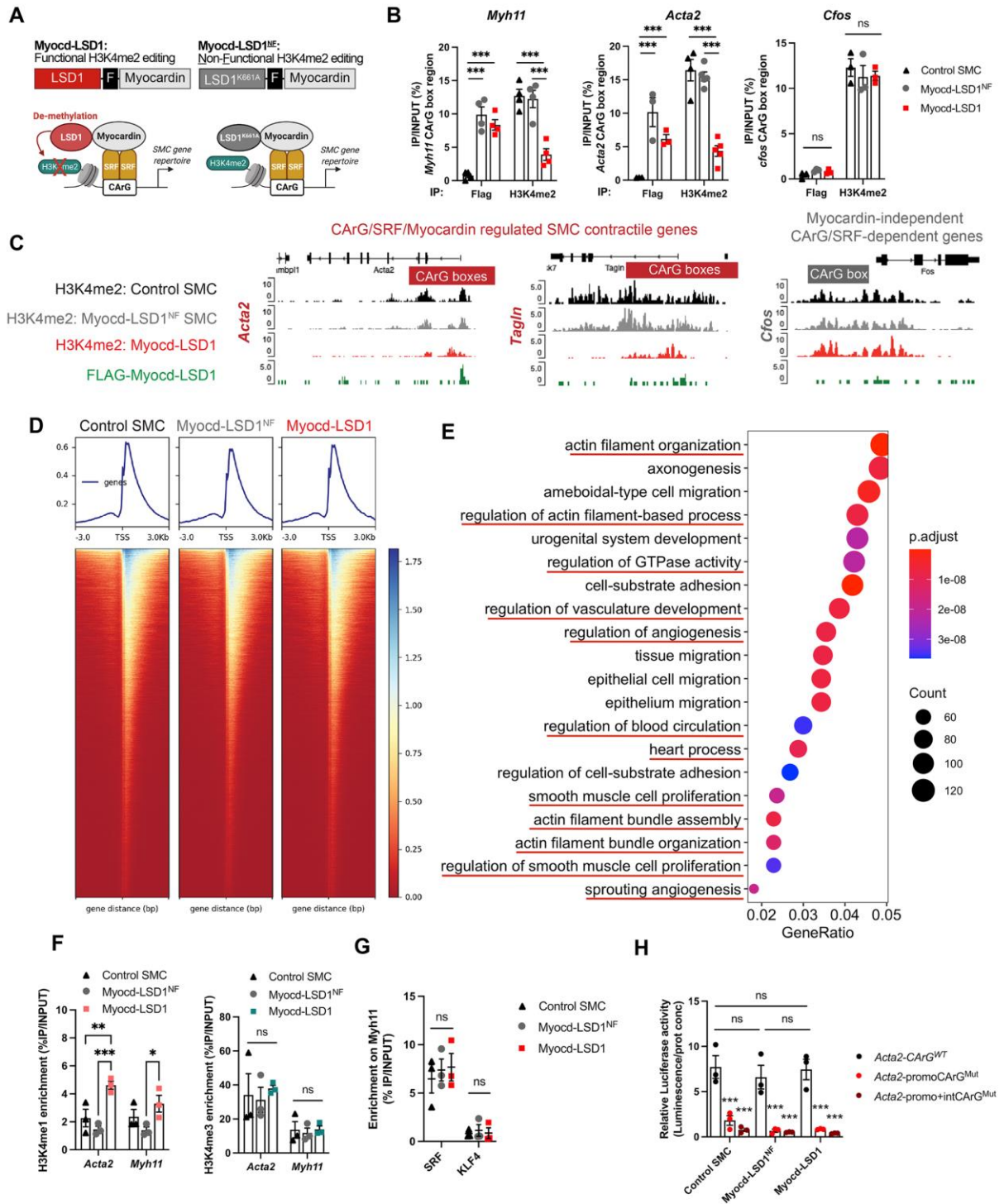


Figure 4 Myocd-LSD1 selectively performs H3K4me2 demethylation on myocardin-regulated SMC gene repertoire

A. Schematic representation of Myocd-LSD1-mediated H3K4me2 editing. Functional (Myocd-LSD1) and non-functional (Myocd-LSD1^{K661A} or Myocd-LSD1^{NF}) constructs of Myocd-LSD1 were generated, both containing a Flag sequence (F) in the linker region. **B.** Myocd-LSD1/LSD1^{NF} and H3K4me2 enrichment on CArG box regions of *Acta2*, *Tagln* and *cfos* in control non-transduced SMC, and SMC transduced with either Myocd-LSD1 or Myocd-LSD1^{NF}. **C.** H3K4me2 and Myocd-LSD1 CUT&Tag sequencing tracks in CArG box regions of *Acta2*, *Tagln* and *cfos* in control, Myocd-LSD1, and Myocd-LSD1^{NF} SMC. **D.** Heatmap of H3K4me2 enrichment around gene transcription start sites (TSS). **E.** Top 20 GO pathways enriched in genes with significant loss of H3K4me2 in Myocd-LSD1 SMC vs Myocd-LSD1^{NF} SMC. **F.** H3K4me1 and H3K4me3 enrichment on CArG box regions of *Myh11* and *Acta2* in control, Myocd-LSD1 and Myocd-LSD1^{NF} SMC. **G.** Measurement of SRF and KLF4 binding on CArG box region of *Myh11* in control, Myocd-LSD1 and Myocd-LSD1^{NF} SMC. **H.** Luciferase activity assay using *Acta2* promoter-enhancer construct with intact (*Acta2*-CArG^{WT}) or mutated CArG boxes (*Acta2*-promoCArG^{Mut} and *Acta2*-promo+intCArG^{Mut}). Data are represented as mean ± s.e.m of 3-5 independent experiments. Groups were compared by One-Way ANOVA or Two-way ANOVA. * p<0.05, ** and ## p<0.001, *** p<0.0001.

2.3.2 H3K4me2 editing impairs SMC contractile function

SMC expressing Myocd-LSD1 presented a marked decrease in expression of the myocardin-regulated contractile genes at the transcript and protein levels (**Figures 5A, 5B, 5C, and 5D**). These alterations in SMC contractile gene expression were observed specifically in Myocd-LSD1 SMC as compared to Myocd-LSD1^{NF} and control SMCs. Moreover, Myocd-LSD1 SMC presented a defect in contractility in 3D-collagen culture (**Figures 5E, Appendix Figure 2F, and 2G**). SMC contractility *ex vivo* in response to potassium was decreased by 25-30% in vessels transduced with Myocd-LSD1 (**Figure 5F**). Interestingly, over-expression of full-length myocardin in Myocd-LSD1 infected SMCs failed to rescue expression of contractile genes (**Figure 5G**). Similarly, rapamycin, a potent SMC differentiation inducer, did not increase SMC contractile

gene expression or SMC contractility (**Figures 5H** and **5I**). Finally, Myocd-LSD1 SMCs failed to re-differentiate to a contractile state after transient PDGF-BB treatment (**Appendix Figure 2H**).

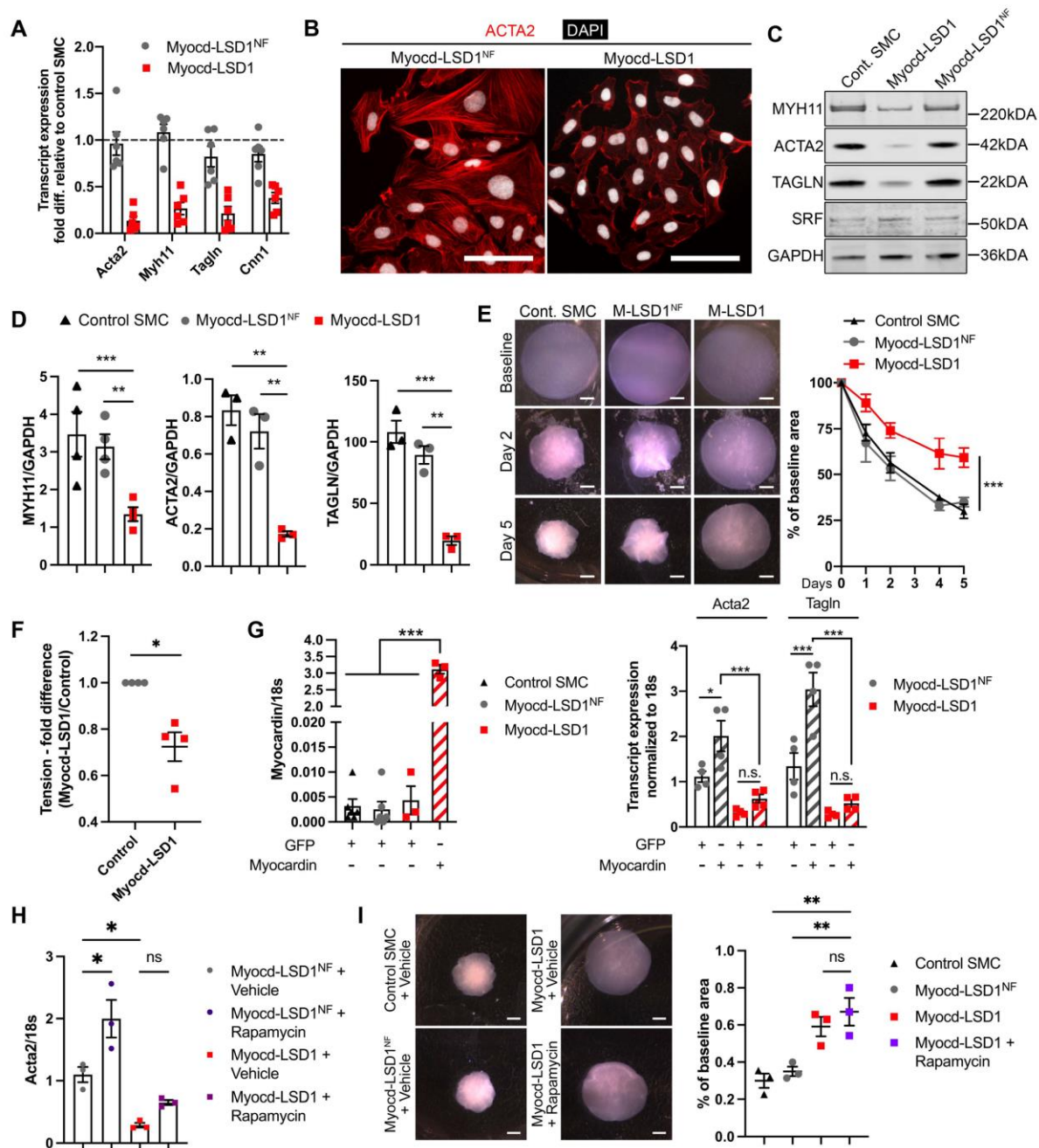


Figure 5 H3K4me2 editing induces loss of SMC contractility *in vitro*

A. Transcript expression of contractile genes in Myocd-LSD1 and Myocd-LSD1^{NF} SMC. Expressed as fold change compared to control SMC. **B.** ACTA2 and DAPI immunofluorescent staining in Myocd-LSD1 and Myocd-LSD1^{NF} SMC. Scale bar = 100 μ m. **C.** SMC-related gene protein expression in control, Myocd-LSD1/LSD1^{NF} SMC. **D.** Protein expression quantification normalized to GAPDH. **E.** Collagen contraction assay using control, Myocd-LSD1 and

Myocd-LSD1^{NF} SMC. Scale bar = 1mm. Measurement of diameter over time. **F.** *Ex-vivo* wire myography combined with potassium chloride infusion in thoracodorsal artery rings incubated with Myocd-LSD1 or control lentivirus for 48h (n=4 mice per group). **G.** mRNA expression of myocardin, Acta2 and Tagln in Myocd-LSD1 and Myocd-LSD1^{NF} SMC transduced with Adv-GFP or Adv-Myocardin. **H.** Acta2 transcript expression in Myocd-LSD1 and Myocd-LSD1^{NF} SMC treated with rapamycin (100 nM). **I.** Collagen contraction assay using control, Myocd-LSD1^{NF}, Myocd-LSD1 and Myocd-LSD1 SMC treated with rapamycin (100 nM). Gel area variation at day 5 post-gelation normalized to baseline area. Scale bar = 1 mm. Data are represented as mean \pm s.e.m of 3-6 independent experiments. Groups were compared by Student t-test, One-way ANOVA, Two-way ANOVA, or Mann-Whitney (F). * p<0.05, ** p<0.001, *** p<0.0001.

Next, we locally delivered lentivirus encoding Myocd-LSD1 or Myocd-LSD1^{NF} on the right carotid arteries of *Myh11* CreER^{T2}-YFP mice by Pluronic gel application (**Figure 6A**). Upon tamoxifen treatment at 6 weeks, Myh11⁺ SMC are permanently and specifically labeled with YFP. Consequently, SMC identity can be traced regardless of conventional SMC marker gene expression (e.g., ACTA2, MYH11), which could be altered upon H3K4me2 editing. Two weeks after virus delivery, Myocd-LSD1 was highly expressed in transduced carotid arteries and SMCs (**Appendix Figure 3A, 3B, 3C, and 3D**). While Myocd-LSD1 did not induce significant changes in vessel morphology (**Appendix Figure 3E and 3F**), a marked reduction in ACTA2 and MYH11 expression was observed in YFP⁺ SMCs (**Figures 6B and 6C**). Importantly, there was a direct association between expression of Myocd-LSD1 (mCherry⁺) and reduced ACTA2 expression (**Figure 6D**). Expression of Myocd-LSD1 was not associated with a change in SMC proliferation, survival, or apoptosis rate (**Appendix Figure 3G, 3H, 3I, and 3H**). Our studies provide evidence that the presence of H3K4me2 on the CArG box regions of SMC contractile genes is essential for maintenance of SMC contractile phenotype and function *in vitro* and *in vivo*.

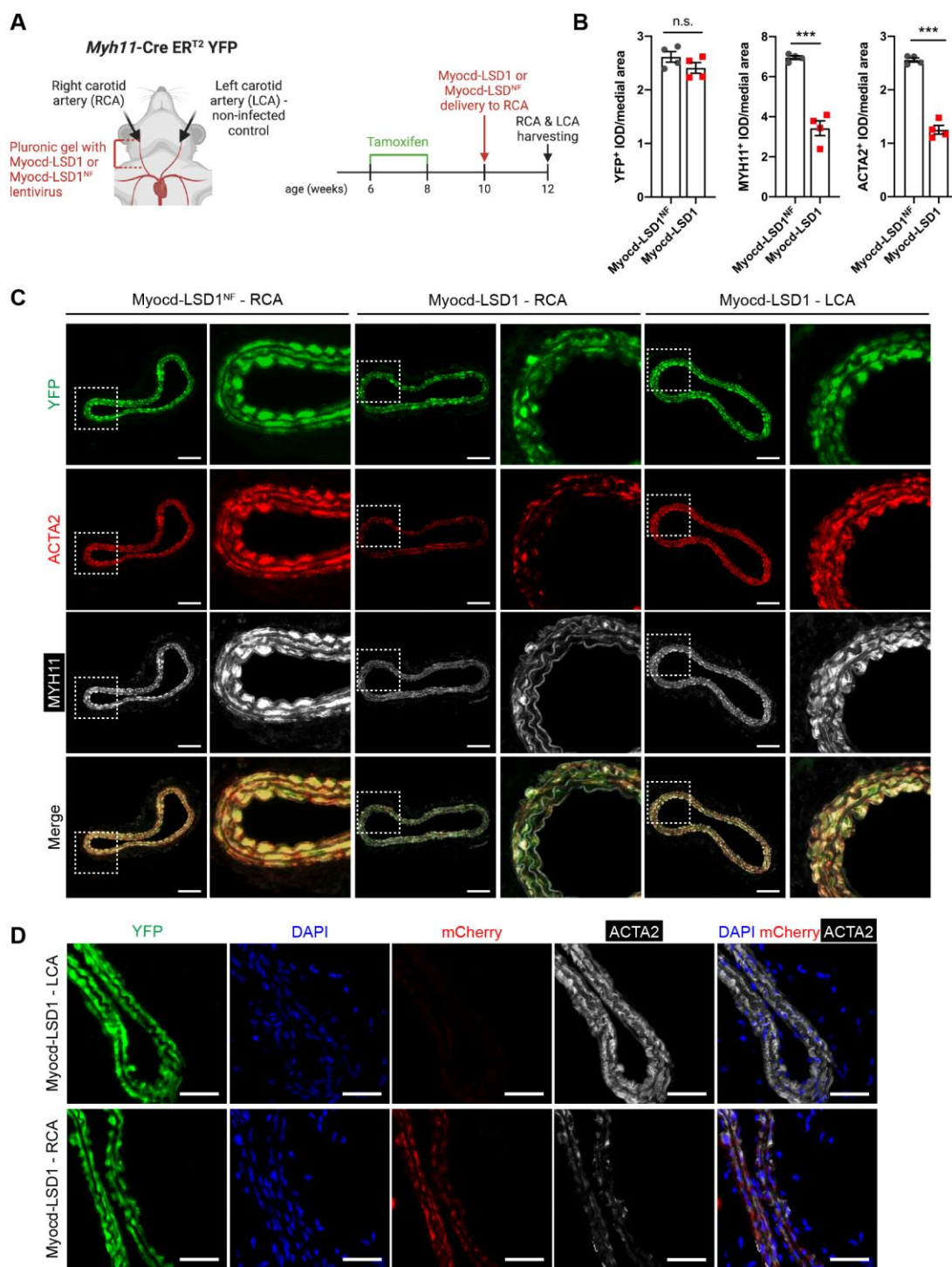


Figure 6 H3K4me2 editing impairs SMC contractile gene expression *in vivo*

A. Schematic of lentiviral-mediated H3K4me2 editing *in vivo*. **B.** Quantification YFP⁺, ACTA2⁺ and MYH11⁺ Integrated Optical Density (IOD) normalized to medial area in carotid cross-sections of *Myh11*-CreER^{T2} YFP mice locally infected with Myocd-LSD1 or Myocd-LSD1^{NF} lentivirus (n=4 mice per group). **C.** YFP, ACTA2, and MYH11 staining in non-infected left carotid arteries (LCA), Myocd-LSD1 and Myocd-LSD1^{NF} infected right carotid arteries (RCA). Scale bar = 100 μ m. **D.** YFP, mCherry and Acta2 staining in non-infected left carotid or Myocd-LSD1 infected right carotid arteries. Scale bar = 100 μ m. Data are represented as mean \pm s.e.m of 4 independent biological replicates. Groups were compared by Student t-test (B). * p<0.05, ** p<0.001, *** p<0.0001.

2.3.3 H3K4me2 mediates TET2 recruitment on myocardin-regulated contractile genes

H3K4me2 enrichment on myocardin-regulated genes has been reported irrespective of their activation status^{114,162} which suggests that H3K4me2 may not exhibit intrinsic gene activation functions but rather control transcriptional and epigenetic factor recruitment. We found that loss of H3K4me2 induced marked changes in DNA methylation. Myocd-LSD1 expression induced an increase in DNA methylation (5mC) and a simultaneous reduction in DNA hydroxymethylation (5hmC) on *Acta2* and *Myh11* CArG box promoter regions (**Figure 7A**). Correspondingly, we observed a striking loss of TET2 recruitment to these loci in Myocd-LSD1 SMC, while expression of TET2 was not altered (**Figures 7B** and **Appendix Figure 2C**). It has been reported that TET2 promotes SMC differentiation by converting 5mC into 5hmC on SMC marker genes²³⁸. Overexpression of TET2 rescued *Acta2* and *Myh11* expression in Myocd-LSD1 SMC, suggesting that H3K4me2 editing-mediated defect in TET2 recruitment causes loss of SMC contractile gene expression (**Figure 7C**).

The mechanisms by which TET2 selectively binds to given genomic regions have not been fully characterized. Unlike the other TET enzyme isoforms, TET1 and TET3, TET2 lacks a defined CXXC DNA-binding domain to mediate its recruitment²⁵¹. By performing HA-tag CUT&Tag

sequencing in control or Myocd-LSD1 SMCs expressing HA-TET2, we found that H3K4me2 editing was associated with a partial loss of TET2 recruitment in Myocd-LSD1 SMC (**Figures 7D, Appendix Figure 4A, and 4B**), including in the *Acta2* CArG box region (**Figure 7E**). Genes exhibiting a loss of TET2 occupancy in Myocd-LSD1 are associated with several biological processes related to SMC differentiation and functions (**Figure 7F**). Genome-wide, we found that 86.6% of TET2 occupancy overlapped with H3K4me2 in control SMCs, while the number of genes with TET2 and H3K4me2 co-distribution was reduced by more than 50% in Myocd-LSD1 SMCs (**Figure 7G**). We next examined the co-distribution between H3K4me2 and 5hmC in human coronary artery SMC using publicly available H3K4me1/me2/me3 datasets (**Figure 7H**)²⁵². 73% of genes enriched in 5hmC in human SMC also presented an enrichment for H3K4me2 (**Figures 7H, Appendix Figure 4C, and 4D**). Remarkably, we found that 5hmC is preferentially distributed with H3K4me2 compared to H3K4me1 and H3K4me3 (**Figure 7H, and Appendix Figure 4D**). While 73% of 5hmC-enriched genes overlapped with H3K4me2-enriched genes, the co-enrichment with 5hmC dropped to 36% and 51% for H3K4me1 or H3K4me3 respectively. If we analyze the co-distribution of 5hmC with only one type of H3K4 methylation, 13.4% of 5hmC distribution overlaps with genes enriched in H3K4me2 only, compared to 2.7% and 1% for H3K4me1 and H3K4me3 respectively.

Proximity Ligation Assay (PLA) showed the proximity between H3K4me2 and TET2 in cultured SMCs (**Appendix Figure 4E, 4F, and 4G**) and mouse aorta (**Appendix Figure 4H**). We found a decrease in the number of H3K4me2/TET2 interactions in Myocd-LSD1 SMCs, suggesting that a significant subset of these interactions occurs on myocardin-regulated genes impacted by Myocd-LSD1 (**Figures 7I and 7J**). We next performed co-immunoprecipitation (Co-IP) between biotinylated H3K4me2 peptides and nuclear extracts of 293T cells expressing HA-

tagged TET2. We found that H3K4me2 was immunoprecipitated with HA-TET2 (**Figures 7K** and **Appendix Figure 4I**). Co-IP with Biotin-H3K4me1, me2, or me3 peptides revealed a preferential interaction between TET2 and H3K4me2 (**Figures 7L** and **7M**). Together, these data provide evidence that H3K4me2 serves as a hub for dynamic TET2 recruitment to SMC gene repertoire in SMC.

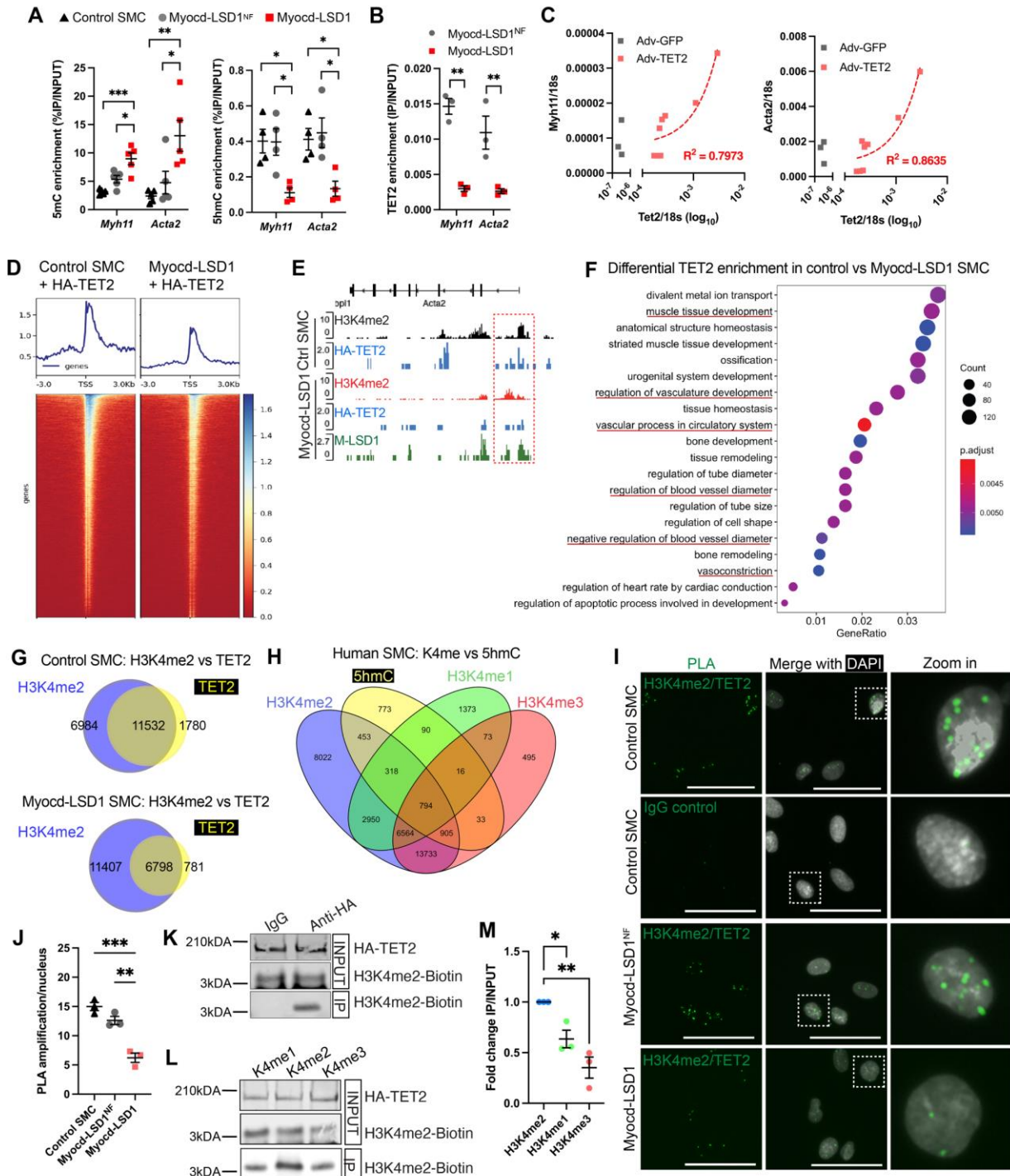


Figure 7 H3K4me2 interacts with TET2 and is required for its recruitment on the SMC contractile genes

A. 5mC and 5hmC levels on *Myh11* and *Acta2* CARG box regions in control, Myocd-LSD1, and Myocd-LSD1^{NF} SMC. **B.** TET2 enrichment on *Acta2* and *Myh11* CARG box regions in Myocd-LSD1^{NF} and Myocd-LSD1 SMC. **C.** Correlation between *Myh11*, *Acta2* and *Tet2* mRNA levels in Myocd-LSD1 SMC transduced with Adv-TET2. R² is calculated by linear regression. **D.** Heatmap of HA-TET2 enrichment around transcription start sites (TSS) measured by CUT&Tag sequencing in control SMC and Myocd-LSD1 SMC transduced with Adv-HA-TET2. **E.** Visualization of HA-TET2 enrichment peaks on the *Acta2* gene in control SMC and Myocd-LSD1 SMC. **F.** GO pathway analysis of genes with decreased TET2 enrichment in Myocd-LSD1. **G.** Venn diagrams of annotated genes with HA-TET2 enrichment and H3K4me2 enrichment in control SMC or Myocd-LSD1 SMC. **H.** Venn Diagram comparing H3K4me1, H3K4me2, H3K4me3, and 5hmC distribution in human SMC. **I.** Proximity Ligation Assay (PLA) detecting proximity between H3K4me2 and TET2. Scale bar = 25µm. **J.** Quantification of H3K4me2/TET2 PLA signals in control SMC, Myocd-LSD1^{NF}, and Myocd-LSD1 SMC. **K.** HA-tagged TET2 and biotin-H3K4me2 peptide co-immunoprecipitation (IP). IP: anti-HA antibody or IgG control; Blotting: anti-biotin antibody. **L.** HA-tagged TET2 and biotin-H3K4me1/2/3 peptide co-immunoprecipitation. IP: anti-HA antibody; Blotting: anti-biotin antibody. **M.** Quantification of HA-TET2 and Biotin-H3K4me1/2/3 peptide co-immunoprecipitation. IP signals normalized with INPUT Biotin-H3K4me1/2/3 signals. Fold changes were represented as compared to H3K4me2 IP signal. Data are represented as mean ± s.e.m of 3-5 independent experiments. Groups were compared by One-Way ANOVA. * p<0.05, ** p<0.001, *** p<0.0001.

2.3.4 H3K4me2 editing induces profound transcriptomic changes consistent with loss of SMC lineage identity

Bulk RNAseq revealed profound changes in the transcriptomic profile of SMC expressing Myocd-LSD1 as compared to Myocd-LSD1^{NF} (**Figure 8A**). GO pathway analysis showed that H3K4me2 editing impaired pathways associated with contractility, vascular development and differentiation (**Figures 8B, Appendix Figure 5A, and 5B**). Down-regulated genes with loss of H3K4me2 enrichment (RNAseq/CUT&Tag seq comparison) were also associated with SMC

differentiation and contraction (**Figure 8C**). There was significant enrichment in SRF binding motifs in genes downregulated in Myocd-LSD1 SMC, providing further evidence of the specificity of H3K4me2 editing (**Appendix Figure 5C**).

We found remarkable differences in the transcriptomic profiles of Myocd-LSD1 SMC and SMC stimulated by PDGF-BB (**Figures 8D, 8E, 8F, and Appendix Figure 5E**). Interestingly, while both groups showed comparable levels of SMC contractile gene downregulation, H3K4me2 edited SMC displayed a selective downregulation of regulators of SMC differentiation and lineage determination (e.g., *Mef2c*, *Notch3*, *Gata6*, *Rbpms*) suggesting that H3K4me2 editing causes a loss of SMC lineage identity (**Figure 8G**). Interestingly, transient expression of Myocd-LSD1 in SMC only induced downregulation of myocardin-dependent contractile genes while expression of *Smtn* (myocardin-independent gene) and SMC master regulators (*Mef2c*, *Tet2*) was unchanged (**Figure 8H**). This discrepancy suggests that constitutive H3K4me2 editing in Myocd-LSD1 expressing SMC may induce secondary downregulation of a cohort of genes responsible for maintenance of SMC lineage identity. Finally, we treated Myocd-LSD1 SMC with all-trans retinoic acid (ATRA), which has been widely used to induce SMC differentiation from SMC precursors, embryonic stem cells or iPS cells²⁵³⁻²⁵⁶. ATRA-treatment induced a significant recovery of early contractile genes (*Acta2*, *Tagln*) and *Gata6* (**Figure 8I**). This recovery was associated with a gain in H3K4me2 enrichment on myocardin-regulated gene CArG box regions (**Figure 8J**).

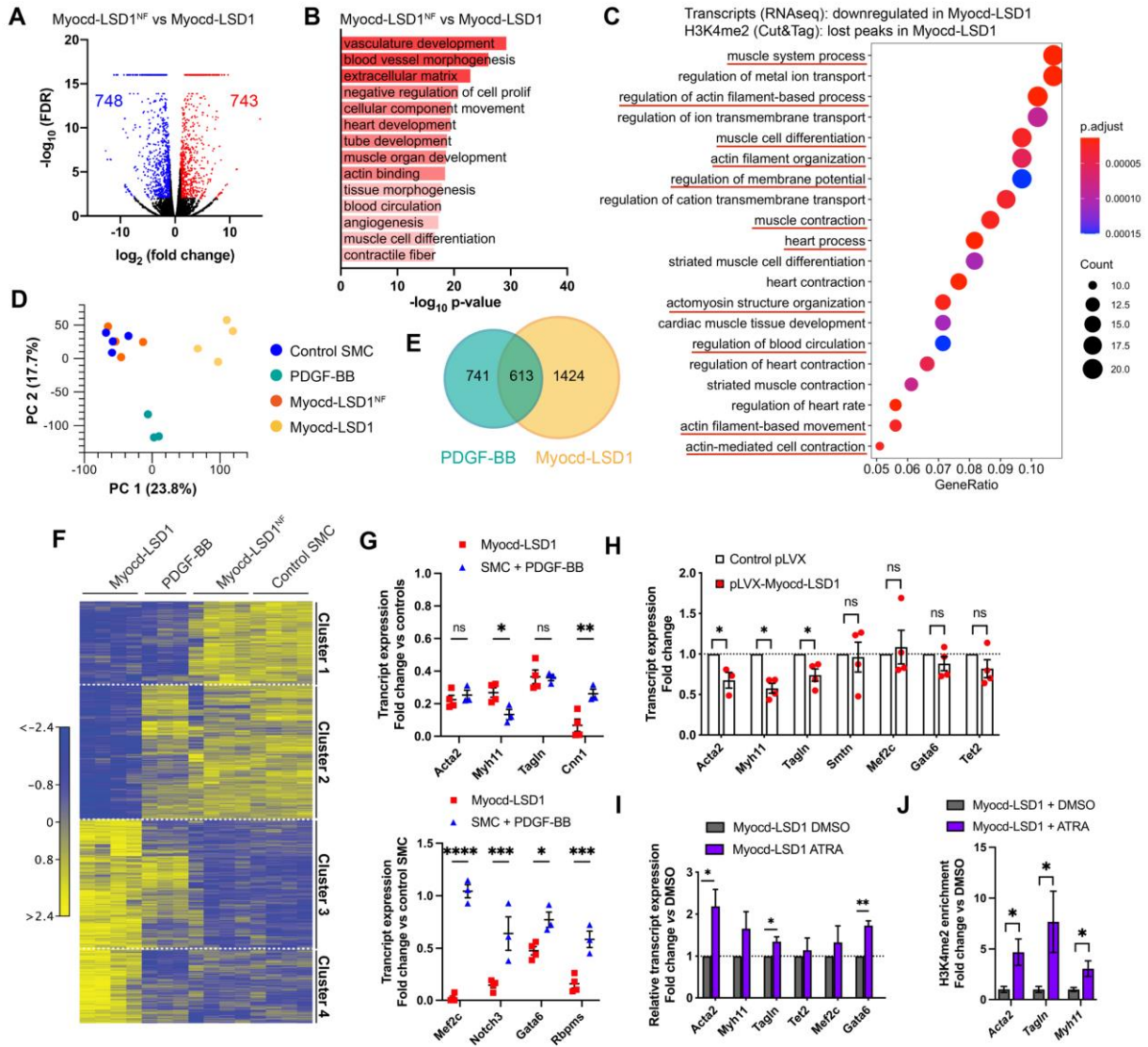


Figure 8 H3K4me2 editing is associated with a profound loss of SMC lineage identity.

Bulk RNAseq performed on control, Myocd-LSD1, Myocd-LSD1^{NF}, and PDGF-BB-treated SMC. **A.** Volcano plot representing genes differentially expressed in Myocd-LSD1 vs. Myocd-LSD1^{NF} SMC. **B.** GO Pathway analysis showing the most significantly downregulated pathways in Myocd-LSD1 vs. Myocd-LSD1^{NF} SMC. **C.** GO pathway analysis on intersected gene sets with transcript downregulation and H3K4me2 loss in Myocd-LSD1 SMC vs Myocd-LSD1^{NF} SMC. **D.** Principal component analysis. **E.** Venn diagram representing the overlap between differentially expressed genes in Myocd-LSD1 and PDGF-BB treated SMC. **F.** Heat map of differential transcript expression in Myocd-LSD1, PDGF-BB treated, Myocd-LSD1^{NF}, and control SMC. **G.** Expression levels of SMC contractile genes

(cluster 1, top graphs) and SMC master differentiation regulators (cluster 2, bottom graphs) in Myocd-LSD1 and PDGF-BB treated SMC. Expression normalized to the expression in pooled control and Myocd-LSD1^{NF} SMC. **H.** Normalized transcript expression in control SMC transiently transfected with Myocd-LSD1 or control plasmid. **I.** Transcript expression in Myocd-LSD1 SMC treated with vehicle or all-trans retinoic acid (ATRA). **J.** ChIP-qPCR of H3K4me2 on CARG box region of *Acta2*, *Tagln* and *Myh11* in Myocd-LSD1 SMC treated with vehicle or ATRA. Data are represented as mean \pm s.e.m of 3-4 independent biological replicates. Groups were compared by multiple Student t-test. * p<0.05, ** p<0.001, *** p<0.0001.

2.3.5 H3K4me2 editing exacerbates SMC phenotypic plasticity

Remarkably, genes with gain of H3K4me2 enrichment in Myocd-LSD1 were associated with stemness, developmental programs, and lineage specification and differentiation pathways (**Figure 9A**). This result was confirmed at the transcript level with increased expression of genes involved in multiple lineages differentiation (**Figures 9B** and **Appendix Figure 6A**). Interestingly, we found that H3K4me2 editing led to the upregulation of genes associated with atherosclerosis-related SMC plasticity and phenotypic modulation, including genes associated with synthetic SMC (*s100a4*, *fn1*), mesenchymal stem cells (*Eng*, *Nt5e*), phagocytic cells (*Lgals3*, *CD68*) and osteochondrogenic cells (*Runx2*, *Sox9*) (**Figures 9C**, **Appendix Figure 6B**). Surprisingly, genes associated with SMC transition to an atheroprotective fibrocyte state (*lum*, *tnfrsf11b*) were down-regulated in Myocd-LSD1 SMC (**Figure 9C**)²³¹. Notably, the increase in expression of plasticity markers was significantly higher in Myocd-LSD1 SMC as compared to PDGF-BB treated SMC, supporting again a deeper loss of SMC lineage identity induced by H3K4me2 editing (**Appendix Figure 6C**).

When exposed to cholesterol, Myocd-LSD1 SMC exhibited higher lipid uptake capacities and increased expression of phagocytosis markers compared with Myocd-LSD1^{NF} SMC (**Figures**

9D, Appendix Figure 6D, and 6E). We then performed lineage differentiation assays on Myocd-LSD1 and Myocd-LSD1^{NF} SMC by treatment with adipogenic and chondrogenic differentiation supplements. After 14 days of culture in adipogenic differentiation medium, 30% of Myocd-LSD1 SMC were positive for both AdipoRed (lipid droplets) and FABP4 (adipocyte marker) (**Figure 9E**). In contrast, the ability of Myocd-LSD1^{NF} SMC to express FABP4 was extremely limited. We also found that Myocd-LSD1 SMC cells formed chondrogenic structures and expressed Aggrecan (chondrogenesis marker) after 28 days in differentiation media (**Figure 9F**). Together, our data show that H3K4me2 is a key regulator of SMC lineage identity and restrains phenotypic plasticity.

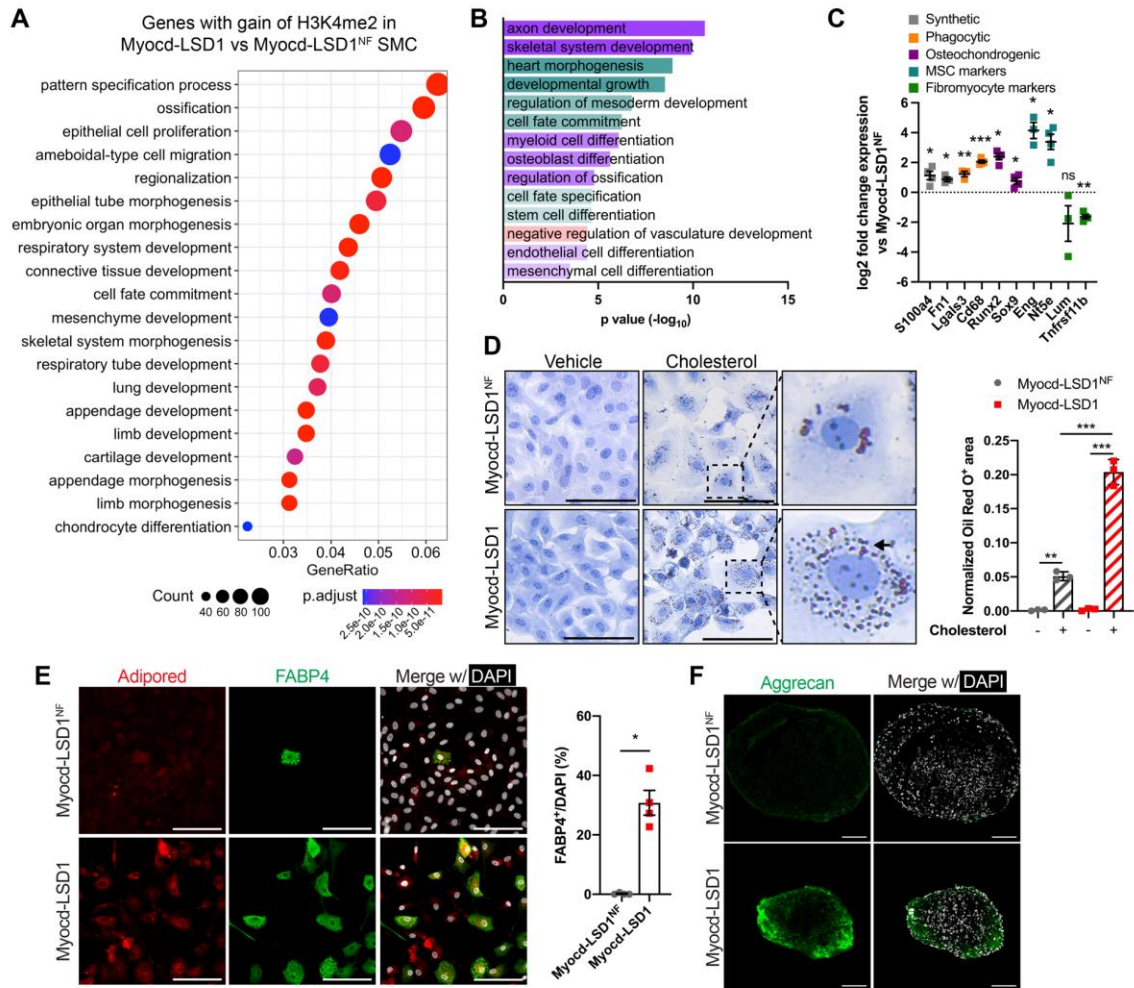


Figure 9 Loss of H3K4me2 on myocardin-regulated genes exacerbates SMC plasticity.

A. Top20 Gene Ontology pathways of genes with enhanced H3K4me2 enrichment in Myocd-LSD1 SMC compared with Myocd-LSD1^{NF} SMC. **B.** Significantly upregulated GO pathways related with lineage plasticity from RNAseq in Myocd-LSD1 vs Myocd-LSD1^{NF} SMC. **C.** Expression of markers of SMC phenotypic transitions in Myocd-LSD1 SMC. **D.** Oil Red O staining in Myocd-LSD1 and Myocd-LSD1^{NF} SMC treated with cholesterol (40 μ g/ml) or vehicle for 48h and quantification of Oil Red O⁺ area normalized to cellular area. Arrow: example of intracellular Oil Red O⁺ lipid vacuoles. Scale bar: 100 μ m. **E.** FABP4 and lipid droplets staining (left) and quantification of FABP4⁺ SMC (right) in Myocd-LSD1 and Myocd-LSD1^{NF} SMC cultured in adipogenic differentiation media. Scale bar: 100 μ m. **F.** Immunofluorescent staining with Aggrecan in SMC cultured in chondrogenic differentiation media. Scale bar: 100 μ m.

Data are represented as mean \pm s.e.m of 3-4 independent experiments. Groups were compared by One-Way ANOVA (D) and Student t-test (C, E). * $p < 0.05$, ** $p < 0.001$, *** $p < 0.0001$.

2.3.6 H3K4me2 editing impairs SMC participation in adaptive vascular remodeling

Based on the impact of H3K4me2 editing on SMC phenotype, we sought to investigate the functional consequences of alteration of H3K4me2 distribution on SMC participation in vascular remodeling. We combined local Myocd-LSD1 lentivirus delivery and unilateral ligation of the right carotid. Three weeks after injury, ligated vessels displayed high expression of Myocd-LSD1 constructs (**Appendix Figure 7A**). Surprisingly, a significant decrease in neointima formation in ligated carotids transduced with Myocd-LSD1 was observed (**Figures 10A and 10B**). SMC investment in the neointima was nearly abolished after Myocd-LSD1 delivery (**Figures 10C and 10D**). Mechanistically, we found that expression of Myocd-LSD1 in SMC induced loss of migration capacity in response to PDGF-BB (**Figures 10E and 10F**), despite unaltered PDGF- β receptor (PDGF β R) expression and PDGF β R-dependent downstream signaling cascade (**Appendix Figure 7B, 7C, and 7D**). Defective migration is rather due to disorganization of the SMC cytoskeleton network (including actin polymerization and Talin distribution) (**Figure 10G**). These results further demonstrate that H3K4me2 controls SMC contractility but also the intrinsic physiological properties of SMC adaptation in response to vascular injury.

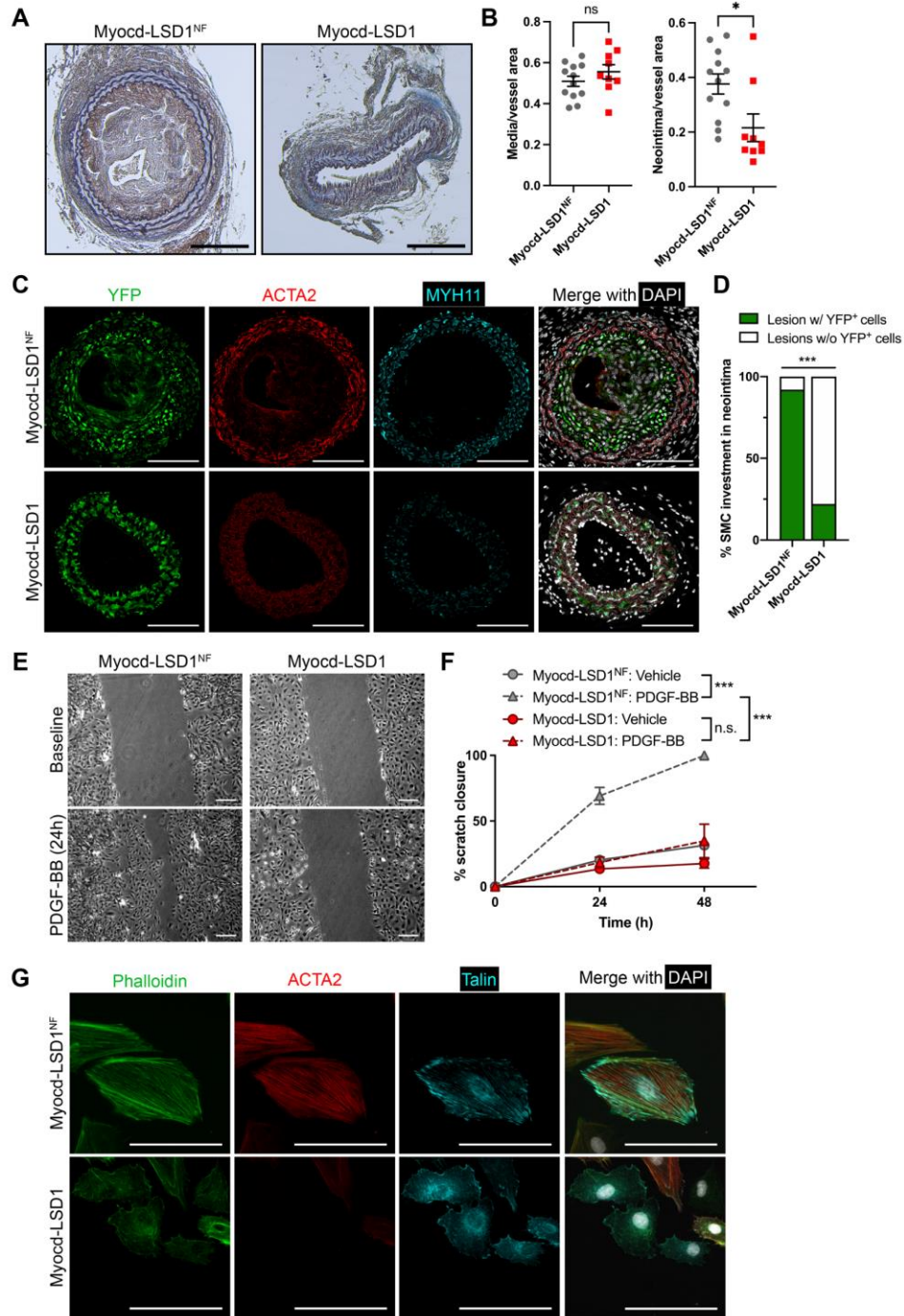


Figure 10 H3K4me2 editing inhibits SMC investment in the neointima after vascular injury.

A. Mason staining of ligated carotid cross sections. Scale bar = 100 μm . **B.** Morphometric analysis of neointima and media area in Myocd-LSD1 and Myocd-LSD1^{NF} infected carotids. N = 9-12 mice per group. **C.** Immunofluorescent staining for YFP (SMC-fate tracing), ACTA2, MYH11, and DAPI on cross-sections from ligated right carotids infected with Myocd-LSD1 or Myocd-LSD1^{NF}. Scale bar = 100 μm . **D.** Percentage of neointimal lesion populated by YFP⁺ SMC. N = 9-12 mice per group. **E.** Scratch wound assay on Myocd-LSD1^{NF} and Myocd-LSD1 SMC. Representative images at baseline or after 24h treatment with PDGF-BB (30 ng/ml). Scale bars: 100 μm . **F.** Quantification of SMC migration: percentage closure normalized to the wound area at baseline. **G.** Immunofluorescent staining of cytoskeleton components: F-actin (phalloidin), ACTA2, and Talin in Myocd-LSD1^{NF} and Myocd-LSD1 SMC. Scale bar: 50 μm . Data are represented as mean \pm s.e.m of 9-12 independent biological replicates. Groups were compared by unpaired Student t-test, Fisher's exact test, or Two-Way ANOVA. * p<0.05, ** p<0.001, *** p<0.0001.

2.3.7 H3K4me2/TET2 complex impairment leads to miR145 repression and loss of miR145-dependent cytoskeleton dynamics

Remarkably, the impaired participation of SMC in remodeling observed in Myocd-LSD1 transduced vessels is a feature shared with miR-145 deficient mice²⁵⁷. We found that miR-145 was markedly downregulated in Myocd-LSD1 SMC compared to Myocd-LSD1^{NF} and PDGF-BB treated counterparts (**Figures 11A** and **Appendix Figure 8A**) and the expression of miR-145 target genes involved in plasticity and migration inhibition was increased (**Figures 11B**, **Appendix Figure 8B**, and **8C**). GO analysis on upregulated miR-145 target genes showed enrichment in several pathways associated with negative regulation of cell motility (**Appendix Figure 8D**). The increased expression of migration inhibitory genes (*Srgap1*, *Ssh2*, *Sema3a*) was specifically observed in H3K4me2-edited SMC, but not in PDGF-BB treated SMC (**Figure 11C**).

The *miR145* locus contains a distal functional CArG box²⁵⁷. By analyzing ENCODE datasets, we found that the CArG region of the *miR145/miR143* cluster was enriched in H3K4me2

in human SMC, suggesting that these genes could be primary targets of Myocd-LSD1 (**Figure 11D**). In line with this hypothesis, a marked loss of H3K4me2 enrichment, TET2 recruitment and decreased 5hmC level were observed at the *miR145* CArG region in Myocd-LSD1 SMC (**Figures 11E, 11F, and Appendix Figure 8E**). Interestingly, we observed a dose-dependent rescue of PDGF-BB-dependent migration in Myocd-LSD1 SMC after miR-145 overexpression (**Figure 11G**). Meanwhile, higher expression of miR-145 inhibited migration, which can be due to the loss of expression of other key miR-145 targets like KLF4, a potent inducer of SMC migration ²⁵⁸. Together, these results provide evidence for the regulation of miR-145 expression by the H3K4me2/TET2 complex and that loss of the SMC-specific H3K4me2 signature leads to miR-145-dependent disorganization of cytoskeleton dynamics, explaining, at least in part, the defect in participation in vascular remodeling of H3K4me2 edited SMC.

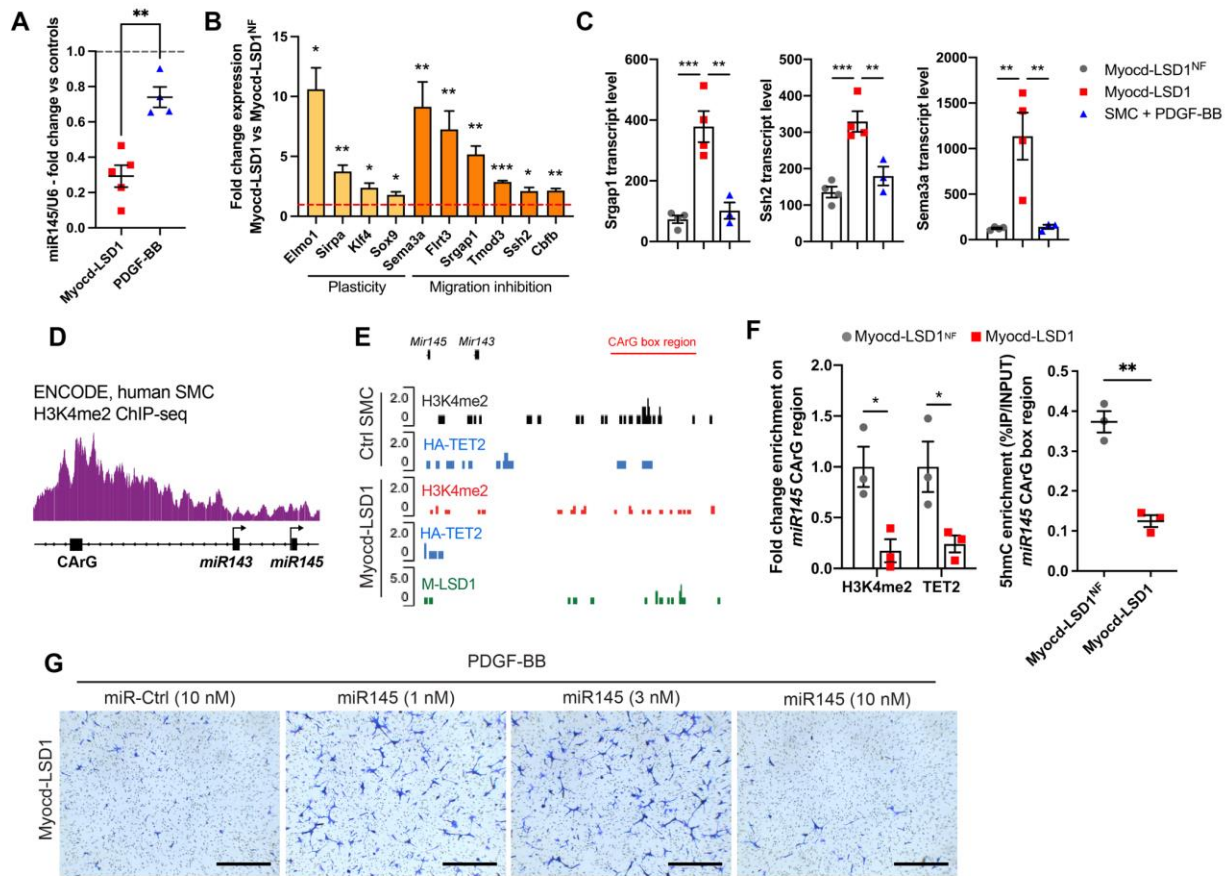


Figure 11 H3K4me2/TET2 complex impairment leads to miR145 repression and loss of miR145-dependent cytoskeleton dynamics.

A. miR145 expression in Myocd-LSD1 and PDGF-BB treated SMC (30 ng/ml, 24h). **B.** Expression of miR145 target genes associated with cell plasticity (yellow) and migration inhibition (orange) in Myocd-LSD1 SMC vs Myocd-LSD1^{NF} SMC. **C.** Transcript levels of Srgap1, Ssh2, and Sema3a in Myocd-LSD1^{NF}, Myocd-LSD1 SMC and SMC treated with PDGF-BB (normalized transcript counts). **D.** ChIPseq track showing H3K4me2 distribution on the *miR143/miR145* gene cluster in human SMC. Source: ENCODE Project. **E.** CUT&Tag sequencing tracks for H3K4me2, HA-TET2 and Myocd-LSD1 occupancy at the *miR143/miR145* gene in control and Myocd-LSD1 SMC. **F.** Enrichment of H3K4me2, TET2 and 5hmC level on *miR145* CARG region Myocd-LSD1^{NF} and Myocd-LSD1 SMC. **G.** Transwell assay using Myocd-LSD1 SMC transfected with miR-Control (10 nM) or miR-145 at different doses (1 nM, 3 nM, and 10 nM) for 24 hours. Scale bar = 0.5 mm. Data are represented as mean \pm s.e.m of 3-4 independent

biological replicates. Groups were compared by unpaired Student t-test or One-Way ANOVA. * $p < 0.05$, ** $p < 0.001$, *** $p < 0.0001$.

2.4 Discussion

It has been widely assumed that H3K4 methylation is a mechanism of gene activation based on the correlation between the distribution of H3K4 methylated residues and actively transcribed genes^{259,260}. However, our studies and others provide evidence contradicting this paradigm. H3K4me2 enrichment was also found on transcriptionally poised and inactive genes, suggesting that presence of H3K4me2 is not sufficient to induce gene activation^{114,261,262}. Moreover, H3K4me2 enrichment on the SMC gene repertoire is stably retained during SMC dedifferentiation and repression of these genomic loci *in vitro* and *in vivo*^{114,162,163}. The present functional studies support a model in which H3K4me2 serves as a lineage memory mechanism by priming lineage-specific genes for dynamic activation and ensuring appropriate gene re-expression after transient repression.

Our studies uncovered that H3K4me2 serves as a stable hub for selective recruitment of the methylcytosine dioxygenase TET2 on SMC gene repertoire. H3K4me2-mediated TET2 binding promotes activation of SMC pro-differentiation gene program via DNA demethylation and hydroxymethylation^{238,263,264}. We found a strong genome-wide co-distribution of TET2 and H3K4me2 and a marked alteration of TET2 genome occupancy after H3K4me2-editing. The property of H3K4me2 in regulating factor recruitment may be broader since H3K4me2 distribution closely overlaps with transcription factor binding regions²⁶⁵. TET2 recruitment may also be dependent on the cooperation with other factors. Indeed, studies have shown that TET2 also

interacts with transcription factors such as SNIP1²⁶⁶, TFCP2L1, KLF4, C/EBP α ²⁶⁷ and histone methylations, such as H3K36me2²⁶⁸ in other cell types. Whether these mechanisms play a role in TET2-mediated SMC differentiation will need to be empirically evaluated. H3K4me2 mediates TET2 recruitment on SMC contractile genes and *miR145*^{257,269,270}, highlighting the complexity and interdependency of several epigenetic mechanisms, namely, histone modifications, DNA methylation, and non-coding RNAs.

H3K4me2 appears as a key epigenetic mediator of SMC lineage identity maintenance. We hypothesize that this mechanism is required for retention of a transcriptional memory in SMC undergoing transient dedifferentiation and acts in concert with other mechanisms associated with this process²⁷¹. For example, the histone variant H2A.Z mediates the subnuclear localization of genes to confer memory of previous activation and promote reactivation²⁷². The establishment of lineage-specific DNA methylation patterns throughout the genome has also been implicated in cell differentiation and lineage commitment by determining the expression or repression of differentiation programs. Moreover, there is evidence that these methylated or demethylated DNA patterns are stably retained in adult cells and represent an epigenetic memory of the cell lineage origin²⁷³. It has been shown, for example, that MSCs from different tissues and different origins present distinct DNA methylation patterns while similarly expressing MSC markers such as CD106, CD146²⁷⁴. Our data showed that H3K4me2 editing led to a profound loss of lineage identity, not only characterized by the repression of the SMC contractile genes, but also by the redistribution of H3K4me2. Loss of H3K4me2 in Myocardin-regulated genes induces a gain of H3K4me2 on genes involved in embryonic development and differentiation programs associated with other lineages. This suggests that after “erasure” of the SMC lineage H3K4me2 signature, the cell regains poising and priming of other lineage-specific gene subsets for context-dependent *de*

novo lineage determination. This hypothesis is consistent with the increased plasticity and the remarkable ability of H3K4me2 edited SMC to transdifferentiate into other lineages upon adequate treatment.

Importantly, the upstream mechanisms responsible for the acquisition of the H3K4me2 signature during vascular development remain to be identified. Several histone methyltransferases are potential candidates for performing H3K4 di-methylation ²⁷⁵. In cardiomyocytes, the lysine methyltransferase, KMT2D, contributes to H3K4me2 appearance and is required for proper cardiac development ²⁴⁷. Yet, our understanding of H3K4me2 contribution during SMC differentiation and which histone modifiers “write” the H3K4me2 signature is remarkably limited. Our data obtained in adult SMC have also potential implications for cell reprogramming. Indeed, it raises the question of the persistence of H3K4me2 signature from the original cell type during induced pluripotent stem (iPS) cell reprogramming. Seminal studies have demonstrated that iPS cells retain, at least partially, the epigenetic memory of the original cell type and tissue ²⁷⁶. Conversely, one could wonder if reprogrammed iPS cells recapitulate stable epigenetic signatures of the desired somatic lineage. Further identification and functional characterization of stable lineage-specific epigenetic programming associated with targeted epigenome editing could increase cell reprogramming efficiency.

H3K4me2 signature on the SMC gene repertoire appears as a fundamental mechanism engraving SMC lineage identity and restraining SMC plasticity. Our unbiased transcriptional profiling revealed notable differences between SMC treated with PDGF-BB and SMC subjected to Myocd-LSD1-mediated chromatin editing. Moreover, H3K4me2 editing profoundly altered SMC participation in adaptive vascular remodeling *in vivo*. Interestingly, a recent study showed a similar lack of neointima formation in a model of wire-induced femoral artery injury in SMC-

specific TET2 deficient mice²⁷⁷. These findings motivate the reevaluation of central SMC biology paradigm. First, SMC phenotypic switching has classically been described as a dedifferentiation process due to the loss of expression of SMC contractile genes. However, our data and previous studies suggest that phenotypically modulated SMC (i.e., ACTA2⁻ and MYH11⁻) do not lose their H3K4me2 epigenetic signature, nor their lineage identity¹⁶². Second, our results demonstrate that the SMC ability to undergo reversible loss of contractility is a fundamental and epigenetically programmed property of SMC. SMC reversible phenotypic modulation in response to modifications of the environment is an evolutionary-conserved process necessary for the maintenance of vascular homeostasis. H3K4me2 plays a key role in allowing this reversible loss of contractility.

We anticipate that H3K4me2 programming biases SMC phenotype and behavior in chronic vascular diseases by promoting the re-expression of the contractile gene repertoire and limiting SMC plasticity. For example, in atherosclerosis, we and others have reported that the H3K4me2 signature on contractile gene promoters was retained during SMC phenotypic modulation, including dedifferentiated SMC (ACTA2⁻), and SMC expressing phagocytosis markers (LGALS3⁺, CD68⁺)^{162,163,165}. Interestingly, there is evidence that SMC-derived foam cells have defective and limited phagocytosis capacities compared with their myeloid-derived counterparts^{231,278}. There is a possibility that retention of SMC-lineage H3K4me2 programming restrains the full transition to a phagocytic macrophage-like cell. It remains to be determined how loss of the H3K4me2 signature, if occurring during development or progression of vascular diseases, would impact SMC fate and contribution to the disease. Epigenetic programming can be subject to alterations induced by various environmental influences relevant to cardiovascular disease pathogenesis, including metabolic disorders^{279,280} and aging^{281,282}. Further investigation of the persistence of H3K4me2

signature in the context of vascular disease and comorbidity (aging, obesity) would greatly enhance our understanding of SMC behavior and offer new strategies to restore SMC functions and modulate SMC phenotype and fate in these pathological contexts.

2.4.1 Limitations of the study

Although our approach consisting of utilizing myocardin as a recruitment system for the H3K4me2 demethylase is proven to be effective for the selective and coordinate editing of the SMC lineage related genes, the striking lack of reliable tools (e.g., antibodies) to study endogenous myocardin leads to a possible partial understanding of myocardin recruitment mechanisms and target genes²⁸³. Further analysis of Myocd-LSD1 and H3K4me2 CUT&Tag datasets could help identify new CArG-dependent or CArG-independent regulatory roles for Myocardin. Myocd-LSD1 potently induced the decrease in expression of a large cohort of SMC lineage-related genes, leading to loss of lineage identity and specialized functions. Interestingly, single mutations in some of these key genes have been associated with vascular diseases. For example, mutations in *ACTA2* or *MYH11* are associated with aortic dilation and SMC dysfunction^{284,285}. Although impossible with our experimental system, it would be interesting to determine the minimal and core H3K4me2-enriched genes necessary for maintenance of the lineage identity.

2.5 Acknowledgement

We thank the Center for Biologic Imaging (supported by NIH 1S10OD019973-01), at the University of Pittsburgh, the Health Sciences Sequencing Core at Children's Hospital of Pittsburgh,

the Health Sciences Library System at the University of Pittsburgh, and the Yale Cancer Center Sequencing facility at Yale University. We thank Dr. Q. Gan, J. Krasner, R. Tripathi, J. Krzemien, and Dr. A. Ostriker for their help. Schematics were created with Biorender.

2.6 Source of funding

This work is supported by the National Institute of Health R01HL146465 and the American Heart Association 15SDG25860021 grants to DG; the National Institute of Health R01 HL133864, R01 HL128304, R01 HL153532 and AHA Established Investigator Award to A.C.S; the National Institute of Health R01 HL142090-01, R01 HL146101 to K.A.M; and the National Institute of Health R01 HL136314 and R01 HL057353 to G.K.O.

2.7 Methods

2.7.1 Myocd-LSD1 cloning and expression

Myocardin-LSD1 (Myocd-LSD1) was generated by association of the full length human LSD1 cDNA (GenBank: NM_001363654.2) and a partial mouse Myocardin cDNA sequence (GenBank: NM_146386.3) encoding from amino acid 129 to 506. hLSD1 and mMyocd are linked by a 75 base pair linker containing a FLAG tag sequence (DYKDDDDK) and ensuring an unshifted open reading frame. The mMyocd sequence includes the SRF-binding domains, the CARG box/promoter recognition domains, and the nuclear localization signals to allow nuclear

localization and CARG/SRF specific recruitment. The cytoplasmic localization/actin binding domain, the dimerization domain, and the transactivation domain were excluded from the construct to avoid cytoplasmic sequestration and transcriptional activation through Myocd-LSD1.²⁴⁸ To control for potential H3K4me2 demethylation-independent effects of Myocd-LSD1 (e.g., steric hindrance, positive or negative dominant effects), we designed a catalytically inactive and non-functional Myocd-LSD1 (Myocd-LSD1^{NF}) by introducing a loss-of-function mutation, LSD1^{K661A}, which leads to an almost complete loss of LSD1 demethylase activity.²⁴⁹

For *in vitro* studies, male rat aortic SMC constitutively expressing Myocd-LSD1 or Myocd-LSD1^{NF} were generated by retroviral transduction. For *in vivo* studies, Myocd-LSD1 and Myocd-LSD1^{NF} were cloned into a lentiviral vector with a reporter system (pLVX-IRES-mCherry, Addgene: #68857) and packaged into lentivirus. Lentivirus titer was determined by Lenti-X qRT-PCR Titration Kit (Takara) following the manufacturer's protocol. Myocd-LSD1 and Myocd-LSD1^{NF} lentivirus were delivered in SMC-lineage tracing mice as detailed below.

2.7.2 Mice

The animal protocols including all listed mouse strains and procedures were reviewed and approved by the University of Pittsburgh Institutional Animal Care and Use Committee. Mice were housed and all experimental procedures were performed in an American Association for Accreditation of Laboratory Animal Care-accredited laboratory animal facility at University of Pittsburgh. All mice were housed in routinely sanitized cages at a controlled temperature and humidity condition with standard rodent chow and water supply. *Myh11-Cre*^{ERT2}²⁸⁶ and R26R-EYFP²⁸⁷ were crossed to obtain *Myh11-CreERT2-YFP* lineage tracing mice as previously described¹⁶². All strains are on a C57BL/6J background and mice were genotyped by PCR. Male

mice were exclusively used as experimental animals due to the location of the *Myh11*-Cre^{ERT2} transgene on the Y chromosome. At 6 weeks of age, male mice were injected daily with 1mg of tamoxifen in peanut oil (10 mg/mL). After 10 injections over the course of two weeks, mice recovered for one week to allow tamoxifen to be fully metabolized. Littermates received 10⁶⁻⁷ lentiviral particles encoding for Myocd-LSD1 or Myocd-LSD1^{NF} which were delivered unilaterally to the right carotid by application of Pluronic gel (20% Wt/Vol). Briefly, a 1 cm incision was made along the midline of the cervical region. The cranial bifurcation of the right carotid was exposed and separated from the surrounding fascia. Pluronic gel was applied directly to the right carotid, using retractors to keep the artery exposed while the gel solidified. A similar procedure was employed in association with permanent carotid ligation. In this case, the right carotid was ligated caudal to the bifurcation using 7-0 silk suture. Pluronic gel was then applied at the site of the ligation. 14- or 21-days following surgery, mice were euthanized by CO₂ asphyxiation and perfused with PBS and 4% paraformaldehyde (PFA) using a gravity perfusion system via the left ventricle. Left and right carotid arteries, starting at the cranial bifurcation, were excised and fixed overnight in 4% PFA at 4°C. Tissues were processed and embedded in paraffin vertically and serial 10 µm sections were collected from the cranial bifurcation or the ligation site.

2.7.3 Cell culture

Male rat aortic smooth muscle cells constitutively expressing Myocd-LSD1 or Myocd-LSD1^{NF} were generated by lentiviral transduction. Uninfected control SMC, Myocd-LSD1 and Myocd-LSD1^{NF} SMC were routinely cultured in growth medium (DMEM:F12, Gibco, 11320-033) supplemented with fetal bovine serum (10%, Corning, 35-015-CV), L-glutamine (1.6 mM, Gibco, 25030081), and penicillin-streptomycin (100 U/mL, Gibco, 15140122) at 37°C with 5% CO₂.

Before stimulation and for all baseline measurements, SMC were starved in a serum-free, insulin-free medium supplemented with L-glutamine (1.6 mM, Gibco, 25030081), L-ascorbic acid (0.2 mM, Sigma Aldrich, A4403), Apo-Transferrin (5 mg/ml, Sigma Aldrich, T5391) and Na Selenite (6.25 ng/ml, Sigma-Aldrich, S5261) for 48-72 hours. SMC from 3-5 constitutive passages were used to repeat independent experiments. Human recombinant PDGF-BB (Sigma Aldrich, SRP3138) was reconstituted in 10 mM acetic acid at 30 ng/ml for treatment. Rapamycin (Sigma Aldrich, R0395) was reconstituted in DMSO at 100 nM for treatment. SMC were treated with PDGF-BB or Rapamycin for 24h before being harvested for analysis. All-trans Retinoic Acid (Sigma, R2625) was reconstituted in DMSO at 1 mM for treatment. Transient overexpression of Myocd-LSD1 was performed by transfecting pLVX-Myocd-LSD1 with Lipofectamine 3000 Transfection Reagent (Invitrogen, L3000015). Myocardin and TET2 overexpression was achieved by transduction of Ad-m-Myocd-GFP (Vector Biolabs, ADV-265349) or Ad-HA-mTET2 (Applied Biological Materials, 465200540200) adenovirus with 10% polybrene infection/transfection reagent (Millipore, TR1003) at 2×10^6 to 10^7 IFU per well in 6-well-plates.

Human coronary artery smooth muscle cells (hCASMCs, Lonza) were propagated in M199 medium (Gibco, 11150-067) supplemented with 10% FBS, 100 U/ml each penicillin-streptomycin, 2.7 ng/ml rhEGF (Biolegend, 713008), and 2 ng/ml rhFGF (Biolegend, 713034). Cells were starved in 2% serum medium for 24 hours before treatment with 50 nM rapamycin for 48 hours to enhance SMC differentiation.

2.7.4 Chromatin Immunoprecipitation

Chromatin Immunoprecipitation (ChIP) was performed as previously described^{162,288}. In brief, passage-matched control, Myocd-LSD1, Myocd-LSD1^{NF} SMC were fixed with 1% PFA for

10 min at room temperature. Cells were sonicated with a Bioruptor Pico (Diagenode) to obtain chromatin fragments of 200-500 base pairs. Chromatin was incubated with Protein G Dynabeads (Invitrogen, 10004D) and one of the following antibodies: H3K4me2 (2 μ g; #07-030, Millipore), Flag (4 μ g; #F3165, Sigma Aldrich), H3K9me3 (2 μ g; ab176916, Abcam), H3K27me3 (2 μ g; 07-449, Sigma Aldrich), SRF (2 μ g; sc-13029, Santa Cruz), KLF4 (2 μ g; sc-20691, Santa Cruz), TET2 (5 μ g; ABE364, Millipore), H3ac (2 μ g; 06-599, Millipore), rabbit IgG (Abcam, ab171870) or mouse IgG (Abcam, ab37355). Genomic DNA was extracted with phenol-chloroform from immunoprecipitated (IP) and non-immunoprecipitated (INPUT) samples. Histone modification and protein enrichment was measured by qPCR using primer sets targeting CARG regions of the SMC contractile genes. Results were expressed as IP/INPUT. Primers used for ChIP-qPCR are listed in Key Resources Table.

2.7.5 CUT & Tag sequencing and data analysis

CUT&Tag seq²⁸⁹ was performed using CUT&Tag-ITTM Assay Kit (Active motif, 53160) following manufacturer's protocol. Briefly, 5×10^5 cells were harvested using ACCUTASETM cell detachment solution (Stem Cell Technologies, 07920). After binding with Concanavalin A beads, cells were incubated with primary antibody targeting H3K4me2 (Active motif, 39141), FLAG (Sigma Aldrich, F7425) or HA-tag (Abcam, ab9110) overnight at 4°C. Samples were then incubated with Guinea Pig anti-Rabbit Antibody, followed by CUT&Tag-IT Assembled pA-Tn5 Transposomes. After tagmentation in tagmentation buffer at 37°C for 1 hour, released DNA was extracted by DNA purification column for library preparation and SPRI Beads clean-up. Paired-

end sequencing was performed with illumina MiSeq (MS v2 50 cycle kit 12-15M reads) at Health Sciences Sequencing Core at UPMC Children's Hospital of Pittsburgh.

Paired-end raw reads were aligned to Rn6 using Bowtie2 ²⁹⁰. Tracks were generated by deepTools2 Bamcoverage ²⁹¹ with normalized counts as bins per million (BPM) and visualized with IGV ²⁹². Peaks were called using MACS2 ²⁹³ callpeak with cut off FDR (q-value) at 0.05. Global heatmap was produced with deepTools2 ²⁹¹. Peaks were annotated by CHIPseeker with rn6.ncbiRefSeq as the annotation source ²⁹⁴. Differential binding analysis of H3K4m2 enrichment was performed by DiffBind with significant threshold at FDR<0.05 ²⁹⁵. Geno-ontology analysis for annotated peaks were performed by ClusterProfiler ²⁹⁶. Reduced H3K4me2 peaks in Myocd-LSD1 SMC was compared with published SRF ChIPseq dataset in mouse vascular SMC (GSM3069844) ²⁹⁷. Bioinformatic analysis was performed on Galaxy platform ²⁹⁸ and data visualization was performed in R.

2.7.6 Methylated/Hydroxymethylated DNA Immunoprecipitation (MeDIP/hMeDIP)

MeDIP/hMeDIP was performed using MeDIP kit (Diagenode, C02010010) and hMeDIP kit (Diagenode, C02010031) following manufacturer's protocol. Briefly, genomic DNA was extracted from control, Myocd-LSD1 and Myocd-LSD1^{NF} SMC starved in serum-free medium for 48 hours. DNA was sheared into fragment around 400 bp on Bioruptor Pico (Diagenode) prior to immunoprecipitation. 10% - 20% of sheared DNA was used as the INPUT control. Hydroxymethylated DNA or methylated DNA was captured by 5-hmC monoclonal antibody (Diagenode, C15200200) or anti-5mC antibody (Diagenode, MAb-081-100) with Protein G-coated magnetic beads at 4 °C overnight respectively. Captured DNA was isolated with DNA isolation buffer supplemented with proteinase K (Diagenode). 5hmC/5mC enrichment levels were

determined by qRT-PCR following manufacturer's protocol. Primers used for MeDIP/hMeDIP-qPCR are listed in Key Resources Table.

2.7.7 hMeDIP Sequencing and Data Processing

Genomic DNA was isolated from human coronary SMC. hMeDIP was performed as described previously²³⁸. Briefly, DNA with 5-hmC modification was immunoprecipitated with the hydroxymethylated DNA IP kit (Diagenode, C02010031) following manufacturer's instructions. Precipitated genomic DNA was sonicated to 200 – 500 bp using the Covaris sonicator (Covaris). 1 µg of fragmented genomic DNA was immunoprecipitated with a 5-hmC monoclonal antibody (Diagenode, C15200200) provided in hMeDIP kit. The DNA-antibody mixture was then incubated with magnetic beads overnight at 4°C, washed and DNA purified using purification kit (Qiagen, 69504). The purified DNA was adapter ligated using NEBNext DNA Library Prep Master Mix Set for Illumina 6040 (New England Biolabs) and NEBNext Multiplex Oligos for Illumina (Index Primers Set 1) E7335 (New England Biolabs). Each library was layered on one of the eight lanes of the Illumina flow cell at appropriate concentration and bridge amplified to get around 180 million raw reads. The DNA reads on the flow cell were then sequenced on HiSeq 2000 using appropriate base pair sequencing recipe. The quality of the sequence and its alignment to reference genome was carried out by the Illumina supported Consensus Assessment of Sequence and Variation (CASAVA) software program. For sequencing data analysis, raw reads were aligned to hg38 using Bowtie2²⁹⁰. Peaks were called using MACS2²⁹³ callpeak with cut off FDR (q-value) at 0.05. Peaks were annotated by ChIPseeker with hg38.ncbiRefSeq as the annotation source²⁹⁴. Annotated peaks were compared to H3K4me1 (ENCSR130IMV_2), H3K4me2

(ENCSR783AXV_2) and H3K4me3 (ENCSR515PKY_2) enriched peaked derived from ENCODE project ²⁹⁹. Bioinformatic analysis was performed on Galaxy platform ²⁹⁸.

2.7.8 Real-time Quantitative PCR (RT-qPCR)

Passage-matched control, Myocd-LSD1, Myocd-LSD1^{NF} SMC were collected and total RNA was extracted by TRIzol Reagent (Invitrogen, 15596026) according to manufacturer's protocol. Total RNA was quantified by Qubit RNA Broad Range Assay kit (Invitrogen, Q10210). cDNA was synthesized from 1 µg of RNA using iScript cDNA Synthesis Kit (Bio-Rad, 1708891) and real-time quantitative PCR was performed with PowerUpTM SYBRTM Green Master Mix (Applied Biosystems, A25742) using CFX Connect Realtime System (Bio-Rad, 1855201). mRNA levels of target genes were normalized to 18s/Gapdh expression. Primers used for qPCR are listed in Key Resources Table.

2.7.9 RNA extraction from FFPE sections

Tissue was scraped from 5 µm thick FFPE tissue slides and deparaffinized with Xylene solution in 1.5 ml tubes, followed by a 100% EtOH wash. Protein contamination was removed by incubation with Proteinase K and genomic DNA was removed using DNase I (Qiagen). The remaining pellet was in 100% EtOH and RNA was isolated with RNeasy FFPE Kit (Qiagen, 73504) following manufacturer's instructions.

2.7.10 RNA-sequencing and Data Analysis

Total RNA was extracted, and column purified from control SMC (n = 4), Myocd-LSD1 SMC (n = 4), Myocd-LSD1^{NF} SMC (n = 4), and SMCs treated with PDGF-BB (30 ng/ml, Sigma Aldrich, SRP3138) for 24 hours (n = 3) using RNeasy Mini Kit (Qiagen, 74104) following manufacturer's protocol. Genomic DNA was removed using DNase I (Qiagen). RNA quality control, library preparation and sequencing were performed by Health Sciences Sequencing Core at UPMC Children's Hospital of Pittsburgh. Briefly, RNA quality was checked with Agilent RNA Screen Tape Assay Tape Station System. RNA library was prepared by TruSeq Stranded mRNA (PolyA+) according to manufacturer's protocol. Libraries were sequenced with illumina NextSeq High Output 150 cycle kit (2 x 75 bp) with reading depth of 20 million reads per sample. The 75 bp paired-end reads were mapped to Rattus Norvegicus reference genome and gene ID were mapped to Rattus Norvegicus ensembl_v91 using default setting by CLC Genomic Workbench (Qiagen). All mapped reads were normalized by Trimmed Mean of M values (TMM normalization) for differential gene expression analysis in CLC Genomic Workbench. Principle Component Analysis (PCA), volcano plots and heatmaps were created by CLC Genomic Workbench at default setting. Global heatmap was generated with statistic parameters as Euclidean distance measure and complete linkage cluster. Cutoff value for data filtration is minimum fold-change of 1.2. Venn Diagram of differentially expressed genes was plotted with cutoff value at minimum fold-change of 1.5. Corrected FDR p-value < 0.05 is considered statistically significant. Pathway enrichment analysis was performed using the Biogroups app from Correlation Engine (Illumina) clustering the different biosets taking into account the direction of each gene³⁰⁰. Gene Ontology (GO)^{301,302}, and the microRNA target database Targetscan³⁰³ were used to analyze the up-regulated and down-regulated genes separately. P value ≤ 0.05 was considered as statistical significance.

2.7.11 MicroRNA Isolation and Quantification

microRNA-enriched RNA was isolated using the miRNeasy Mini Kit (Qiagen, 217004) based on Qizol/Chloroform extraction³⁰⁴. Reverse transcription of 100 ng RNA was performed using TaqMan™ MicroRNA Reverse Transcription Kit (Applied Biosystems, 4366596) and specific microRNA RT primers according to the manufacturer's instructions. qPCR was performed using specific microRNA TaqMan primers (miR-145 assay ID: 002278; U6 assay ID: 001973, Applied Biosystems)³⁰⁵. The relative quantification of microRNA expression was determined using the $2^{-\Delta\Delta C_t}$ method, obtaining the fold changes in gene expression normalized to the internal control small nuclear RNA U6. Primers used for qPCR are listed in Key Resources Table.

2.7.12 MicroRNA Transfection

SMC was seeded at 1.5×10^5 cells per well in routine growth medium into 6-well plates. When cells reached 70-80% confluency, miR-145-5p mimic (ThermoFisher, mirVana, MC11480) or the negative control mimic (ThermoFisher, miRvana, 4464058) were prepared in designated concentration and transfected into cells using Lipofectamine RNAiMax Reagent (ThermoFisher, 13778075) according to manufacturer's instructions.

2.7.13 Western Blot

Total proteins were extracted using CHAPS buffer (1% CHAPS hydrate, 150 mM NaCl, 25 mM HEPES Buffer). Extracts were separated by electrophoresis on NuPAGE 4-12% Bis-Tris Gels (Invitrogen, NP0321PK2) or 3-8% Tris-Acetate Gels (Invitrogen, EA0375PK2), followed by

transfer onto 0.45 μm Nitrocellulose Membranes (Bio-Rad, 1620115). Histone proteins were extracted by Histone Extraction Kit (Abcam, ab113476), separated on NuPAGE 4-12% Bis-Tris Gels (Invitrogen, NP0321PK2) and transferred on 0.2 μm Nitrocellulose Membranes (Thermo Scientific, 77012). Membranes were incubated with antibodies specific to ACTA2 (Sigma A2547), MYH11 (Kamiya Biomedical Company KM3669), TAGLN (Abcam ab14106), GADPH (Abcam ab8245/ab9485), unmodified H3 (Abcam ab1791), H3K4me1 (Millipore, 07-436), H3K4me2 (clone CMA303, Millipore 05-1338), H3K9me3 (Abcam ab176916), p-Akt-S473 (Cell Signaling Technology 4060), AKT1/2 (Santa Cruz sc8312). IRDye® anti-rabbit IgG secondary antibody (LI-COR, RRID AB_621843) or anti-mouse IgG secondary antibody (LI-COR, RRID AB_10953628) were used for immune-blotting. Membranes were imaged on the LI-COR Odyssey CLx imaging system.

2.7.14 Ex-vivo Myography

Thoracodorsal artery (TDA) from C57BL/6J mice were excised after euthanasia and perfusion with PBS. TDA were cleaned of fat, cut into 2 mm rings and incubated in supplemented smooth muscle cell media (Lonza) containing 10^6 lentiviral particles encoding for Myocd-LSD1 or Myocd-LSD1^{NF}. Following 48 hours of incubation, two 25 μm wires were passed through the lumen of the rings and placed on a small vessel myograph (DMT 620M) filled with physiological salt solution (PSS) containing (in mM): NaCl 119, KCl 4.7, MgSO₄ 1.17, KH₂PO₄ 1.18, D-glucose 5.5, NaHCO₃ 25, EDTA 0.027, CaCl₂ 2.5, pH 7.4 when bubbled with 95% O₂ 5% CO₂ at 37°C. Following a 30 min rest, vessels were stretched to an internal diameter equivalent to 80 mm Hg. Vessels were constricted by the addition of 60 mM potassium solution (KPSS) for 5 min

2.7.15 Immunofluorescent Staining

Tissues were embedded vertically and serial 10 μm sections were collected beginning at the ligation site. For immunofluorescent staining, sections at 180 μm from the ligation site were selected. Following deparaffinization, antigen retrieval was performed (Vector Laboratories H-3300). Staining was performed to evaluate gene expression in cells using primary antibodies for GFP (Abcam ab6673 1:250), MYH11 (Kamiya Biomedical Company MC-352 1:250, Abcam ab683 1:250), Ki67 (Abcam ab15580), cleaved Caspase 3 (Cell Signaling Technology 9661), FLAG tag (Cell Signaling Technology 14793s), mCherry (Abcam ab167453) or IgG as a control. Secondary antibodies included donkey anti-goat 647 (Life Technologies A21447) and donkey anti-rat 555 (Abcam ab150154). Along with the secondary antibodies, sections were also stained for ACTA2 (Sigma-Aldrich F3777 1:500) and DAPI (1:1000). Slides were mounted using Prolong Gold Antifade Reagent (Fisher P36930). For immunofluorescent staining on cultured cells, cells were fixed with 4% paraformaldehyde (Electron Microscopy Sciences) and permeabilized with 0.5% Triton-X-100 (Sigma). Smooth muscle α -actin was stained by FITC-conjugated ACTA2 antibody (Sigma F3777). For cytoskeleton dynamic studies, SMC were transduced with Talin-GFP (Cell Light, Invitrogen, C10611) for 24h, and stained with phalloidin (conjugated with Alexa-647; A22287, Invitrogen) and ACTA2 (conjugated with Cy3; C6198, Sigma Aldrich).

Images were acquired on a fluorescent microscope (Leica, DMI8) using the Ocular Advanced Scientific Camera Control software (Digital Optics Limited) or Nikon A1 Confocal microscope using NIS-Elements software (Nikon). Image processing was performed using ImageJ and Image Pro Premier (Media Cybernetics).

2.7.16 Collagen Contraction Assay

Control, Myocd-LSD1, and Myocd-LSD1^{NF} SMC were resuspended in a 10% FBS F12:DMEM media at the density 5×10^5 cells/mL after starvation in serum-free, insulin-free media for 48 to 72 hours. The cell suspension was incorporated in a collagen solution [bovine collagen I solution (PurCol®, Advanced Biomatrix, #5005), 10 mM NaOH, 1X PBS] and the cell-collagen solution was deposited on non-treated tissue culture 12-well plates. Plates were incubated at 37°C for 2 to 3 hours to allow gelation. Then, gels were immersed in 10% FBS culture medium and lifted from the bottom of the plate. Gel images were acquired immediately (baseline) and every 24 hours under a dissection microscope. Gel diameter and area were calculated using Image Pro Premier software. Gels were stained with ACTA2-FITC and DAPI (overnight incubation) after Triton-X-100 permeabilization and blocking in 5% BSA 10% horse serum PBS. Cell density was evaluated by counting the number of DAPI⁺ cells in 3 individual fields/gel and normalized to the field area (cells/mm²). Estimation of the cell number per gel was done as follow: number of cells = Area x Cell density.

2.7.17 Proximity Ligation Assay

Proximity Ligation Assay (PLA) was performed using Duolink In Situ PLA reagents according to the manufacturer's instructions (Sigma Aldrich). Cultured rat SMC were fixed after treatment with PDGF-BB, rapamycin, or control vehicle with 4% PFA for 15 min and permeabilized with 0.25% Triton X-100 PBS for 15 min at room temperature. Aorta cryosections were post-fixed with pre-cooled acetone for 10 min. The same protocol was then used for cultured cells and cryosections. Incubation with antibodies against H3K4me2 (clone CMA303, Millipore,

05-1338) and TET2 (Abcam, ab124297) was done overnight at 4°C. Cells and sections were incubated with Duolink® *In Situ* PLA Probe anti-rabbit PLUS (Sigma Aldrich, DUO92002) and anti-mouse MINUS (Sigma Aldrich, DUO92004) secondary antibodies, followed by ligation and amplification with Duolink® *In Situ* Detection reagents Orange (555nm) (Sigma Aldrich, DUO92007). Finally, staining with ACTA2-FITC antibody (4.4 µg/ml, Clone 1A4, Sigma Aldrich, F3777) was performed on cryosection. Slides were mounted using Duolink® *In Situ* mounting medium with DAPI (Sigma Aldrich, DUO82040). Images were acquired on a fluorescent microscope (Leica, DMI8) using the Ocular Advanced Scientific Camera Control software (Digital Optics Limited). Image processing and PLA dot quantification was performed using ImageJ.

2.7.18 Peptide Binding Assay

HA-tagged mTET2 was overexpressed in 293T cells by adenoviral transduction. Nuclear proteins were extracted from transduced 293T cells using NE-PER Nuclear and Cytoplasmic Extraction Reagents (Thermo Scientific, 78833) following manufacturer's instructions. 200 µg of nuclear protein extract from 293T cells overexpressing HA-tagged mTET2 was incubated with 20 µg of synthetic biotinylated H3K4me1 (Active Motif, 81040), H3K4me2 (Active Motif, 81041) and H3K4me3 peptide (Active motif, 81042) in binding buffer (150 mM NaCl, 50 mM HEPES, 0.1% Tween, 10% Glycerol, protease inhibitor cocktail, 1 mM PMSF) at least 4 hours at 4°C. 7 µg of rabbit anti-HA antibody (Abcam, ab91110) and anti-Biotin antibody (Abcam, ab53494) was used to Immunoprecipitate HA-TET2 or Biotinylated H3K4me2 peptide respectively in presence of Dynabeads Protein G (Invitrogen, 10004D) overnight at 4°. The immunoprecipitation complex was washed 3 times with binding buffer. After discarding Dynabeads, immunoprecipitated or

INPUT control biotinylated histone peptides were run on 4-12% Bis-Tris Gel (NuPAGE, Invitrogen, NP0321PK2) and followed by Western Blotting with IRDye 800CW Streptavidin (LI-COR, 926-32230). Immunoprecipitated or INPUT control HA-tagged Tet2 were run on 3-8% Tris-Acetate Gel (NuPAGE, Invitrogen, EA0375PK2) and followed by Western Blotting with Conjugated secondary antibodies (Li-COR). One-twelves the amount of immunoprecipitation was run in parallel as the INPUT control and 7 μ g of rabbit IgG was used as negative control for immunoprecipitation. Immunoblotting was imaged by the LI-COR Odyssey CLx imaging system.

2.7.19 Plasticity Assays

SMC were loaded with Cholesterol–methyl- β -cyclodextrin (Sigma Aldrich, C4555) for 24 to 72h as previously described^{163,306}. Cholesterol was used at 20, 40, or 80 μ g/ml. After cholesterol loading, SMC were either harvested for RT-qPCR analysis as described above or stained for lipid uptake with Oil Red O staining kit (Sigma Aldrich, MAK194), following manufacturer's instructions. Oil Red O staining was quantified using Image Pro Premier. SMC phenotypic plasticity was characterized by Rat Mesenchymal Stem Cell Functional Identification Kit (R&D Systems, SC020) following manufacture's protocol. Briefly, for adipogenic differentiation assay, control, Myocd-LSD1, and Myocd-LSD1^{NF} SMC were plated on 6-well-plates and 2-well chamber slides and cultured until confluency in F12:DMEM containing 10% FBS. Culture media was then replaced with Adipogenic Differentiation Media (α MEM, 10% FBS, adipogenic supplement, R&D Systems) and changed every 4 days for 2 weeks. Cells were incubated with AdipoRed Assay (Lonza, PT-7009) and immunofluorescent stained for mFABP4 (R&D Systems) following manufactures' protocols. For chondrogenic differentiation assay, 10⁶ Myocd-LSD1 and Myocd-LSD1^{NF} SMC were transferred and centrifuged down in 15 ml Falcon tubes to form cell pellets.

Chondrogenic differentiation media (DMEM/F12, ITS supplement, chondrogenic supplement, R&D Systems) were used and replaced every 3 days for 28 days without disturbing cell pellets. Cell pellets were then harvested and immunofluorescent stained for hAggrecan (R&D Systems) following manufactures' protocol. Images were acquired by Ocular Advanced Scientific Camera Control software (Digital Optics Limited) on a fluorescent microscope (Leica, DMI8). Cell counting was performed on acquired images using ImageJ.

2.7.20 Cell Viability Assay

Uninfected control, Myocd-LSD1, and Myocd-LSD1NF SMC were seeded in a 96-well-plate at a confluency of 1000 cells/well and were cultured in growth medium (DMEM:F12, Gibco) supplemented with fetal bovine serum (10%, Corning), L-glutamine (1.6 mM, Gibco), and penicillin-streptomycin (100 U/mL, Gibco). Cell viability was assessed by measuring ATP content at 24, 48 and 72 hours by using the Cell Titer-Glo luminescent cell viability assay following manufacture's recommendations (Promega, G7570). Luminescence measurements were performed in a Synergy-HTX multi-mode reader (Biotek).

2.7.21 Transwell Assay

Myocd-LSD1 SMC were seeded (8×10^5 cells/ml, 150ul) with serum-free insulin-free media in 8 μ m pore size polycarbonate transwell inserts (Corning, 3422). Serum-free insulin-free media supplemented with PDGF-BB (Sigma-Aldrich, SRP3138) was added to the lower compartment in a final concentration of 30 ng/ml as the chemo-attractant. After 24 hours incubation, cells were fixed with 4% PFA (Electron Microscopy Science, 15710) and stained with

0.1% crystal violet (Sigma-Aldrich, V5265). Cells on the upper compartment were carefully removed by a cotton swab. The membrane was excised and mounted onto a glass slide with Prolong Gold Mounting Media (ThermoFisher, P10144). Images were taken by microscope (Leica DM500) with the Leica LAS EZ software and processed using ImageJ software.

2.7.22 Luciferase Assay

SMCs were seeded at 1.5×10^5 cells per well in growth medium into 6-well plates and transfected at 70-80% confluency, with control pGL3, pGL3-*Acta2-CAR^{WT}* (-2.6/+2.8kb with intact CARG boxes), pGL3-*Acta2-promoCAR^{Mut}* (-2.6/+2.8kb with mutated CARG boxes within the promoter region), and pGL3-*Acta2-promo+intCAR^{Mut}* (-2.6/+2.8kb with mutated CARG boxes within the promoter and the first intron region)³⁰⁷. After 24 hours post transfection, SMCs were cultured in serum-free media for 24h. Cells were collected and luciferase activity was quantified using Firefly Luciferase Assay System (Promega, E1500) according to manufacturer's instructions. The luciferase signal results were normalized to total protein level.

2.7.23 Quantification and Statistical Analysis

All data are presented as the mean \pm SEM. *In vitro* experiments were repeated independently at least 3 times with duplicated technical repeats. One single data symbol represented the mean value of technical repeats for one independent experiment. For *in vivo* experiments, 4 to 12 mouse littermates were used for each group. All statistics were performed using GraphPad Prism 8. Two-tailed unpaired Student's t-tests with a confidence level of 95% were used to compare two groups with continuous variables with normal distribution and equal

variances tested by Kolmogorov-Smirnov test. Two-tailed unpaired Student's t-tests followed by a Welch's correction with the confidence level of 95% were performed if two groups have unequal variances. Two-tailed unpaired Mann-Whitney U-tests with the confidence level of 95% were used if variables were non-normally distributed. For comparison between multiple groups with a single factor or two factors, we used one-way or two-way ANOVA, respectively. For categorial data, we used two-sided Fisher's exact test. $P \leq 0.05$ was considered as statistically significant.

3.0 H3K4me2 regulates perivascular cell participation in microvascular remodeling in mouse hindlimb ischemia model

Mingjun Liu^{1,2}, Maryam Alanjawi^{1,6}, Lee L Ohayon², Cristina Espinosa-Diez¹, Jianxin Wei¹, Partha Dutta^{2,5}, Adam C. Straub^{1,3,4}, Luke Brewster⁷, Delphine Gomez^{1,2}

¹ Pittsburgh Heart, Lung, Blood, and Vascular Medicine Institute, University of Pittsburgh;
Pittsburgh, PA, USA

² Division of Cardiology, Department of Medicine, University of Pittsburgh; Pittsburgh, PA,
USA

³ Department of Pharmacology & Chemical Biology, University of Pittsburgh School of
Medicine; Pittsburgh, PA, USA

⁴ Center for Microvascular Research, University of Pittsburgh School of Medicine; Pittsburgh,
PA, USA

⁵ Department of Immunology, University of Pittsburgh School of Medicine, Pittsburgh, PA, USA

⁶ Dietrich School of Arts & Sciences, University of Pittsburgh; Pittsburgh, PA, USA

⁷ Division of Vascular Surgery, Department of Surgery, Emory University School of Medicine;
Atlanta, GA, USA

3.1 Summary

Peripheral artery disease (PAD), caused by occlusion of arteries in lower extremities, affects millions of patients worldwide. Inefficient compensatory microvascular remodeling exacerbates PAD complications, including claudication and amputation, due to an insufficient supply of blood, nutrition, and oxygen. Molecular mechanisms associated with defective microvascular remodeling and improper SMC-mediated arteriogenesis and perivascular coverage are not fully understood. We previously identified an SMC-specific epigenetic program consisting of the enrichment of H3K4 di-methylation (H3K4me2) on the SMC gene repertoire, which is required for SMC-lineage identity, contractility, and participation in vascular remodeling in large vessels. Yet, the role of H3K4me2 in regulating SMC-Pericytes (SMC-P)-mediated microvascular remodeling associated with hindlimb ischemia has not been investigated. Using a newly generated mouse model allowing for simultaneous SMC-P fate mapping and expression of Myocd-LSD1 for selective H3K4me2 demethylation on the SMC-related genes, we observed that H3K4me2 ablation impaired blood perfusion recovery after femoral artery ligation/excision-induced hindlimb ischemia. The defect in perfusion was associated with a loss of SMC-P coverage in injured limbs. Co-culture assays revealed that H3K4me2 ablation in SMC led to reduction of endothelial cell (EC)-mediated tube formation and altered SMC/EC interaction, as well as expansion disadvantage compared to control SMC. Mechanistically, the Notch signaling pathway, essential for effective SMC-EC interactions, was defective in H3K4me2 edited SMC. Importantly, we observed a reduction of H3K4me2 levels in perivascular cells in gastrocnemius muscle tissues from PAD patients. In conclusion, the SMC-specific H3K4me2 program regulates SMC-P participation in microvascular remodeling and interaction with endothelial cells, possibly via Notch signaling, in the murine hindlimb ischemia model.

3.2 Introduction

Lower extremity peripheral artery disease (PAD) is a prevalent disease affecting over 230 million people worldwide.³⁰⁸ The primary cause of PAD is an obstruction from the aortoiliac segments to the pedal arteries in the lower extremity due to the development and expansion of atherosclerotic plaques.³⁰⁸ Due to the limited blood supply caused by the arterial occlusion and a lack of compensatory neovascularization, late-stage PAD patients can develop severe clinical complications, such as walking disability, pain, ischemic ulceration, gangrene, and patients may eventually require amputation.³⁰⁹ Unfortunately, no specific therapeutic strategy has been proven effective in slowing, stopping, or reversing PAD progression besides preventive therapies that lower PAD risk factors or surgical revascularization, which showed limited long-term clinical benefits.^{308,310} PAD progression is commonly associated with inadequate compensatory microvascular remodeling, a protective mechanism aiming to bypass artery occlusion and restore blood supply in the lower extremity. Efforts to improve microvascular remodeling by stimulating endothelial cell-mediated angiogenesis with pro-angiogenesis factors, such as vascular endothelial growth factor (VEGF) or fibroblast growth factor (FGF), failed to improve clinical outcomes.³¹¹ One potential reason for the lack of clinical benefits from pro-angiogenic agents is the formation of unstable, leaky neo-vessels without proper maturation and coverage by perivascular cells, including smooth muscle cells and pericytes.^{311,312}

SMC-P participates in microvascular remodeling by mediating the enlargement of existing collateral arterioles and the formation of *de novo* arterioles by muscularization of capillaries to increase blood conduction capacity.^{17,313,314} These diverse cellular processes involve dynamic control of reversible SMC phenotypic modulation between the quiescent contractile state and

dedifferentiated state with capabilities for proliferation, migration and extracellular matrix remodeling.^{315,316}

Despite the extensive studies on these external stimuli triggering SMC participation in microvascular remodeling, internal molecular mechanisms allowing SMC to react to the PAD environment remain partially characterized. The SMC-P-specific knockout of OCT4 impaired ischemia-induced microvascular remodeling, accompanied by defective perivascular cell migration and survival and abnormal endothelial cell migration and barrier function.³¹⁷ Surprisingly, the SMC contractile gene repressor KLF4 is required for SMC-P coverage on resistant arterioles, controlling microvascular permeability and dilation.¹²⁵ These studies suggest the need for investigations on the regulatory mechanisms of microvascular SMC-P behaviors, which could serve as novel therapeutic targets in controlling microvascular remodeling.

Epigenetic mechanisms have been implicated in controlling SMC phenotypes.³¹⁸ Yet, studies exploring epigenetic mechanisms in regulating microvascular remodeling in the context of PAD have been limited. Global gene knockout or pharmacological inhibition of lysine acetyltransferase p300-CBP-associated factor (PCAF) impaired blood reperfusion and SMC-P participation in microvascular remodeling upon hindlimb ischemia by suppressing the expression of pro-inflammatory genes for monocyte recruitment.³¹⁹ Global *HDAC9* knockout reduced angiogenesis and impaired blood reperfusion post-hindlimb ischemia via upregulated antiangiogenic microRNA-17-92 in EC.³²⁰ These studies imply that epigenetic mechanisms are involved in the regulation of ischemia or injury-induced hindlimb microvascular remodeling. We previously identified an “epigenetic memory” mechanism composing stably enrichment of H3K4me2 on SMC-lineage specific genes that is critical in maintaining SMC-lineage identity, contractility, restraining phenotypic plasticity, and participation in macrovascular remodeling in

response to artery injury.³²¹ However, it is unknown if H3K4me2 in perivascular cells of microvasculature is also involved in the process of microvascular remodeling in response to hindlimb ischemia.

Here we investigated the regulatory roles of H3K4me2 in mediating perivascular cell participation in microvascular remodeling using the murine hindlimb ischemia model. We generated a novel transgenic mouse (referred as Myocd-LSD1 mouse) where mature MYH11⁺ SMC-P express simultaneously an H3K4me2 editing system for selective ablation of H3K4me2 on the SMC gene repertoire³²¹ and the SMC fate mapping tracer YFP upon tamoxifen injection. We assayed the microvascular remodeling in a hindlimb ischemia model using Myocd-LSD1 mice.³²¹ By performing selective H3K4me2 editing in SMC-P, we observed impaired blood reperfusion and a lack of YFP⁺ SMC-P participation in the microvascular remodeling within the ischemic muscle *in vivo*. Interestingly, we observed a compensatory cell source (MYH11⁺YFP⁻) replaced YFP⁺ SMC-P during microvascular remodeling. *In vitro* studies indicated that H3K4me2-edited SMC exhibited a survival/proliferation disadvantage when co-cultured with control SMC. *In vitro* tube formation assay demonstrated that H3K4me2-edited SMC interfered with EC-mediated tube formation and changed the SMC-EC interaction pattern. Mechanistically, H3K4me2-editing altered Notch signaling pathways in SMC, which has been proven to play critical roles in controlling SMC differentiation and SMC-P coverage on the microvasculature. Finally, loss of H3K4me2 was observed in SMC-P from human gastrocnemius muscle tissues of PAD patients. In conclusion, our preliminary data demonstrated SMC epigenetic memory marker H3K4me2 is important for perivascular participation in microvascular remodeling in the murine hindlimb ischemia model.

3.3 Results

3.3.1 H3K4me2 editing in SMC-P was associated with an impaired microvascular remodeling in the murine hindlimb ischemia model.

To investigate the roles of the histone post-translational modification H3K4me2 on SMC gene repertoire in regulating SMC-P participation in microvascular remodeling, we generated a novel transgenic mouse line where both cell-fate tracer YFP and selective H3K4me2 editing tool, *Myocd*-LSD1, were specifically expressed in mature SMC-P (*MYH11*⁺) upon tamoxifen injection (*Myocd*-LSD1 mice) (**Figure 12A**). This system performs reliable and specific H3K4me2 ablation on Myocardin-regulated genes in SMC.³²¹ We performed femoral artery ligation and excision to induce hindlimb ischemia and microvascular remodeling in the lower limbs of both control (*Myocd*-LSD1-YFP⁺) and *Myocd*-LSD1⁺YFP⁺ mice. Blood reperfusion to the plantar soles was monitored by laser Doppler for two weeks post-surgery as an indicator of microvascular remodeling. Contralateral limbs without injury were used as the internal control for normalization (**Figure 12B**). Laser Doppler measurement indicated a significant reduction of blood flow to the injured limb immediately after femoral artery excision, demonstrating the successful induction of hindlimb ischemia (**Figure 12C**). We observed an impaired and delayed recovery of blood flow in *Myocd*-LSD1 mice compared with control mice, suggesting that H3K4me2 editing in SMC-P disrupted the efficiency of microvascular remodeling induced by limb ischemia (**Figure 12C**).

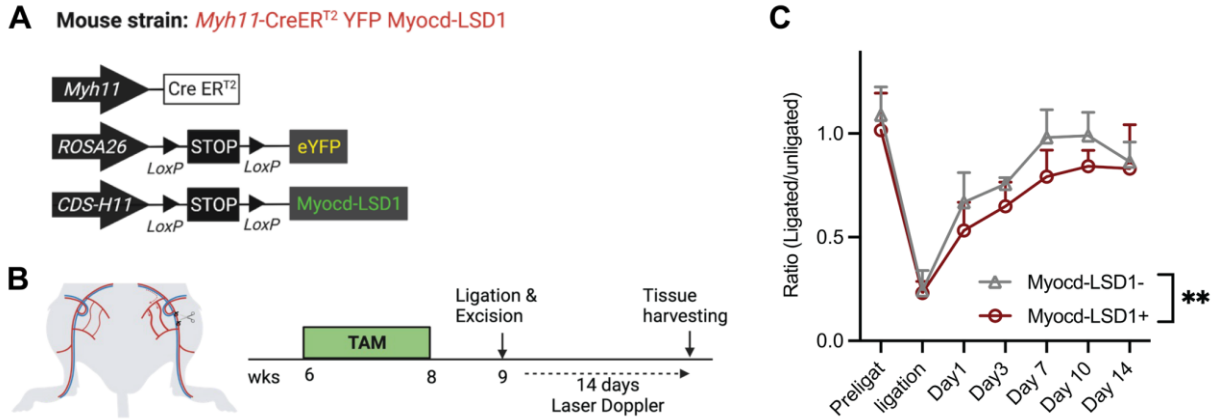


Figure 12 Myocd-LSD1 mice exhibited impaired blood reperfusion in murine hindlimb ischemia model

A. Schematic of Myocd-LSD1 transgenic mouse model. **B.** Schematic of femoral artery excision in control and Myocd-LSD1 mice. Laser doppler was used to measure blood reperfusion post-surgery. **C.** Ratio of blood flow between injured and uninjured limb measured by laser doppler. Data are represented as mean \pm S.D. of $n = 7-10$ mice per group. Groups were compared by Two-Way ANOVA using a mixed-effects model with the Geisser-Greenhouse correction. ** $p < 0.001$.

3.3.2 Defective microvascular remodeling was associated with a lack of SMC-P perivascular coverage in Myocd-LSD1 mice.

To further characterize the cell participation during microvascular remodeling post-surgery, we harvested the gastrocnemius (GC) muscles from both injured and uninjured limbs 14 days after femoral excision for immunostaining. In both control and Myocd-LSD1 mice, there was an increased density of endothelial cells (PECAM⁺) in the injured limbs, suggesting the induction of angiogenesis by femoral artery excision (**Figure 13A, B**). While there was no difference in YFP⁺ SMC-P density in the uninjured limbs between control and Myocd-LSD1 mice, we noticed a reduction of YFP⁺ SMC-P presented in the injured limbs in Myocd-LSD1 mice (**Figure 13A, B**), indicating the lack of SMC-P contribution in microvascular remodeling. Similar to our previous

report, we observed a global reduction of MYH11 intensity in both uninjured and injured limbs of Myocd-LSD1 mice (**Figure 13A, B**), validating the conclusion that H3K4me2 is required for SMC contractile gene expression.³²¹ Notably, we discovered an MYH11⁺YFP⁻ cell population specifically presented in injured limbs from Myocd-LSD1 mice, suggesting compensatory cell sources, including non SMC-P population or unlabeled SMC-P cells due to insufficient Cre activity, participated during the remodeling to replace defective H3K4me2-edited SMC-P (**Figure 13A, B**). We then performed an *in vitro* competition assay by co-culturing previously characterized control rat aortic SMC with Myocd-LSD1-expressing rat aortic SMC (Myocd-LSD1 SMC) prelabeled with different live-cell fluorescent dyes. Both groups of cells were seeded at the same cell density and induced for proliferation by PDGF-BB treatment after serum starvation for two days. We also observed that Myocd-LSD1 SMC was markedly outcompeted by control SMC (**Figure 13C**). Notably, the disadvantage of proliferation or difference in cell survival was not observed when Myocd-LSD1 SMC was cultured alone and treated with PDGF-BB³²¹. A further mechanistic study is needed to determine if the inhibitory effect is caused by paracrine factors or cell-cell contact-dependent mechanisms and whether this disadvantage in cell expansion is a cause of lack of perivascular coverage during the vascular remodeling observed in Myocd-LSD1 mice.

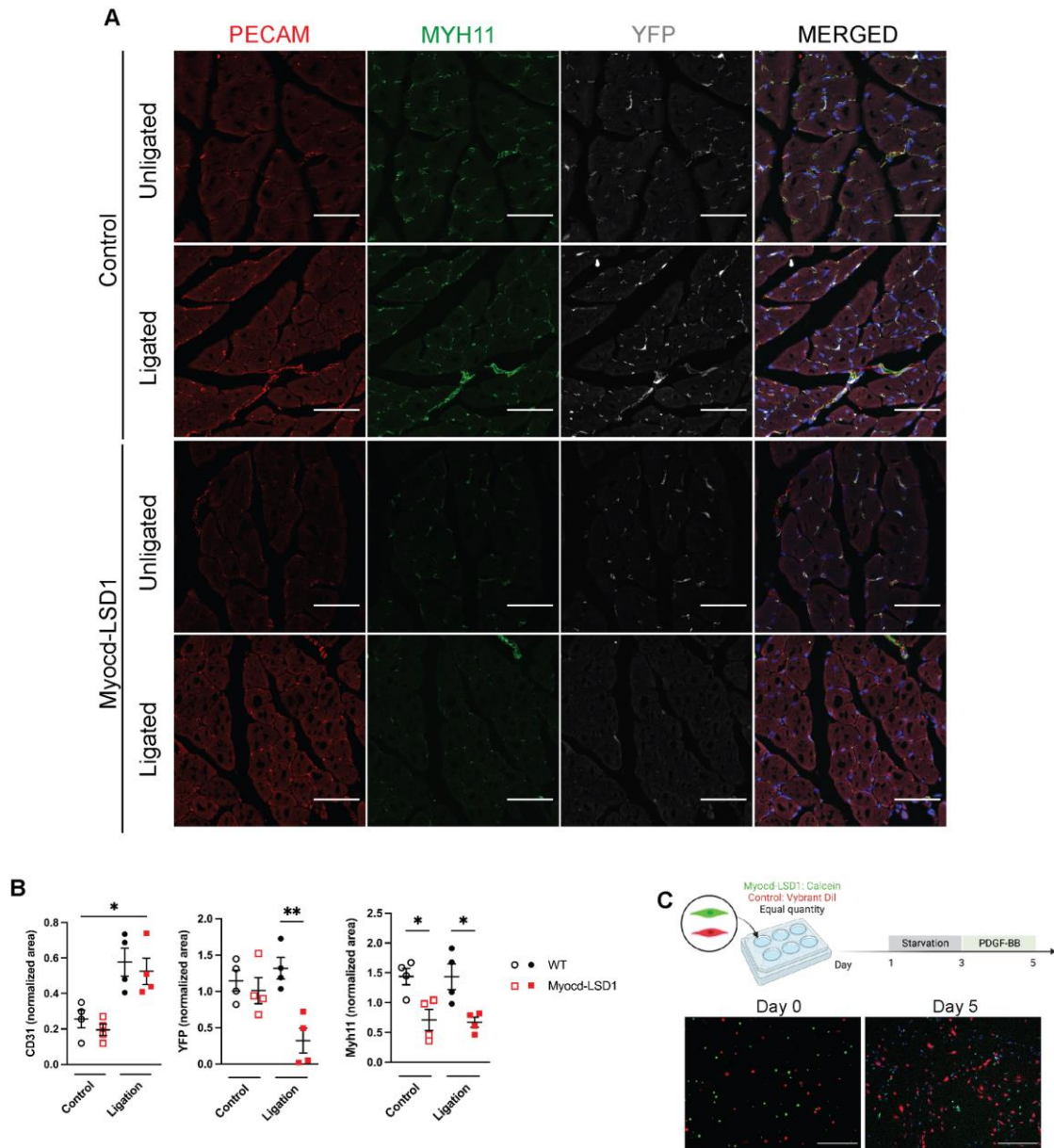


Figure 13 Defective microvascular remodeling was associated with a lack of SMC contribution in Myocd-LSD1 mice

A. immunofluorescent staining of gastrocnemius muscle from control and Myocd-LSD1 mice 14 days post-injury. Collateral limbs were used as the uninjured control. (scale bar = 40 μ m). **B.** Quantification of immunofluorescent staining normalized as a percentage of total area. **C.** *In vitro* competition assay by co-culturing pre-stained control and Myocd-LSD1 SMC. (Scale bar = 400 μ m)

3.3.3 H3K4me2 editing in SMC disrupted tube formation and SMC-EC interaction.

To further investigate the mechanisms by which H3K4me2 editing in SMC-P affects microvascular remodeling, we utilized a well-characterized *in vitro* angiogenesis assay by incubating HUVEC (human umbilical venous endothelial cell) with control or Myocd-LSD1 SMC (the stable rat aortic SMC cell line established in previous chapter) on top of a thin layer of cell basement membrane extract. Cells were exposed to hypoxia (0.2% O₂, 5% CO₂, with N₂ balance) for 4 hours. Interestingly, not only the global tube formation was impaired in Myocd-LSD1 SMC group, as indicated by a decreased density of tubes connected by HUVEC, but we also observed an altered pattern of SMC-EC interaction between HUVEC and Myocd-LSD1 SMC. Instead of adopting a perivascular location, we found that Myocd-LSD1 SMC was stretched and inserted between EC (**Figure 14A**). Morphological changes were also observed when Myocd-LSD1 SMC was cultured with endothelial cell growth media under the hypoxia condition for 24 hours (**Figure 14B**), suggesting a possibility of a phenotypic and functional transition to EC-like state or “SEM” subtype, a multipotent subpopulation of SMC acquiring gene markers of stem cells (*Ly6a*), endothelial cells (*Vcam1*) and monocytes (*Ly6c1*) within atherosclerosis³⁰, in H3K4me2 edited SMC, coinciding with our previous discovery that loss of H3K4me2 exacerbated SMC phenotypic plasticity to acquire features of other lineages, such as adipocyte and osteo-chondrogenesis.³²¹ We further validated if Myocd-LSD1 SMC could acquire EC marker PECAM after culturing with endothelial cells growth media under a hypoxic environment by immunostaining. Interestingly, compared with control SMC cultured in the same environment, a subset of Myocd-LSD1 SMC acquired expression of PECAM with an elongated morphological change (**Figure 14C**). Overall, our data suggest loss of H3K4me2 in SMC exacerbates its phenotypic plasticity, allowing SMC to acquire some features of EC upon pro-angiogenesis stimulations, which in turn disrupts SMC-EC

interaction and angiogenesis. Yet, further characterization of EC-like phenotype under pro-angiogenesis conditions is required before making the conclusion.

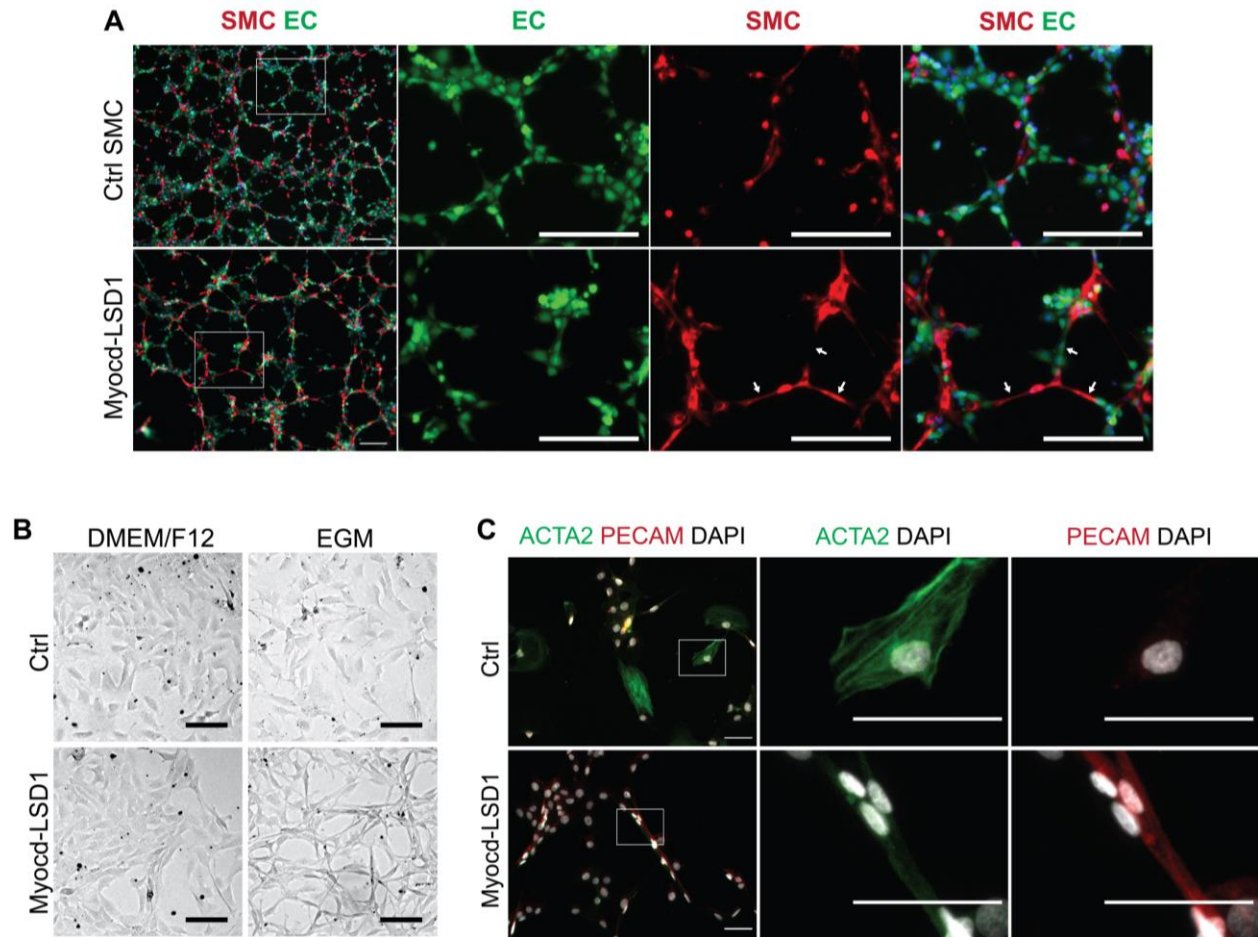


Figure 14 H3K4me2 editing in SMC disrupted angiogenesis and SMC-EC interaction

A. *in vitro* tube formation with pre-stained SMC (red) and HUVEC (green) on Matrigel. Arrow: SMC bridging EC instead of wrapping around EC-mediated tubes. (scale bar = 25 μ m); **B.** SMC morphology cultured in EGM under hypoxia condition for 24 hours. (scale bar = 100 μ m); **C.** Immunostaining of ACTA2, PECAM, and DAPI on SMC cultured in EGM under hypoxia condition for 24 hours. (scale bar = 50 μ m).

3.3.4 H3K4me2 editing altered Notch signaling pathways in Myocd-LSD1 SMC

Given the critical roles of Notch pathways in mediating SMC-EC interaction and SMC lineage specification during development³²², we investigated if Notch pathways were altered upon H3K4me2 editing in SMC. First, we analyzed a previously published RNA-seq dataset (GSE179220) comparing Myocd-LSD1 SMC with control SMC after serum starvation for 2 days. There was an altered pattern of Notch signaling genes in Myocd-LSD1 SMC, including reduction of both Notch1, Notch3 receptors, Jagged-1 and DLL4 ligands, and Notch downstream genes Hey1 and Hey2. Meanwhile, some Notch genes were upregulated in Myocd-LSD1 SMC, such as Notch2 and DLL1, which possibly functions as a compensatory mechanism to overcome Notch deficiency in Myocd-LSD1 SMC (**Figure 15A**). To evaluate the Notch pathway activation in both control and Myocd-LSD1 SMC, we stimulated SMC with immobilized Jagged-1 Fc peptide or IgG as the control group. Interestingly, Jagged-1 stimulation was unable to induce expression of Notch2 and Notch3 or downstream effector Hey2 in Myocd-LSD1 SMC as compared to control SMC (**Figure 15B**). In contrast, Jagged-1 stimulation strongly upregulated DLL1 in Myocd-LSD1 SMC (**Figure 15B**). Interestingly, we also identified a reduction of H3K4me2 on *Hey2* promoter region in Myocd-LSD1 SMC (**Figure 15C**), similar to SMC-specific contractile genes as previously reported³²¹. By analyzing the previously published serum response factor (SRF, part of Myocd/SRF complex) ChIP-seq dataset in mouse SMC, we also identified enrichment of SRF in *Hey2* (**Figure 15D**).

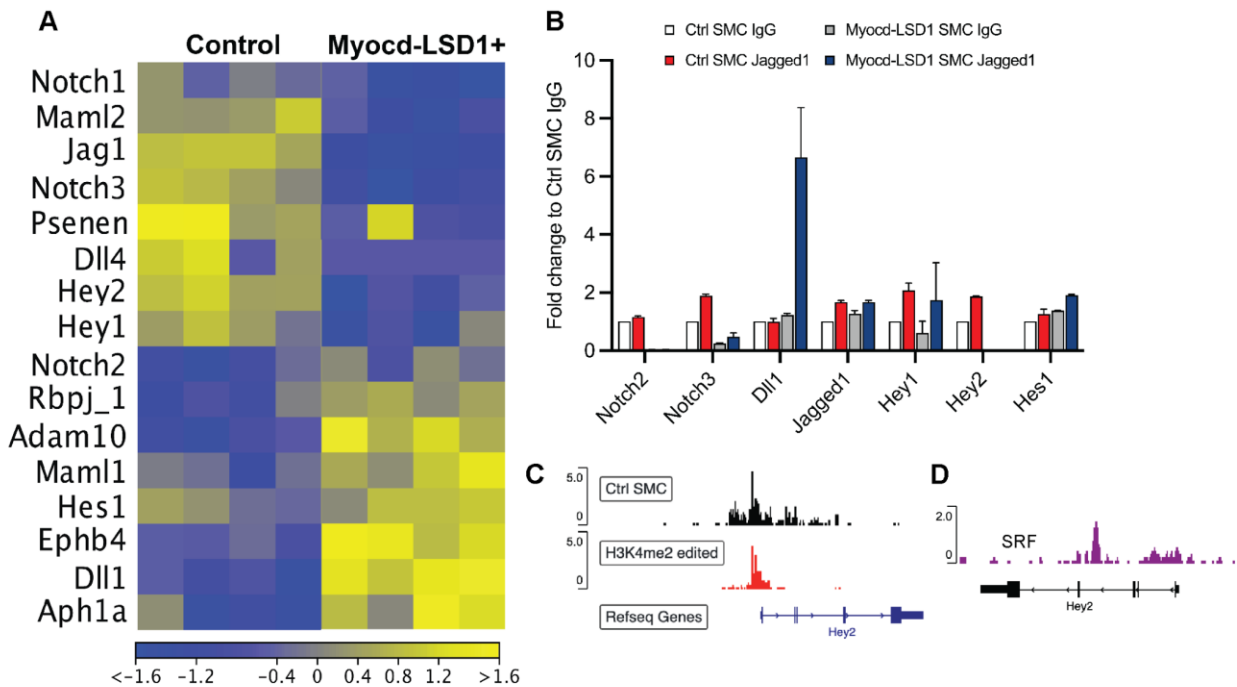


Figure 15 H3K4me2 editing altered Notch signaling pathways in Myocd-LSD1 SMC

A. Heatmap of differential expressed genes associated with Notch pathway signaling from RNA-seq dataset (GSE179220) comparing control SMC and Myocd-LSD1 SMC. **B.** Gene expression of Notch pathway genes upon *in vitro* Jagged-1 Fc stimulation. (n = 2 independent repeat). **C.** Genome track of H3K4me2 enrichment on *Hey2* in control and Myocd-LSD1 SMC. (H3K4me2 CUT&Tag-seq from GSE179220). **D.** Genome track of SRF enrichment on *Hey2* in mouse SMC. (SRF ChIP-seq from GSM3069844).

3.3.5 Reduction of H3K4me2 in perivascular cells was associated with peripheral artery disease

With our data demonstrating a functional role of H3K4me2 in mediating SMC-P participation in hindlimb microvascular remodeling, we aimed to determine if alteration of H3K4me2 is associated with PAD progression in patient samples. By performing immunofluorescent staining on calf muscles from PAD and control patients, we observed a reduction of H3K4me2 intensity in perivascular cells associated with reduced ACTA2 expression,

suggesting a positive correlation between the presence of H3K4me2 and perivascular cell maturation (**Figure 16A, B**). In fact, reduction of H3K4me2 was not homogenously observed in perivascular cells, but we observed an increased percentage of H3K4me2^{low} and ACTA2^{low} SMC-P in PAD patients by quantifying H3K4me2 and ACTA2 intensity in perivascular regions (**Figure 16C**) Together, we provided evidence suggesting the alteration of H3K4me2 in perivascular cells is also presented in human microvasculature with PAD conditions.

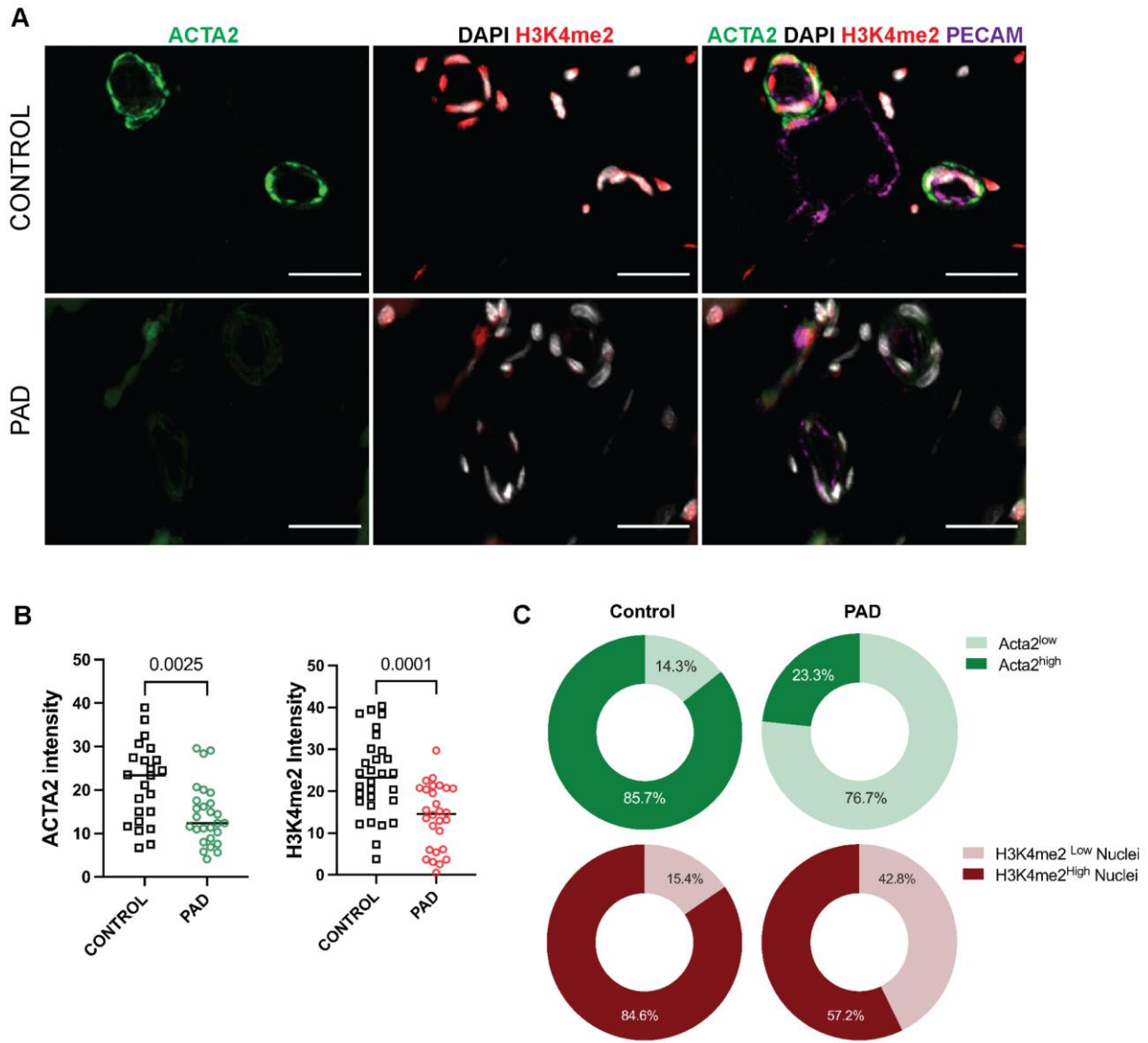


Figure 16 Reduction of H3K4me2 in perivascular cells was associated with human PAD

A. immunofluorescent staining of mature SMC (ACTA2), EC (PECAM), H3K4me2, and DAPI on GC muscles from PAD or Control patients. (Scale Bar = 25 μ m). **B.** Quantification of ACTA2 and H3K4me2 mean intensity in perivascular cells from control or PAD patients. **C.** Summary of the percentage of ACTA2^{low/high} cells and H3K4me2^{low/high} nuclei in the perivascular regions in control and PAD patients.

3.4 Conclusion and Future Directions

The recently developed locus-selective H3K4me2 demethylation tool makes possible the investigation of the functional roles of H3K4me2 enriched on SMC-lineage relevant genes without H3K4me2 enrichment.³²¹ In combination with the SMC fate tracing mouse model, our ongoing experiments provided valuable preliminary evidence proving that H3K4me2 also plays an essential role in mediating microvascular SMC-P behaviors during hindlimb ischemia-induced microvascular remodeling. These observations set a direction for the future investigations:

First, we observed an EC-like morphological change of Myocd-LSD1 SMC when exposed to pro-angiogenesis conditions, such as endothelial growth medium (containing VEGF) and hypoxia. This observation echoes our previous discovery that loss of H3K4me2 exacerbates SMC phenotypic plasticity and accelerates SMC acquisition of gene markers of other lineages upon stimulation.³²¹ In support of the transdifferentiation concept, a recent single-cell RNA-seq study in the murine hindlimb ischemia model identified a small population of fibroblasts that could give rise to EC-like cells during microvascular remodeling, suggesting a bidirectional endothelial-mesenchymal transition.³²³ Yet, further experiments are needed to validate if Myocd-LSD1 SMC acquires EC phenotypes or transcriptome features and to identify molecular mechanisms that control the transdifferentiation processes, such as VEGF or hypoxia-related pathways.

Second, we identified a distinct expression pattern of Notch signaling genes in Myocd-LSD1 SMC. Importantly, *in vitro* stimulation of Notch signaling using immobilized Jagged-1 Fc peptide failed to upregulate several upstream regulators, such as receptors Notch2, Notch3, and downstream effector Hey2, which are likely to be involved in perivascular recruitment during angiogenesis and SMC fate specification. Global Notch3 knockout (Notch3^{-/-}) strongly impaired mural SMC coverage in nascent vessels during maturation in the postnatal retina angiogenesis

model.³²⁴ Endothelial cell-specific knockout or inactivation of Notch ligand Jag1 presented a similar inhibitory effect in mural cell recruitment and microvascular maturation.^{325,326} In the context of peripheral artery occlusion, Notch ligand Dll4 genetic knockdown (*Dll4*^{+/-}) induced leaky immature angiogenesis, likely due to the lack of perivascular cell coverage in the hindlimb ischemia model.³²⁷ Meanwhile, Notch downstream effector Hey2 has been shown to be necessary for SMC proliferation, migration, and neointima formation in Hey2 deficient mice³²⁸, phenocopying the absence of neointima formation in response to carotid ligation after H3K4me2 editing³²¹. Besides, a recent study in *Drosophila* suggested Hey protein is required in maintaining mature enterocyte lineage identity by guarding nuclear organization.³²⁹ Notably, there is no study using the SMC-specific knockout mouse model to determine the SMC-specific roles of the Notch pathway in mediating microvascular remodeling. Therefore, it is interesting to examine if Notch pathways play a central role in the phenotypes observed in Myocd-LSD1 SMC during the microvascular remodeling. Future studies, including overexpression of Hey2 or Notch receptors in Myocd-LSD1 SMC, can answer this question.

Third, we reported a compensatory population of YFP-MYH11⁺ cells that participated in the vascular remodeling in Myocd-LSD1 mice. Our attempt to compare H3K4me2-edited SMC with control SMC in the competition co-culture assay indicated the survival or proliferation of H3K4me2-edited SMC was strongly inhibited by control SMC, which was not observed when H3K4me2-edited SMC was cultured alone³²¹. Clearly, the inhibitory effect is derived from the competing healthy SMC, whereas whether such inhibition is induced by released paracrine factors or via contact-dependent inhibition remains unclear. Besides, further characterization of cellular composition in muscle tissues undergoing vascular remodeling via flow cytometry or single-cell transcriptome profiling is needed to profile the detailed changes in cell populations, cell-cell

interactions, and phenotypes of H3K4me2-edited SMC-P in response to hindlimb ischemia. Besides, exploration using single-cell transcriptomics in our model is likely to identify novel regulators governing perivascular cell participation upon peripheral artery occlusion.

Finally, although we observed a global reduction of H3K4me2 intensity in perivascular cells from PAD patients, whether enrichment of H3K4me2 on SMC-specific genes is altered remains unknown, despite a similar decrease of contractile gene expression in H3K4me2^{low} cells. There are more questions to be addressed in the future studies, including (1) the molecular mechanisms responsible for H3K4me2 alterations in variable pathophysiological conditions, such as common co-morbidities in PAD patients, including aging, metabolism syndromes, and hypertension; (2) Is the loss of H3K4me2 level due to the dysfunction of H3K4me2 maintenance mechanism or an active H3K4me2 demethylation mechanism triggered by pathophysiological conditions? (3) Does the H3K4me2 level of perivascular cells fluctuate across time? This answer might explain why we observed heterogenous H3K4me2 levels in perivascular cells since immunostaining only captures a snapshot. Single-cell or spatial CUT&TAG epigenome profiling can be used to answer these questions. Overall, a more precise understanding of epigenetic programming will eventually help pave the road to developing novel therapeutic strategies for treating PAD.

3.5 Methods

3.5.1 Mice model

Myh11-Cre^{ERT2} YFP Myocd-LSD1 transgenic mouse was generated by crossing the SMC fate tracing mouse line *Myh11*-Cre^{ERT2} R26R-EYFP with H11b-*loxP*-STOP-*loxP*-Myocd-LSD1 mouse generated with Cyagen. Briefly, the gRNA to mouse *Hipp11* locus, a safe harbor locus enabling robust and stable transgene expression, donor vector containing “CAG promoter-*loxP*-3*SV40 pA-*loxP*-Kozak-LSD1-CDS-FLAG-Myocd-CDS-rBG-pA” designed according to previous published Myocd-LSD1 sequence³²¹, and Cas9 mRNA were co-injected into fertilized mouse eggs to generate targeted conditional knock-in offspring. F0 founder animals were identified by PCR followed by sequence analysis, which were bred to wildtype mice to test germline transmission and F1 animal generation. *Myh11*-Cre^{ERT2} YFP Myocd-LSD1^{flox/wt} male mice were crossed with YFP Myocd-LSD1^{wt/wt} female mice to generate experimental male *Myh11*-Cre^{ERT2} YFP Myocd-LSD1^{flox/wt} mice. *Myh11*-Cre^{ERT2} YFP Myocd-LSD1^{wt/wt} male siblings were used as the control group. At 6 weeks of age, male mice were intraperitoneally injected daily with 1mg of tamoxifen in peanut oil (10 mg/mL). After 10 injections over the course of two weeks, mice recovered for one week to allow tamoxifen to be fully metabolized.

3.5.2 Hindlimb ischemia model and laser doppler measurement

Hindlimb ischemia experiments were performed as described before³³⁰ with minor modifications. After anesthesia by inhaling isoflurane, a small incision was made on skin to expose femoral artery. Two ligations were made on the proximal end of the femoral ligation artery with

3-5 mm distance. Femoral artery between the ligations was excised to induce acute ischemia in lower limb. Blood flow in the plantar soles³²¹ was measured by a Laser Doppler perfusion imaging system at several time points: before surgery, immediately after surgery, day 1, 3, 7, 10 and 14. Perfusion was expressed as the ratio between injured to contralateral uninjured hindlimb. Mice were kept on heating pad during the surgery and laser Doppler image acquisition to maintain a constant body temperature at 37 °C.

3.5.3 Cell culture

Rat aortic SMC expressing Myocd-LSD1 was generated as previously stated³²¹. Myocd-LSD1 and control SMC were routinely cultured in growth medium (DMEM:F12, Gibco, 11320-033) supplemented with fetal bovine serum (10%, Corning, 35-015-CV), L-glutamine (1.6 mM, Gibco, 25030081), and penicillin-streptomycin (100 U/mL, Gibco, 15140122) at 37°C with 5% CO₂. Before stimulation and for all baseline measurements, SMC were starved in a serum-free, insulin-free medium supplemented with L-glutamine (1.6 mM, Gibco, 25030081), L-ascorbic acid (0.2 mM, Sigma Aldrich, A4403), Apo-Transferrin (5 mg/ml, Sigma Aldrich, T5391) and Na Selenite (6.25 ng/ml, Sigma-Aldrich, S5261) for 48-72 hours. SMC from 3-5 constitutive passages were used to repeat independent experiments. Human recombinant PDGF-BB (Sigma Aldrich, SRP3138) was reconstituted in 10 mM Acetic Acid at 30 ng/ml for treatment.

3.5.4 In vitro tube formation assay

In vitro tube formation assay was performed according to protocol from ibidi. Briefly, 10 µl of Cultrex basement membrane extract (R&D Systems Bio-technie, 3432-010-01) was loaded

in the lower chamber of ibidi μ -Slide Angiogenesis slides (ibidi, 81506) and incubated at 37 °C for 1 hour for polymerization in cell incubator. HUVEC and SMC were stained with Calcein AM Viability Dye (ThermoFisher eBioscience, 65-0853-39) and Vybrant Dil Cell-labeling Solution (Invitrogen, V22885) respectively. Pre-stained HUVEC and SMC were mixed at cell number ratio (2:1) in EGM-2 Endothelial Cell Growth Medium-2 (Lonza, CC-3162) with supplements and loaded on the upper chamber of the slide. Loaded slides were exposed to hypoxia using a modular hypoxia chamber for 4 hours. Tube formation was captured on a fluorescent microscope (Leica, DMI8) using the Ocular Advanced Scientific Camera Control software (Digital Optics Limited).

3.5.5 Competition assay

Myocd-LSD1 SMC and control SMC stained with Calcein AM Viability Dye and Vybrant Dil Cell-labeling solution respectively were mixed at the same cell density in SMC growth medium. Mixed cell suspension was seeded on 6-well-plates at 3000 cells/cm². Day 1 after seeding, cells were serum starved for the following 2 days and treated with PDGF-BB for 48 hours. Multiple regions of interest were imaged with the fluorescent microscope (Leica, DMI8).

3.5.6 Immunofluorescent staining

Muscle tissues were harvested according to the published protocol.³³⁰ Briefly, calf muscle from both injured and uninjured limb was dissected after fixation by 4% PFA perfusion. Muscles were further processed by 15% sucrose, 30% sucrose and embedded with Tissue-Tek O.C.T. Compound (Sakura, 4583). Embedded tissues were frozen-sectioned into 10 μ m sections for staining. Staining was performed to evaluate gene expression in cells using primary antibodies for

GFP (Abcam ab6673 1:250), MYH11 (Kamiya Biomedical Company MC-352 1:250), CD31/PECAM-1 (Novus Biologicals, NB100-2284, 1:250) or IgG as a control. Images were acquired by Nikon A1 Confocal microscope using NIS-Elements software (Nikon). Image processing was performed using ImageJ and Image Pro Premier (Media Cybernetics).

3.5.7 Immobilized Jagged-1 Fc stimulation

Immobilized Jagged-1 coated plates were prepared as previously described.³³¹ Briefly, goat anti-rat IgG (Fc-specific) antibody (Millipore, SAB3700539) was resuspended in PBS at 10 $\mu\text{g/ml}$. IgG solution was added to cell culture plate at a density of 1.3 $\mu\text{g/cm}^2$ and incubated at room temperature for 1 hour. After washing with PBS, suspended rat Jagged-1-Fc fusion protein (R&D systems, 599-JG-100) at 10 $\mu\text{g/ml}$ was added on IgG-coated plate at surface density of 1.3 $\mu\text{g/cm}^2$ and incubated for 2 hours at room temperature. Coated surface with only IgG antibody was used as the control group. After incubation, surface was rinsed with PBS to remove the unbound Jagged-1-Fc. Cells were seeded at 25000 cells/ cm^2 on coated surface for stimulation.

3.5.8 RNA-seq and CUT&Tag seq analysis

RNA-seq and H3K4me2 CUT&Tag-seq data of Myocd-LSD1 and control SMC were described in previous paper.³²¹ Briefly, Notch pathway heatmap was generated using RNAseq_Expression_Browser_TPM file from GSE179215. H3K4me2 enrichment on rat *Hey2* region was generated in integrative genomics viewer³³² with bigwig files from GSE179217. SRF enrichment on mouse *Hey2* region was generated with bigwig files from GSM3069844.

4.0 General Conclusion and Discussion

Vascular smooth muscle cell is an essential element in maintaining vascular homeostasis with the unique feature of reversible phenotypic modulation. The roles of SMC in pathophysiological conditions have been underestimated until the availability of reliable cell-fate tracing and single-cell transcriptomic tools that unveiled the SMC phenotypic dynamics. Based on the classic phenotypic switching model, important transcription factors have been identified and characterized, yet mechanisms controlling SMC lineage identity and restraining phenotypic plasticity remain unexplored. Epigenetic programming regulates both *cis*-element accessibility and *trans*-factor recruitment via multiple mechanisms. Convincing evidence has proved the critical roles of epigenetic programming in lineage determination during the development and maintenance of lineage transcription memory in adult cells. Stable H3K4me2 presented on SMC-specific genes is proposed to serve as the epigenetic memory system to permit quick recovery of contractile gene expression in response to external stimuli, based on its features of lineage-specificity, stability, and independence of transcription activity.

In this dissertation, we studied the functional relevance of H3K4me2 on SMC-specific gene loci during phenotypic modulation by innovating a novel epigenome editing tool. To avoid the “off-target” effects caused by global manipulation of epigenetic modifiers, we designed a gene-specific H3K4me2 demethylation system, where part of Myocd, the master regulator of SMC differentiation, functions as the recruitment unit, fused with H3K4me2 demethylase LSD1 (Myocd-LSD1) for active demethylation. To exclude the hindrance effect by the Myocd-LSD1, we designed a non-functional fusion protein by introducing a catalytically inactive point mutation on LSD1 (Myocd-LSD1^{NF}). Compared with recently developed CRISPR-based epigenetic editing

tools, such as deactivated Cas9 (dCas9)-LSD1, which targets a limited number of gene loci depending on the number of guide RNAs (gRNAs) delivered into the cells³³³, our system used Myocd as the recruitment unit to systematically perform H3K4me2 on SMC-lineage specific genes. The efficiency and selectivity of Myocd-LSD1 induced H3K4me2 demethylation were extensively validated by comprehensive epigenome profiling via CUT&Tag-seq in SMC stably expressing Myocd-LSD1/LSD1^{NF}.

By performing selective H3K4me2 editing in SMC, we made several key observations. *First*, the presence of H3K4me2 is required for SMC contractile gene expression and contractility in vitro and in vivo. *Second*, H3K4me2 governs SMC lineage identity by controlling the expression of master regulators essential for SMC-lineage specification. *Third*, stable H3K4me2 functions as a lineage-specific recruitment system for the dynamic recruitment of TET2, which primes the reactivation of contractile genes during phenotypic re-differentiation. *Forth*, H3K4me2 restrains SMC lineage plasticity. Selective removal of H3K4me2 from SMC-lineage relevant genes surprisingly induced a profound redistribution of H3K4me2 reprogramming to a “stem cell-like” state with enhanced capacities to acquire other lineage features. *Finally*, the ability of SMC to participate in vascular remodeling is epigenetically encoded by H3K4me2, which requires dynamic yet restrained phenotypic modulation. Losing the stable H3K4me2 mark disrupted SMC-mediated neointima upon carotid artery injury or microvascular remodeling in the hindlimb ischemia model. Retaining H3K4me2 in SMC is surprisingly required for SMC migratory response to the chemoattractant PDGF-BB through the H3K4me2/TET2/miR145 regulatory axis. Besides, loss of H3K4me2 enrichment also disrupted the interaction between SMC-P and EC, associated with loss of Notch receptors (Notch1/2) and Notch downstream transcription factor Hey2.

In conclusion, we identified H3K4me2 as an epigenetic memory mechanism important for maintaining SMC lineage identity and functions. Disruption of the H3K4me2 program in SMC is harmful to vascular homeostasis and could potentially contribute to cardiovascular diseases, such as atherosclerosis and peripheral artery disease. Our work on this central epigenetic memory mechanism engendered new questions to be further investigated.

4.1 Epigenetic heterogeneity across vascular beds

Single-cell RNA-seq (scRNA-seq) techniques provide an unprecedented opportunity to decipher transcriptomic profiles at single-cell resolution. Several groups have constructed the single-cell mapping in healthy aorta³³, atherosclerosis³⁰⁻³² and aneurysm³³⁴. Despite distinct animal models, tissue of interest, and single-cell processing protocols, these scRNA-seq studies further validated the diverse spectrum of SMC phenotypes in both physiological and pathological conditions. An important pilot study by Dr. Hellen Jorgensen group characterized the subpopulations of SMC within the healthy aorta and identified a rare subpopulation expressing multipotent progenitor marker *Sca1* that is associated with SMC phenotypic modulation and highly expressed in a subpopulation of SMC within the atherosclerotic lesions.³³ Besides, they also reported distinct regional transcriptome status between ascending aorta and descending aorta.³³ This study elegantly implies the rich transcriptomic heterogeneity in SMC within healthy aorta that has been largely overlooked due to technical difficulties. In fact, a series of cell fate tracing studies revealed SMC from different aortic regions is derived from multiple embryonic origins, such as epicardium, second heart field, neural crest, and sclerotome.³³⁵ Importantly, the developmental origins of SMC have been associated with the propensity or resistance to major

cardiovascular diseases.^{336,337} Addressing the epigenome heterogeneity of SMC in either healthy or diseased aorta is on the edge of the next wave of single-cell studies. Single nucleus chromatin accessibility profiling via single nucleus assay for transposase-accessible chromatin with sequencing (snATAC-seq) has been performed in human atherosclerotic lesions or human coronary arteries, associating chromatin accessibility in a subpopulation of SMC with Genome-Wide Association Study (GWAS) loci associated with cardiovascular diseases.^{338,339} Importantly, single-cell CUT&Tag-seq (scCUT-Tag-seq) techniques are being developed to provide information regarding genomic distribution of histone modifications at single-cell resolution.^{340,341} Application of scCUT-Tag-seq on multiple histone modifications, including H3K4me2, could answer several interesting questions related to epigenome heterogeneity in SMC:

- 1) Do all SMC derived from variable embryonic origins have similar or distinct H3K4me2 distribution patterns? Do SMC from the same vascular region or embryonic origin display heterogeneity in the H3K4me2 enrichment pattern?
- 2) Is there a subpopulation of SMC in the healthy or diseased aorta that resembles Myocd-LSD1 SMC H3K4me2 distribution, which could be associated with SMC clonal expansion and exacerbated plasticity?
- 3) Are there epigenetic priming systems in a subset of SMC associated with disease progression?

Such priming mechanisms could be critical mechanisms mediating detrimental SMC phenotypic transitions, which could not be determined via scRNA-seq as changes at the transcription level might not appear and require further stimulations. Together, the combination of single-cell resolution techniques will fill the current gaps in our understanding of epigenetic encoding of SMC

function *in vivo* and can help identify novel regulatory mechanisms in mediating SMC phenotypes, which can be potentially used as a therapeutic target in treating cardiovascular diseases.

4.2 Mechanisms regulating H3K4me2 deposition in SMC

Our understanding of the mechanisms establishing and maintaining H3K4me2 programming is limited. Although several epigenetic writers have been identified in depositing H3K4me2 in mammalian cells²⁷⁵, it is more important to identify the recruitment mechanisms guiding the decoration of H3K4me2 on SMC-lineage-specific genes and how H3K4me2 is stably retained during cell replication. iPSC technique can be one of the *in vitro* platforms useful in advancing knowledge of epigenetic specification during development, especially with more defined protocols being established to differentiate SMC from iPSC.³⁴² Interestingly, retinoic acid signaling has been proposed to regulate SMC differentiation from iPSC³⁴², SMC precursor cell A404¹⁵⁶ and within atherosclerotic lesion³⁰. Our data also indicated retinoic acid treatment partially re-differentiated Myocd-LSD1 SMC with a gain of contractile genes and acquisition of H3K4me2 enrichment.³²¹ Future studies investigating the mechanisms of retinoic acid-induced epigenetic programming can provide new insight on treating cardiovascular diseases by rejuvenating SMC from an epigenetic perspective.

Besides SMC specification during development, it would be interesting to further characterize the epigenetic alteration and its underlying mechanisms in SMC in disease models. Similar to what we observed in PAD tissues with respect to a decrease in H3K4me2 (**Figure 16**), global alteration of histone modifications has been identified in other cardiovascular diseases, such as atherosclerosis and restenosis.³⁴³ These observations suggest the potential association between

variation in histone modifications and disease progression. Yet, our understanding of the causal relation between histone modifications and vascular diseases remains to be rudimental because of the limitations of most previous studies. *First*, alterations of histone modifications in cardiovascular diseases rely on global characterization, such as immunofluorescence staining, western blot, or ChIP on a piece of tissue. These techniques can only demonstrate a global intensity change or distribution from a pool of cells commonly presented in vascular diseases, including SMC, EC, immune cells, etc. *Second*, attempts to characterize the functional relevance of epigenetic modifiers in vascular disease often utilize global manipulation tools, such as global knockout or systematic delivery of inhibitors. However, these tools could lead to unexplained systematic effects during clinical translation. *Third*, the majority of mechanism studies still depend on *in vitro* models simulating vascular disease environments, which often cannot represent the real microenvironment given the complex nature of vascular diseases involving multiple systems and types of cells. These limitations are largely caused by the current technical limitations. With the advancement of single-cell, spatial epigenome profiling and gene manipulation tools being actively developed, future studies will generate a more precise and accurate map of epigenetic alterations in different cell types under pathological conditions.

4.3 Lesson learned from H3K4me2 editing

This dissertation reported the role of H3K4me2 in maintaining SMC lineage identity, contractile functions, and the ability to participate in active vascular remodeling upon carotid artery injury or hindlimb ischemia. With respect to adaptive vascular remodeling, loss of H3K4me2 in SMC is detrimental. Conversely, lack of neointima formation can be beneficial

regarding diseases with artery narrowing, such as restenosis. What conclusion can be drawn from this dissertation study from a therapeutic angle?

First, the loss of the H3K4me2 signature in SMC could have detrimental effects, given the fact that SMC is deprived of its lineage identity with exacerbated plasticity. Taking atherosclerosis as an example, the consensus has been achieved that a small subset of SMC undergoes clonal expansion and contributes to a spectrum of diverse phenotypic transitions within the plaque.²⁹ Importantly, recent single-cell transcriptomic studies provided evidence of the existence of a multipotent pioneer population derived from mature SMC, which gives rise to multiple lineages within the lesion.^{30,31} This “stem-cell” like population phenocopies what we observed in H3K4me2-edited SMC. Previous studies identified the persistence of H3K4me2 on *Myh11* promoter at least in a subset of modulated SMC (ACTA2⁺LGALS3⁺YFP⁺) using ISH-PLA.¹⁶² It is unclear if there is a loss of H3K4me2 in other genome loci beyond *Myh11* that triggers the dedifferentiation of SMC. It is also unknown if the persistence of H3K4me2 on *Myh11* contributes to the incomplete phenotypic transition to the defective macrophages compared with myeloid cell-derived macrophages.¹⁶⁵ Future studies characterizing the H3K4me2 distribution from these pioneer cells inside the lesion will answer these questions.

Besides, maintaining SMC lineage identity is also essential for the adaptive vascular remodeling as transition back to contractile state is required for vessel maturation. Although a small subset of fibroblast repertoire is considered beneficial during ischemia-induced microvascular remodeling as they transdifferentiate into EC-like cells and participate in angiogenesis³²³, our results suggest loss of H3K4me2 in SMC facilitates the acquisition of EC-like behavior and disturbs normal SMC-EC interaction during the microvascular remodeling.

Second, despite the lack of neointima formation observed in Myocd-LSD1 treated carotid in the carotid ligation model, it could still be harmful in the long term, such as the formation of vascular calcification. Indeed, clinical cases have been reported that calcified atherosclerosis causes in-stent restenosis.³⁴⁴ Future studies with a more relevant animal model or conditions are needed to determine the long-term effect of H3K4me2 editing in restenosis. Besides, the lack of SMC migration into the atherosclerotic lesions is detrimental due to the lack of protective fibrous cap mainly contributed by SMC. For instance, SMC-specific knockout of OCT4 significantly reduced SMC investment into the lesion, which led to detrimental effects contributing to the unstable plaque formation, including thinner fibrous caps, increased plaque sizes, increased intra-plaque hemorrhage, and increased infiltrated macrophages.³⁴⁵ Similar harmful effects were also observed in another study where radiation completely abolished SMC investment in the brachiocephalic artery (BCA), carotid artery, and aortic arch lesion.⁷⁵ Overall, inhibition of SMC migration can be both protective and detrimental in the context of different vascular diseases, yet uncontrolled SMC phenotypic plasticity should be targeted in developing therapeutic strategies.

Finally, our model of selective H3K4me2 editing provides a novel platform to identify key transcription factors or epigenetic modifiers that can be targeted to bias SMC plasticity. It has been well perceived that restrained participation of SMC is beneficial regarding adaptive vascular remodeling, formation of the protective fibrous cap in atherosclerosis, or maintaining vascular homeostasis by producing ECM. Our strategy of performing gene selective H3K4me2 editing reprograms H3K4me2 from SMC-lineage specific pattern to a stem-cell-like distribution. The generation of the “stem-cell” like SMC can be further used as a cell model to discover novel upstream or downstream transcriptional factors contributing to losing SMC-lineage identity or acquiring features of other lineages. For example, our preliminary data identified the altered

expression profile of Notch pathways in H3K4me2-edited SMC, which could play a role in controlling SMC differentiation and SMC-EC interactions. Given the lack of specificity of epigenetic modifiers and the technical difficulties of translating gene-selective epigenome editing clinically, identification of novel transcription factors can be strategized as pharmacological targets to bias SMC phenotypic transitions in the treatment of cardiovascular diseases.

Appendix A Key Resources Table

Appendix Table 1 Key Resources Table

REAGENT or RESOURCE	SOURCE	IDENTIFIER
Antibodies		
Anti-dimethyl-Histone H3 (Lys4) Antibody	Millipore	Cat# 07-030, RRID:AB_310342
Monoclonal ANTI-FLAG® M2 antibody produced in mouse	Sigma-Aldrich	Cat# F3165, RRID:AB_259529
Recombinant Anti-Histone H3 (tri methyl K9) antibody	Abcam	Cat# ab176916, RRID:AB_2797591
Anti-trimethyl-Histone H3 (Lys27) Antibody	Millipore	Cat# 07-449, RRID:AB_310624
SRF (H-300) antibody	Santa Cruz Biotechnology	Cat# sc-13029, RRID:AB_2302440
GKLF (H-180) antibody	Santa Cruz Biotechnology	Cat# sc-20691, RRID:AB_669567
Anti-Tet2 Antibody	Sigma-Aldrich	Cat# ABE364
Anti-acetyl-Histone H3 Antibody	Millipore	Cat# 06-599, RRID:AB_2115283
Rabbit IgG, polyclonal - Isotype Control (ChIP Grade)	Abcam	Cat# ab171870, RRID:AB_2687657
Mouse IgG - Isotype Control	Abcam	Cat# ab37355, RRID:AB_2665484
Histone H3K4me2 antibody (pAb)	Active Motif	39141, RRID:AB_2614985
ANTI-FLAG® antibody produced in rabbit	Sigma-Aldrich	Cat# F7425, RRID:AB_439687
Anti-HA tag antibody - ChIP Grade	Abcam	Cat# ab9110, RRID:AB_307019
5-hydroxymethylcytosine (5-hmC) monoclonal antibody (mouse)	Diagenode	C15200200-50
5-methylcytosine (5-mC) Antibody - clone 33D3	Diagenode	C15200081-100
Monoclonal Anti-Actin, α -Smooth Muscle	Sigma-Aldrich	Cat# A2547, RRID:AB_476701
Rat Anti-Smooth Muscle Myosin Heavy Chain (sml) Monoclonal Antibody, Unconjugated, Clone KM3669	Kamiya Biomedical Company	Cat# MC-352, RRID:AB_1241986
Anti-TAGLN/Transgelin antibody	Abcam	Cat# ab14106, RRID:AB_443021
Anti-GAPDH antibody [6C5] - Loading Control	Abcam	Cat# ab8245, RRID:AB_2107448
Anti-GAPDH antibody - Loading Control	Abcam	Cat# ab9485, RRID:AB_307275

Appendix Table 1 Continued

Anti-Histone H3 antibody - Nuclear Marker and ChIP Grade	Abcam	Cat# ab1791, RRID:AB_302613
H3K4me1	Millipore	Cat# 07-436, RRID:AB_310614
Anti-Dimethyl Histone H3 (Lys4) Antibody, clone CMA303	Sigma Aldrich	Cat# 05-1338, RRID:AB_1977248
Phospho-Akt (Ser473) (D9E) XP [®] Rabbit mAb	Cell Signaling Technology	Cat# 4060, RRID:AB_2315049
Akt1/2/3 Antibody (H-136)	Santa Cruz Biotechnology	Cat# sc-8312, RRID:AB_671714
IRDye [®] 800CW Donkey anti-Rabbit IgG Secondary Antibody	LI-COR Biosciences	Cat# 926-32211, RRID:AB_621843
IRDye [®] 680RD Donkey anti-Mouse IgG Secondary Antibody	LI-COR Biosciences	Cat# 926-68072, RRID:AB_10953628
Anti-GFP antibody	Abcam	Cat# ab6673, RRID:AB_305643
Anti-Ki67 antibody	Abcam	Cat# ab15580, RRID:AB_443209
Cleaved Caspase-3 (Asp175) Antibody	Cell Signaling Technology	Cat# 9661, RRID:AB_2341188
DYKDDDDK Tag (D6W5B) Rabbit mAb	Cell Signaling Technology	Cat# 14793, RRID:AB_2572291
Anti-mCherry antibody	Abcam	Cat# ab167453, RRID:AB_2571870
Donkey anti-Goat IgG (H+L) Cross-Adsorbed Secondary Antibody, Alexa Fluor 647	Molecular Probes	Cat# A-21447, RRID:AB_141844
Donkey Anti-Rat IgG H&L (Alexa Fluor [®] 555)	Abcam	Cat# ab150154, RRID:AB_2813834
Monoclonal Anti-Actin, α -Smooth Muscle - FITC antibody produced in mouse	Sigma-Aldrich	Cat# F3777, RRID:AB_476977
Anti-Actin, α -Smooth Muscle - Cy3 [™] antibody, Mouse monoclonal	Sigma-Aldrich	Cat# C6198, RRID:AB_476856
Anti-Tet2 antibody	Abcam	Cat# ab124297, RRID:AB_2722695
Anti-Biotin antibody	Abcam	Cat# ab53494, RRID:AB_867860
Bacterial and Virus Strains		
Ad-m-MYOCD-GFP	Vector Biolabs	Cat# ADV-265349
Ad-mTET2-HA	Applied Biological Materials	Cat# 465200540200
Lenti-Myocd-LSD1	This paper	N/A
Lenti-Myocd-LSD1 ^{NF}	This paper	N/A
Biological Samples		
Human Coronary Artery Smooth Muscle Cells	LONZA	Cat# CC-2583
Chemicals, Peptides, and Recombinant Proteins		
Corning [®] Fetal Bovine Serum, 500 mL, Premium, United States Origin	Corning	Cat# 35-015-CV
L-Glutamine (200 mM)	Gibco	Cat# 25030081

Appendix Table 1 Continued

L-Ascorbic acid	Sigma-Aldrich	Cat# A4403; CAS: 50-81-7
apo-Transferrin human	Sigma-Aldrich	Cat# T5391; CAS: 11096-37-0
Sodium selenite	Sigma-Aldrich	Cat# S5261; CAS: 10102-18-8
PDGF-BB human	Sigma-Aldrich	Cat# SRP3138
Rapamycin from <i>Streptomyces hygroscopicus</i>	Sigma-Aldrich	Cat# R0395; CAS: 53123-88-9
Retinoic acid	Sigma-Aldrich	Cat# R2625; CAS: 302-79-4
Lipofectamine™ 3000 Transfection Reagent	Invitrogen	Cat# L3000015
Polybrene Infection / Transfection Reagent	Sigma-Aldrich	Cat# TR-1003-G
Recombinant Human EGF (Animal-Free)	Biologend	Cat# 713008
Recombinant Human FGF-basic (146 aa) (Animal-Free)	Biologend	Cat# 713304
Dynabeads™ Protein G for Immunoprecipitation	Invitrogen	Cat# 10004D
ACCUTASE™ Cell detachment solution	Stem cell technologies	Cat# 07922
PowerUp™ SYBR™ Green Master Mix	Applied Biosystems	Cat# A25742
mirVana® miRNA mimic miR-145-5p	ThermoFisher	Cat# MC11480
mirVana® miRNA mimic negative control	ThermoFisher	Cat# 4464058
Lipofectamine RNAiMax Reagent	ThermoFisher	Cat# 13778075
Invitrogen™ CellLight™ Talin-GFP, BacMam 2.0	Invitrogen	Cat# C10611
Invitrogen™ Alexa Fluor™ 647 Phalloidin	Invitrogen	Cat# A22287
PureCol® Type I Collagen Solution, 3 mg/ml (Bovine)	Advanced BioMatrix	Cat# 5005
Duolink® <i>In Situ</i> PLA Probe anti-rabbit PLUS	Sigma-Aldrich	Cat# DUO92002
Duolink® <i>In Situ</i> PLA Probe anti-mouse MINUS	Sigma-Aldrich	Cat# DUO92004
Duolink® <i>In Situ</i> Detection reagents Orange	Sigma-Aldrich	Cat# DUO92007
Duolink® <i>In Situ</i> mounting medium with DAPI	Sigma-Aldrich	Cat# DUO82040
Histone H3K4me1 Peptide - biotinylated	Active Motif	Cat# 81040
Histone H3K4me2 Peptide - biotinylated	Active Motif	Cat# 81041
Histone H3K4me3 Peptide - biotinylated	Active Motif	Cat# 81042
IRDye 800CW Streptavidin	LI-COR Biosciences	Cat# 926-32230
Methyl-β-cyclodextrin (Cholesterol)	Sigma-Aldrich	Cat# C4555; CAS: 128446-36-6
AdipoRed™ Assay Reagent	LONZA	Cat# PT-7009
Tamoxifen	Sigma-Aldrich	Cat# T5648; CAS: 10540-29-1
Pluronic® F-127	Sigma-Aldrich	Cat# P2443; CAS: 9003-11-6
16% Paraformaldehyde Aqueous Solution, EM Grade, Ampoule 10 ML	Electron Microscopy Sciences	Cat# 15710
Crystal violet solution	Sigma-Aldrich	Cat # V5265; CAS: 548-62-9
Antigen Unmasking Solution, Citrate-Based	Vector Laboratories	Cat# H-3300
Critical Commercial Assays		
Qubit™ RNA BR Assay Kit	Invitrogen	Cat# Q10210
iScript™ cDNA Synthesis Kit	Bio-Rad	Cat# 1708891
RNeasy FFPE Kit	Qiagen	Cat# 73504
miRNeasy Mini Kit	Qiagen	Cat# 217004
TaqMan™ MicroRNA Reverse Transcription Kit	Applied Biosystems	Cat# 4366596

Appendix Table 1 Continued

Histone Extraction Kit	Abcam	Cat# ab113476
NE-PER Nuclear and Cytoplasmic Extraction Reagents	Thermo Scientific	Cat# 78833
Oil Red O staining kit	Sigma-Aldrich	Cat# MAK194
Rat Mesenchymal Stem Cell Functional Identification Kit	R&D Systems	Cat# SC020
CellTiter-Glo® Luminescent Cell Viability Assay	Promega	Cat# 7570
CUT&Tag-IT™ Assay Kit	Active Motif	Cat# 53160
MeDIP kit	Diagenode	Cat# C02010010
hMeDIP kit	Diagenode	Cat# C02010031
Luciferase assay kit	Promega	Cat# E1500
Deposited Data		
H3K4me3 (<i>Homo Sapiens</i> smooth muscle cell originated from H9)	ENCODE project ²⁹⁹	https://www.encodeproject.org/experiments/ENCSR515PKY/
VSMC_SRF	NCBI's Gene Expression Omnibus	GSM3069844
H3K4me1 (<i>Homo Sapiens</i> smooth muscle cell originated from H9)	ENCODE project ²⁹⁹	https://www.encodeproject.org/experiments/ENCSR130IMV/
H3K4 di-methylation controls smooth muscle cell lineage identity and vascular homeostasis	NCBI's Gene Expression Omnibus	GSE179220
H3K4me2 (<i>Homo Sapiens</i> smooth muscle cell originated from H9)	ENCODE project ²⁹⁹	https://www.encodeproject.org/experiments/ENCSR783AXV/
Experimental Models: Cell Lines		
Human coronary artery smooth muscle cells (hCASCs)	LONZA	Cat# CC-2583
Experimental Models: Organisms/Strains		
Mouse: YFP: B6.129X1- <i>Gt(ROSA)26Sor^{tm1(EYFP)Cos/J}</i>	²⁸⁷	MGI: J:80963
Mouse: Myh11-Cre ^{ERT2} : B6.FVB-Tg(Myh11-cre/ERT2)1Soff/J	⁴⁹	MGI: J:141641
Oligonucleotides		
See Supplementary Table 1		
Recombinant DNA		
pLVX-Myocd-LSD1-IRES-mCherry	This paper	N/A
pLVX-Myocd-LSD1 ^{NF} -IRES-mCherry	This paper	N/A
pGL3-Acta2-CArG ^{WT}	³⁰⁷	N/A
pGL3-Acta2-promoCArG ^{Mut}	³⁰⁷	N/A
pGL3-Acta2-promo+intCArG ^{Mut}	³⁰⁷	N/A
Software and Algorithms		
Prism 9	Graph Pad	https://www.graphpad.com/
Adobe Illustrator 2021	Adobe	https://www.adobe.com/products/illustrator.html
Fiji	http://fiji.sc	RRID:SCR_002285
Office 365	Microsoft	https://www.microsoft.com/en-us/microsoft-365

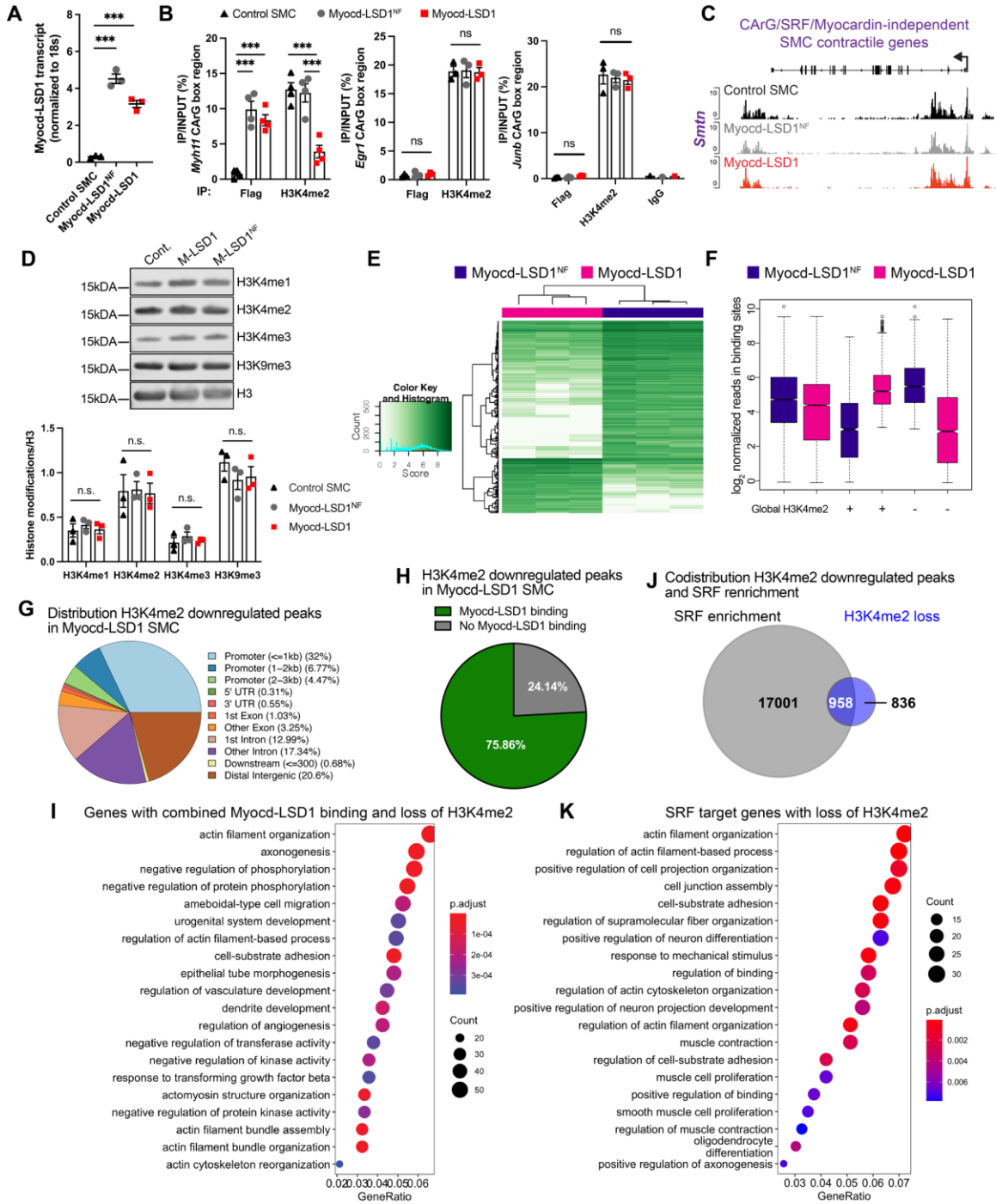
Appendix Table 1 Continued

Adobe Photoshop 2021	Adobe	https://www.adobe.com/products/photoshop.html
R version 4.0.4	http://www.r-project.org/	RRID:SCR_001905
Galaxy	http://galaxyproject.org/	RRID:SCR_006281
Bowtie2	290	RRID:SCR_016368
Deeptools	291	RRID:SCR_016366
Integrative Genomics Viewer	http://www.broadinstitute.org/igv/	RRID:SCR_011793
MACS	https://github.com/macs3-project/MACS	RRID:SCR_013291
Diffind	http://bioconductor.org/packages/release/bioc/html/DiffBind.html	RRID:SCR_012918
ChIPseeker	https://bioconductor.org/packages/ChIPseeker/	RRID:SCR_021322
ClusterProfiler	http://bioconductor.org/packages/release/bioc/html/clusterProfiler.html	RRID:SCR_016884
QIAGEN CLC Genomics Workbench	Qiagen	https://www.qiagen.com/us/products/discovery-and-translational-research/next-generation-sequencing/informatics-and-data/analysis-and-visualization/clc-genomics-workbench/
BaseSpace Correlation Engine	Illumina	https://www.illumina.com/products/by-type/informatics-products/basespace-correlation-engine.html
Targetscan	http://targetscan.org/	RRID:SCR_010845
Ocular Advanced Scientific Camera Control software	Digital Optics Limited	https://www.photometrics.com/products/ocular
Image Pro Premier	Media Cybernetics	https://www.mediacy.com/support/imagepropremier
Other		
Multi Wire Myograph System	DMT	Cat# 620M
LEICA Dmi8 Inverted Fluorescent Microscope	LEICA	https://www.leica-microsystems.com/products/light-microscopes/p/leica-dmi8-id/
Nikon Instruments A1 Confocal Laser Microscope	Nikon	https://www.microscope.healthcare.nikon.com/products/confocal-microscopes/a1hd25-a1rh25
Synergy-HTX multi-mode reader	BioTek	https://www.biotek.com/products/detection-multi-mode-microplate-readers/synergy-htx-multi-mode-reader/

Appendix Table 1 Continued

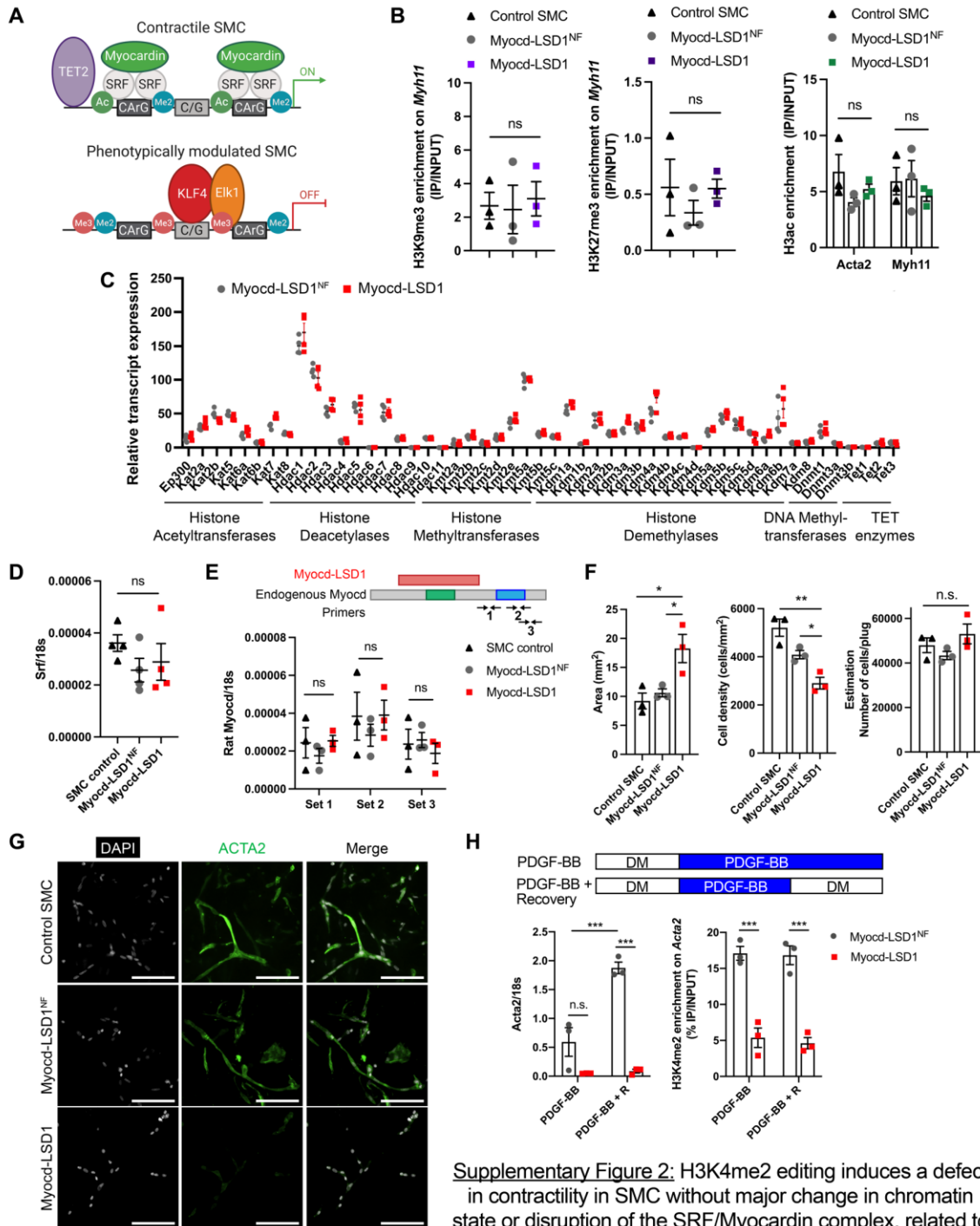
6.5 mm Transwell® with 8.0 µm Pore Polycarbonate Membrane Insert, Sterile	Corning	Cat# 3422
Bioruptor® Pico sonication device	Diagenode	Cat# B01060010
CFX Connect Realtime System	Bio-Rad	Cat# 1855201
Odyssey® CLx Imaging System	LI-COR Biosciences	https://www.licor.com/bio/odyssey-dlx/

Appendix B Supplementary Figures



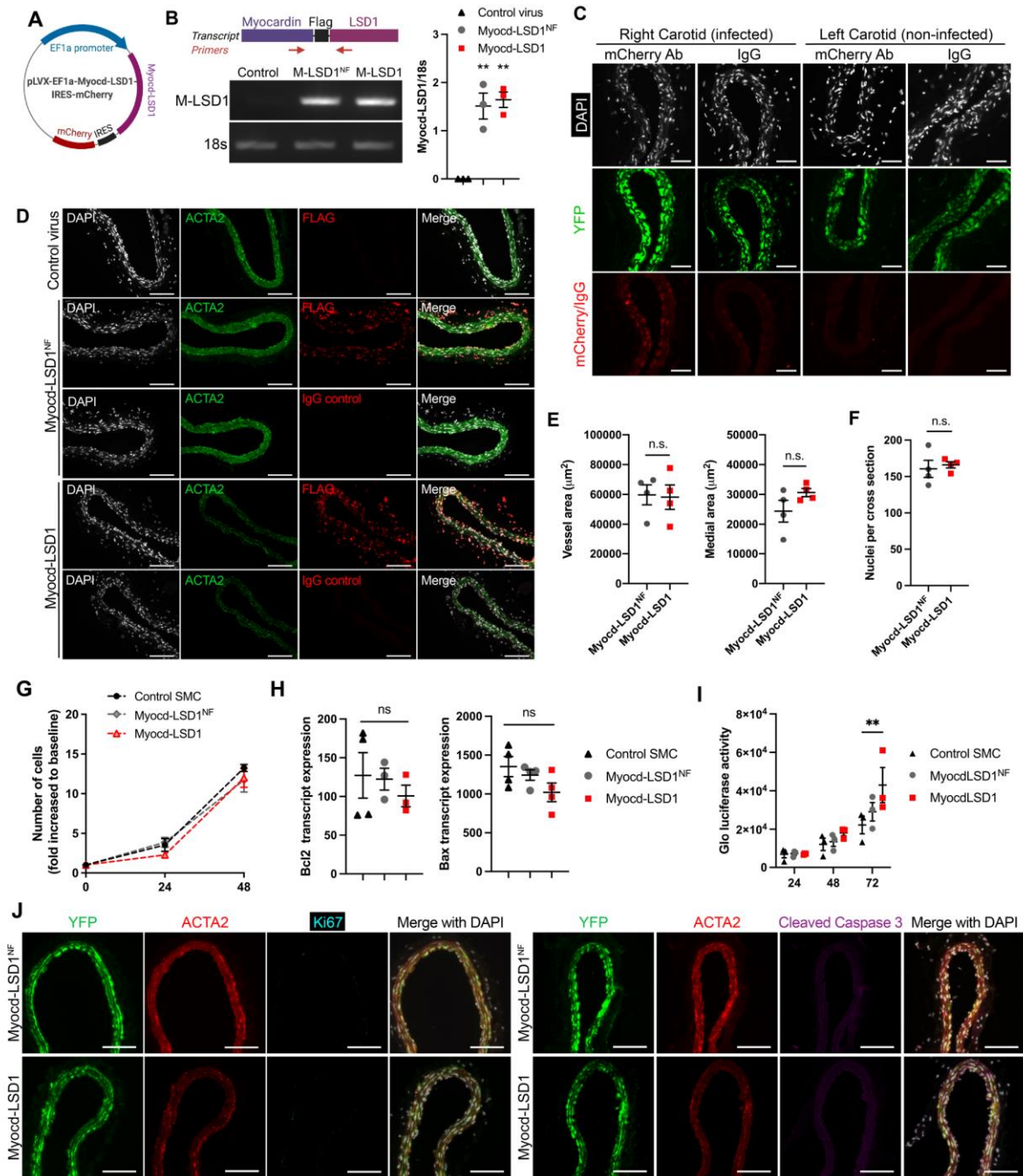
Appendix Figure 1 Myocod-LSD1 mediates loss of H3K4me2 on myocardin-regulated genes.

(A) mRNA expression of Myocd-LSD1 or Myocd-LSD1NF in control SMC, Myocd-LSD1, and Myocd-LSD1^{NF} SMC measured by qRT-PCR. (B) H3K4me2 and Myocd-LSD1 enrichment in CA_RG box regions of myocardin-dependent gene *Myh11* and myocardin-independent SRF-dependent genes *Egr1* and *Junb* in control, Myocd-LSD1NF and Myocd-LSD1 SMC. (C) CUT&Tag sequencing tracks showing H3K4me2 enrichment on the myocardin/SRF-independent contractile gene *Smtn*. (D) Global levels of H3K4me1, H3K4me2, H3K4me3, H3K9me3 measured by histone western blot and quantification normalized to unmodified H3. (E) Heatmap showing affinities for differentially bound sites for H3K4me2 between Myocd-LSD1 and Myocd-LSD1NF SMC. (F) Box plots of read distributions for significantly differentially bound (DB) sites for H3K4me2 between Myocd-LSD1 and Myocd-LSD1NF SMC. + indicates gene loci with a higher level of H3K4me2 in Myocd-LSD1 SMC; - indicates gene loci with a higher level of H3K4me2 in Myocd-LSD1NF SMC. (G) Pie plot of the genomic distribution of loci with a significantly lower level of H3K4me2 enrichment in Myocd-LSD1 SMC than Myocd-LSD1NF SMC. (H) Pie plot showing the relative proportion of genes with decreased H3K4me2 in Myocd-LSD1 SMC with presence or absence of MyocdLSD1 binding. (I) Unbiased top 20 Gene-Ontology pathway analysis of intersected genes with MyocdLSD1 binding and loss of H3K4me2 in Myocd-LSD1 SMC vs. Myocd-LSD1NF SMC. (J) Venn Diagram showing the overlap between genes with significant H3K4me2 decrease in Myocd-LSD1 SMC and genes with SRF binding in mouse SMC (GSE112417). (K) Unbiased top 20 Gene-Ontology pathway analysis of SRF-targeted genes with loss of H3K4me2 in Myocd-LSD1 SMC. Experiments were repeated 3-5 times independently. Data are represented as mean \pm s.e.m. Groups were compared by One-Way ANOVA. * $p < 0.0001$



Appendix Figure 2 H3K4me2 editing induces a defect in contractility without a major change in chromatin state or disruption of the SRF/Myocardin complex.

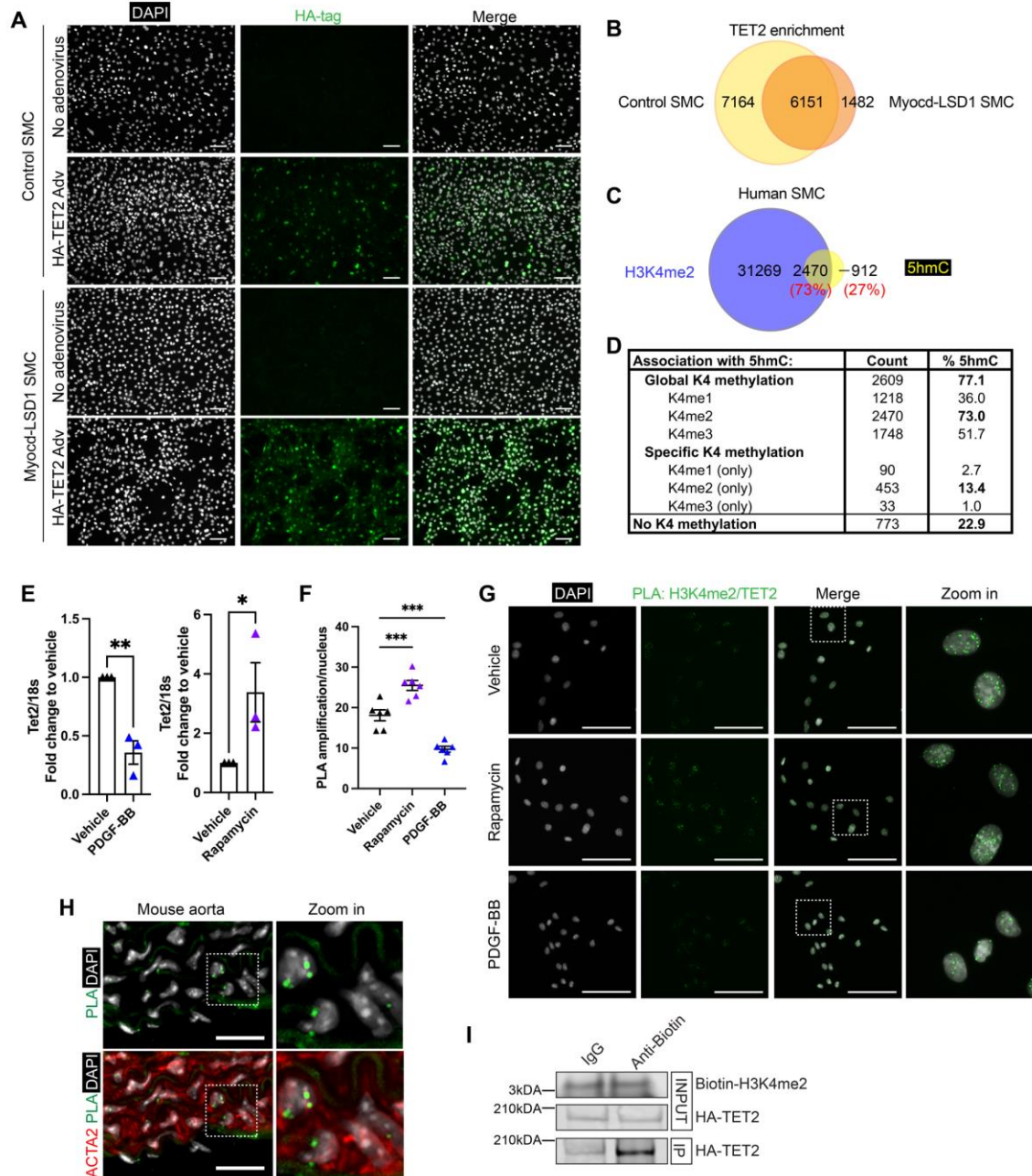
(A) Schematic representation of SMC marker gene activation (top) and repression (bottom) canonical regulators. The recruitment of the SRF/Myocardin complex is a potent mechanism for SMC marker gene activation. Epigenetic mechanisms, including TET2 binding and activating histone modifications such as acetylation, have been associated with activating these genes. Recruitment of KLF4 and histone repressive modifications (e.g., H3K9me3 and H3K27me3) drive SMC marker gene repression. (B) ChIP-qPCR analysis of H3K9me3, H3K27me3, and H3ac enrichment on myocardin-regulated Myh11 and Acta2 promoter regions in control, Myocd-LSD1 and Myocd-LSD1NF SMC. (C) Relative transcript levels of epigenetic modifiers in Myocd-LSD1 and Myocd-LSD1NF SMC. (D) Relative Srf transcript level in control, Myocd-LSD1 and Myocd-LSD1NF SMC measured by qRT-PCR. (E) Schematic of primer sets designed for specifically detecting endogenous myocardin transcript (top). The green box represents the SRF binding domain, and the blue box represents the transactivation domain. Normalized rat endogenous myocardin transcript levels in control, Myocd-LSD1, and Myocd-LSD1NF SMC measured by qRT-PCR (bottom). (F) Quantification of collagen gel area (mm²), cell density, and the number of cells in 3D SMC/collagen gels at five days post gelation. (G) Representative micrographs of ACTA2 and DAPI staining of SMC cultured in 3D collagen gels for five days. Scale bar = 100µm. (H) Acta2 mRNA expression and H3K4me2 ChIP-qPCR in Myocd-LSD1 or Myocd-LSD1NF SMC treated with PDGF-BB (30 ng/mL) for 48 h or 24 h with recovery for 24 h in differentiation media (DM). Experiments were repeated 3-4 times independently. Data are represented as mean ± s.e.m. Groups were compared by One-Way ANOVA (B, D, E, F), multiple Student t-test (C), and Two-Way ANOVA (H). * p<0.0001



Appendix Figure 3 Myocd-LSD1 transduction in mouse carotid arteries inhibits SMC differentiated phenotype without altering cell viability, proliferation, and apoptosis

(A) Schematic representation of the pLVX-Myocd-LSD1-IRES-mCherry plasmid used for lentivirus-mediated Myocd-LSD1 generation. A single transcript containing both Myocd-LSD1 and mCherry sequences is transcribed, which is then translated into two proteins through separated ribosomal initiation (IRES sequence). (B) Schematic

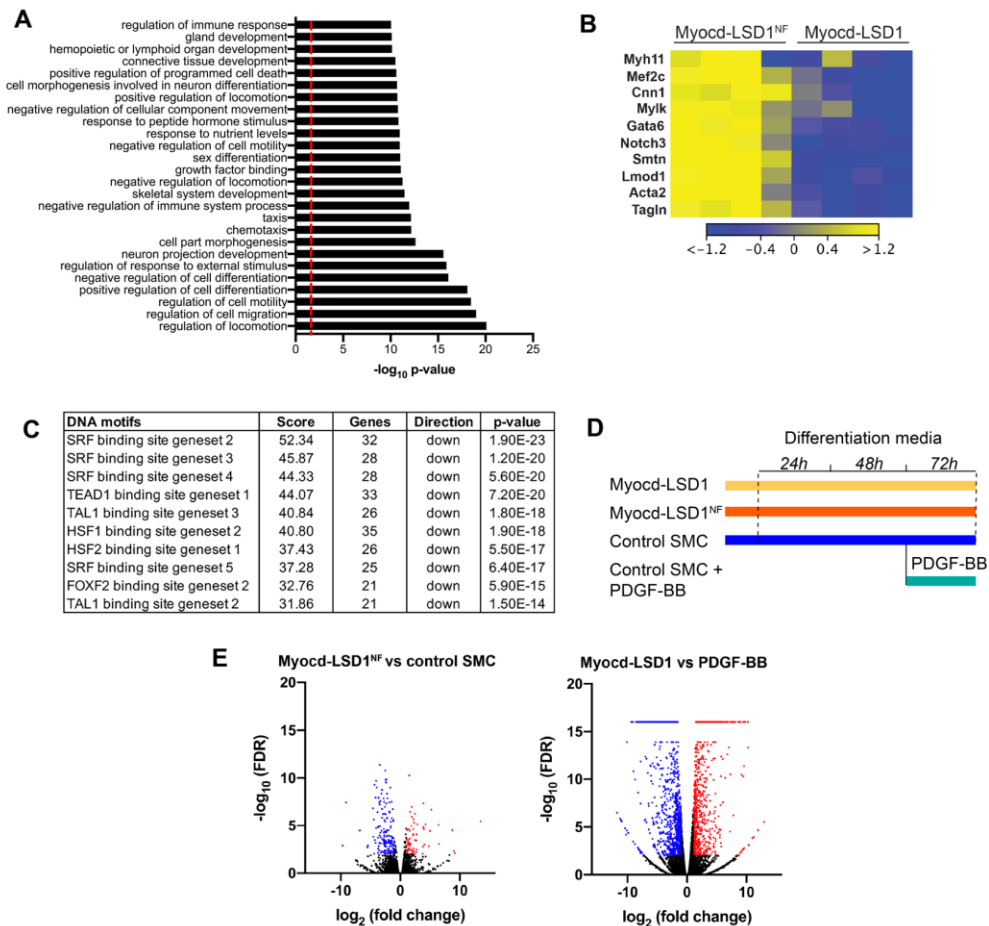
representation of primers used for detection of Myocd-LSD1 expression (top) by qRT-PCR. Myocd-LSD1 quantification in carotid arteries receiving control, Myocd-LSD1, or Myocd-LSD1^{NF} lentivirus (right). qRT-PCR products were visualized on 1% agarose gel (bottom left). (C) Validation of lentivirus delivery and SMC transduction in vivo by YFP and mCherry co-staining. mCherry staining specificity was assessed by comparing to IgG control and staining in both infected (right carotid) and non-infected (left carotid) arteries. A limited endogenous mCherry signal was detected. Scale bar = 100 μ m. (D) Immunofluorescent staining of FLAG-tagged Myocd-LSD1/Myocd-LSD1^{NF} using a FLAG antibody in control, Myocd-LSD1 or Myocd-LSD1^{NF} infected carotid arteries. Scale bar = 100 μ m. (E) Morphometric analysis of Myocd-LSD1 and Myocd-LSD1^{NF} infected carotid artery cross-sections. N=4 per group. (F) Number of nuclei in Myocd-LSD1^{NF} and Myocd-LSD1 lentivirus infected carotid artery cross-sections. N=4 per group. (G) Cell proliferation measured in control SMC, Myocd-LSD1, and Myocd-LSD1^{NF} SMC cultured in media containing 10% FBS for 48 hours. (H) Relative transcript expression of apoptotic markers Bcl2 and Bax in cultured SMC. (I) Cell viability measured by cell titer Glo luciferase assay. (J) Representative images of Immunofluorescent staining for DAPI, YFP, ACTA2, Ki67 (left), or cleaved-caspase 3 (right) to assess SMC proliferation and apoptosis in the right carotid arteries of SMC-lineage tracing mice transduced with Myocd-LSD1 or Myocd-LSD1^{NF}. Scale bar = 100 μ m. In vitro experiments were repeated 3-4 times independently. Data are represented as mean \pm s.e.m. Groups were compared by Student t-test (E, F), One-Way ANOVA (H, I), or Two-Way ANOVA (G). * p<0.0001.



Appendix Figure 4 TET2 interacts with H3K4me2 in SMC

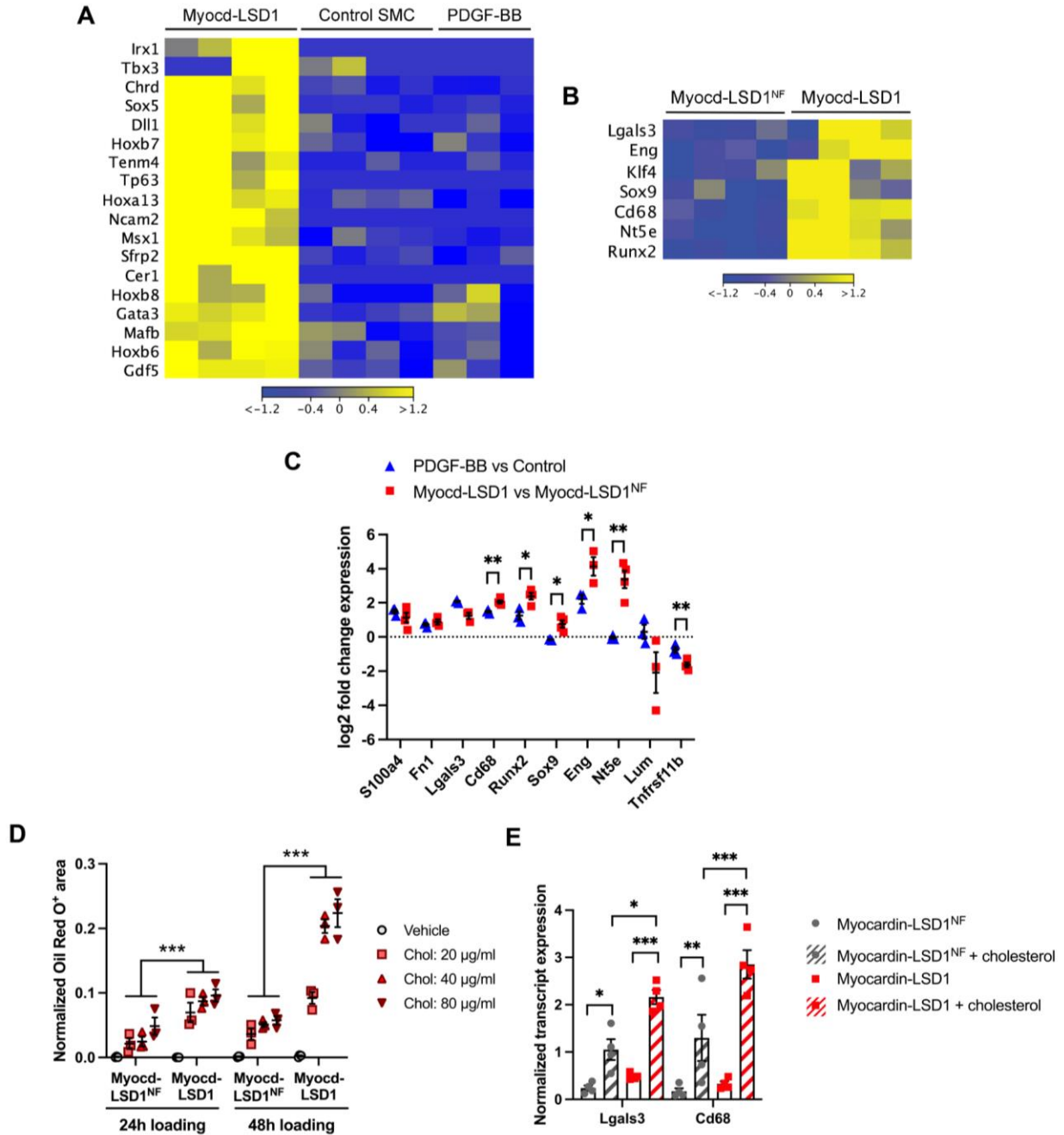
(A) Validation of HA-TET2 expression in control SMC and Myocd-LSD1 SMC transduced with Adv-HA-TET2 and anti-HA tag antibody specificity used in CUT&Tag sequencing. Scale bar: 100 μ m. (B) Venn Diagram showing the overlap between HA-TET2 occupancy in Myocd-LSD1 and control SMC. (C) Venn diagram showing the overlap between 5hmC and H3K4me2 enrichment in human SMC. (D) Summary table comparing the overlap between 5hmC

and H3K4me1/me2/me3 enriched genes in human SMC (based on Fig 4H). (E) TET2 expression levels in PDGF-BB (30 ng/mL) or rapamycin (100 nM) treated SMC measured by qRT-PCR. (F) Quantification of PLA dot number per nucleus per field of view in control SMC treated with rapamycin (100 nM), PDGF-BB (30 ng/mL), or vehicle for 24 h. (G) Representative micrographs of proximity ligation assay (PLA) detecting the interactions between H3K4me2 and TET2 in control SMC treated rapamycin (100 nM), PDGF-BB (30 ng/mL), or vehicle for 24h. Scale bar = 25 μ m. (H) In vivo H3K4me2/TET2 PLA performed in mouse aortic cross-sections in association with ACTA2 staining. Scale bar = 50 μ m. (I) Reverse co-immunoprecipitation (IP) of HA-tagged TET2 and biotin-H3K4me2 peptide. IP was performed with an anti-Biotin antibody or IgG control. Interaction with HA-TET2 was assessed by Western Blot using an anti-HA antibody. Experiments were repeated 3-6 times independently. Groups were compared by Student t-test (E) or One-Way ANOVA (F). * $p < 0.0001$.



Appendix Figure 5 RNAseq reveals marked differences in transcription profiles in Myocd-LSD1 expressing SMC

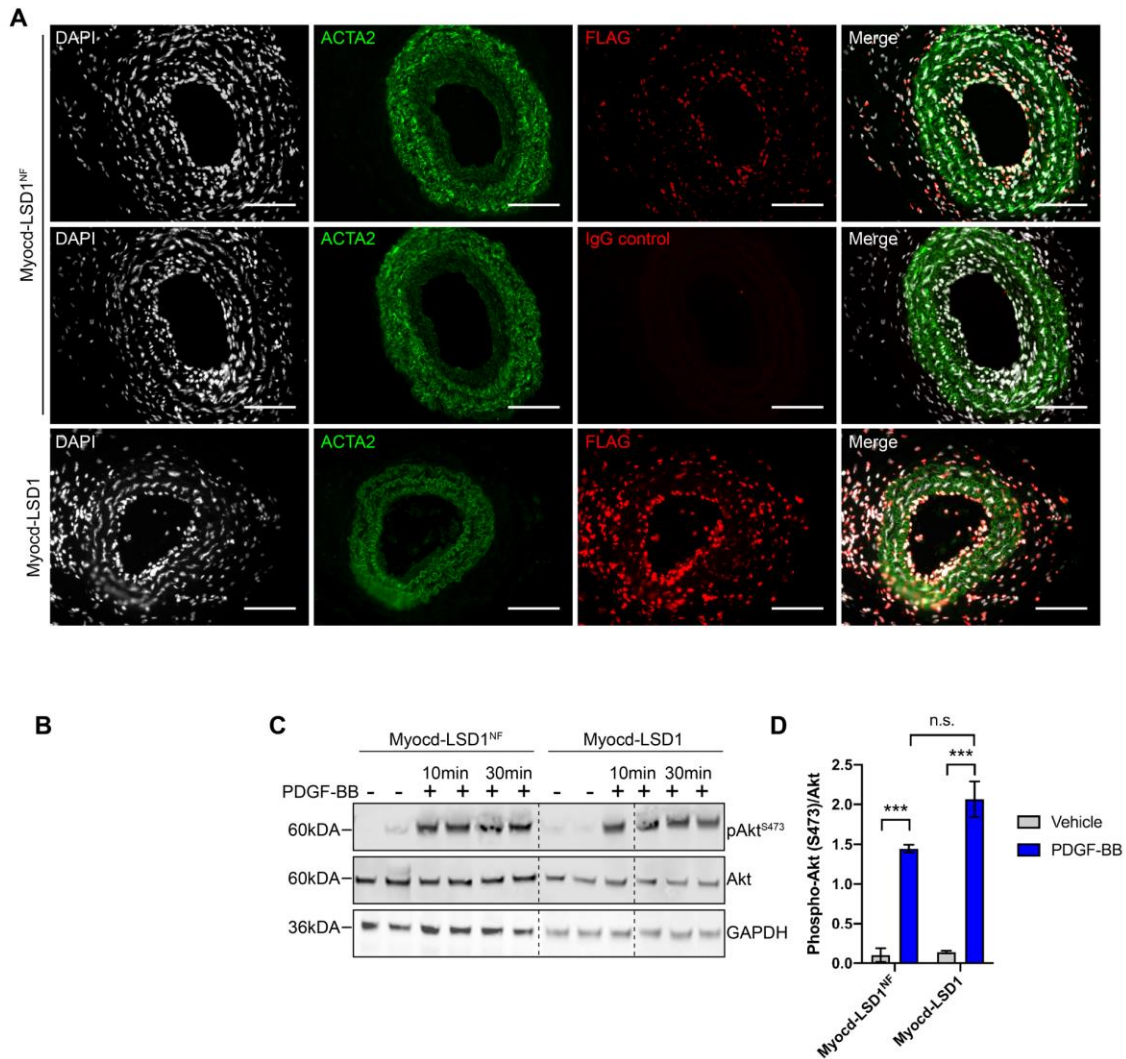
(A) Unfiltered Gene-Ontology pathways upregulated in Myocd-LSD1 SMC vs. Myocd-LSD1^{NF} SMC. (B) Heat map showing the differential expression of SMC contractile genes and master regulators between Myocd-LSD1 and Myocd-LSD1^{NF} SMC. (C) Table listing the most enriched DNA motifs in significantly downregulated genes in Myocd-LSD1 vs. Myocd-LSD1^{NF} SMC. (D) Schematics of RNA- seq experiment design: RNA sequencing was performed on control, Myocd-LSD1, and Myocd-LSD1^{NF} SMC and control SMC treated with PDGF-BB (30ng/ml) for 24 h. (E) Volcano plots showing the differential expression in transcripts in control SMC vs. Myocd-LSD1^{NF} (left) and Myocd-LSD1 vs. PDGF-BB treated SMC (right). Blue dots indicate significantly downregulated genes, and red dots indicate significantly upregulated genes ($p < 0.05$ and fold change > 2 or < -2). The threshold for statistical significance is FDR corrected p-value < 0.05 .



Appendix Figure 6 H3K4me2 editing exacerbates SMC phenotypic plasticity

(A) Heatmap of differential expression of genes related with developmental programs or differentiation of other lineages in Myocd-LSD1, control, and PDGF-BB treated SMC. (B) Heatmap showing differentially expressed genes associated with SMC phenotypic plasticity between Myocd-LSD1 and Myocd-LSD1^{NF} SMC. (C) Comparative expression of genes presented in Fig 6C in Myocd-LSD1 and PDGF-BB treated SMC. Results are expressed as the fold change expression relative to the group's controls (Myocd-LSD1 vs. Myocd-LSD1^{NF} SMC and PDGF-BB treated

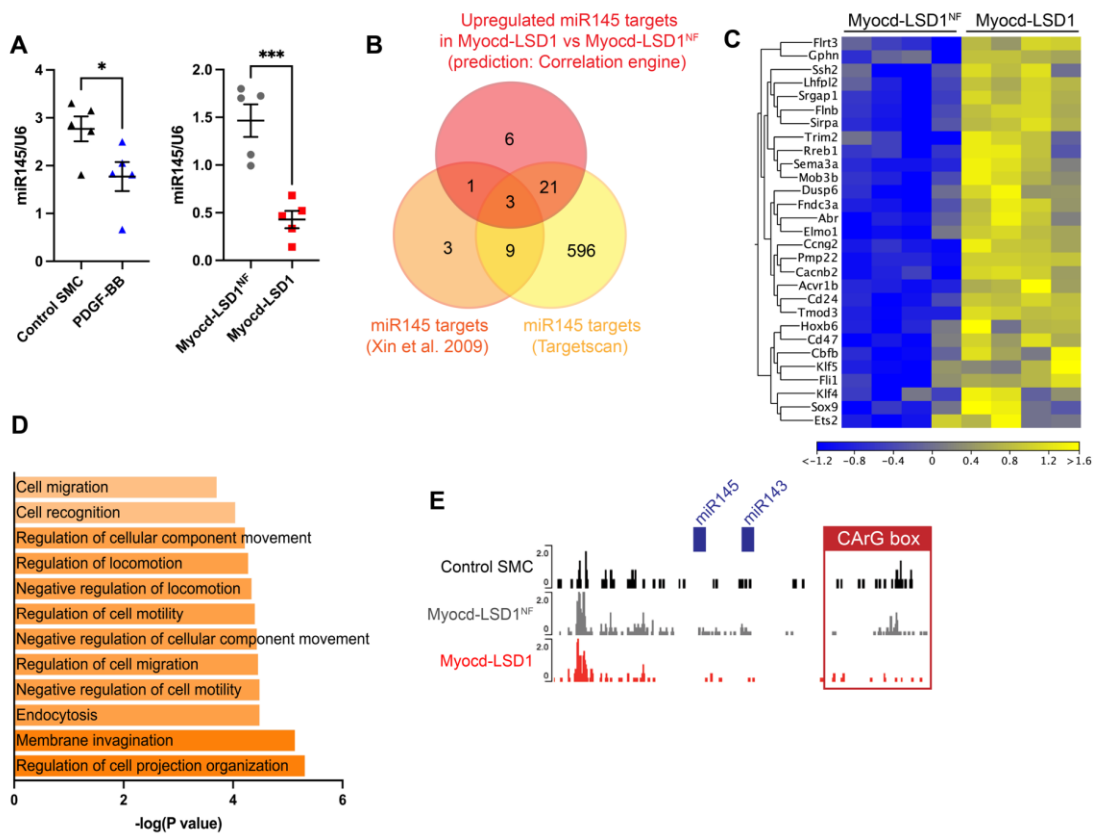
SMC vs. control SMC). (D) Quantification of Oil Red O+ area after cholesterol loading in Myocd-LSD1 and Myocd-LSD1^{NF} SMC (normalized to cellular area). (E) Lgals3 and Cd68 mRNA expression levels of Myocd-LSD1 and Myocd-LSD1^{NF} SMC treated with cholesterol (40 µg/ml) or vehicle for 48 h. Each experiment was repeated 3-4 times, independently. Data are represented as mean ± s.e.m. Groups were compared by Student t-test (C) Two-way ANOVA (D, E). p<0.0001



Appendix Figure 7 Myocd-LSD1 expression in ligated carotid artery induces impaired vascular remodeling due to PDGF-BB signaling-independent defective migration

(A) Immunofluorescent staining of FLAG-tagged Myocd-LSD1/Myocd-LSD1^{NF} and ACTA2 in carotid undergoing ligation and lentiviral delivery. IgG control was used to validate the specification of the anti-FLAG antibody. Scale bar = 100 μ m. (B) *Pdgfrb* transcript levels in Myocd-LSD1^{NF} and Myocd-LSD1 SMC. (C) Western blot detecting activated pAkt^{S473}, total Akt, and GAPDH in Myocd-LSD1^{NF} and Myocd-LSD1 SMC in response to PDGF-BB treatment. The dashed lines indicate breaks in the blot image. (D) Quantification of phosphorylated Akt normalized to total Akt in Myocd-LSD1^{NF}, and Myocd-LSD1 SMC treated with PDGF-BB for 10 min or 30 min. Each experiment

was repeated 3-4 times, independently. Data are represented as mean \pm s.e.m. Groups were compared by Student t-tests (B) and One-Way ANOVA (D). * $p < 0.0001$



Appendix Figure 8 H3K4me2 editing is associated with the upregulation of multiple miR 145 target genes related to cell migration and motility inhibition

(A) Comparison of miR-145 expression normalized to U6 between control, and PDGF-BB treated SMC (left) and Myocd-LSD1 and Myocd-LSD1^{NF} SMC (right). (B) Venn Diagram of miR145 target genes between three groups: (1) upregulated miR145 target genes in Myocd-LSD1 SMC comparing to Myocd-LSD1^{NF} SMC, (2) miR145 targets related with cell migration and cytoskeleton dynamics identified in Xin et al. Genes Dev. 2009²⁰³, (3) miR145 target prediction by Targetscan database. (C) Heatmap of upregulated miR-145 target genes in Myocd-LSD1 SMC vs. Myocd-LSD1^{NF} SMC extracted from the RNAseq dataset. (D) Gene Ontology pathway analysis performed on the significantly downregulated miR145 target genes in Myocd-LSD1 SMC compared to Myocd-LSD1^{NF}. Several significantly enriched pathways are associated with negative regulation of cell motility and migration. (E) CUT&Tag H3K4me2 tracks in the miR145/miR143 cluster and the upstream regulatory CARG box in control, Myocd-LSD1, and Myocd-LSD1^{NF} SMC. Each experiment was repeated 3-5 times, independently. Data are represented as mean ± s.e.m. Groups were compared by Student t-test (A). * p<0.0001

Bibliography

- 1 Basatemur, G. L., Jorgensen, H. F., Clarke, M. C. H., Bennett, M. R. & Mallat, Z. Vascular smooth muscle cells in atherosclerosis. *Nat Rev Cardiol* **16**, 727-744, doi:10.1038/s41569-019-0227-9 (2019).
- 2 Owens, G. K. Molecular control of vascular smooth muscle cell differentiation and phenotypic plasticity. *Novartis Found Symp* **283**, 174-191; discussion 191-173, 238-141 (2007).
- 3 Gabbiani, G. *et al.* Vascular smooth muscle cells differ from other smooth muscle cells: predominance of vimentin filaments and a specific alpha-type actin. *Proc Natl Acad Sci U S A* **78**, 298-302, doi:10.1073/pnas.78.1.298 (1981).
- 4 Gown, A. M., Vogel, A. M., Gordon, D. & Lu, P. L. A smooth muscle-specific monoclonal antibody recognizes smooth muscle actin isozymes. *J Cell Biol* **100**, 807-813, doi:10.1083/jcb.100.3.807 (1985).
- 5 Chamley, J. H., Gröschel-Stewart, U., Campbell, G. R. & Burnstock, G. Distinction between smooth muscle, fibroblasts and endothelial cells in culture by the use of fluoresceinated antibodies against smooth muscle actin. *Cell Tissue Res* **177**, 445-457, doi:10.1007/bf00220606 (1977).
- 6 Miano, J. M., Cserjesi, P., Ligon, K. L., Periasamy, M. & Olson, E. N. Smooth muscle myosin heavy chain exclusively marks the smooth muscle lineage during mouse embryogenesis. *Circ Res* **75**, 803-812, doi:10.1161/01.res.75.5.803 (1994).
- 7 Babij, P., Kelly, C. & Periasamy, M. Characterization of a mammalian smooth muscle myosin heavy-chain gene: complete nucleotide and protein coding sequence and analysis of the 5' end of the gene. *Proc Natl Acad Sci U S A* **88**, 10676-10680, doi:10.1073/pnas.88.23.10676 (1991).
- 8 Duband, J. L., Gimona, M., Scatena, M., Sartore, S. & Small, J. V. Calponin and SM 22 as differentiation markers of smooth muscle: spatiotemporal distribution during avian embryonic development. *Differentiation* **55**, 1-11, doi:10.1111/j.1432-0436.1993.tb00027.x (1993).
- 9 Fisher, S. A. Vascular smooth muscle phenotypic diversity and function. *Physiol Genomics* **42A**, 169-187, doi:10.1152/physiolgenomics.00111.2010 (2010).
- 10 Webb, R. C. SMOOTH MUSCLE CONTRACTION AND RELAXATION. *Advances in Physiology Education* **27**, 201-206, doi:10.1152/advan.00025.2003 (2003).

- 11 Wang, L. *et al.* Mutations in myosin light chain kinase cause familial aortic dissections. *Am J Hum Genet* **87**, 701-707, doi:10.1016/j.ajhg.2010.10.006 (2010).
- 12 Blatter, L. A. & Wier, W. G. Nitric oxide decreases $[Ca^{2+}]_i$ in vascular smooth muscle by inhibition of the calcium current. *Cell Calcium* **15**, 122-131, doi:10.1016/0143-4160(94)90051-5 (1994).
- 13 Campbell, G. R., Uehara, Y., Malmfors, T. & Burnstock, G. Degeneration and regeneration of smooth muscle transplants in the anterior eye chamber. An ultrastructural study. *Z Zellforsch Mikrosk Anat* **117**, 155-175, doi:10.1007/BF00330735 (1971).
- 14 Poole, J. C., Cromwell, S. B. & Benditt, E. P. Behavior of smooth muscle cells and formation of extracellular structures in the reaction of arterial walls to injury. *Am J Pathol* **62**, 391-414 (1971).
- 15 Chamley, J. H., Campbell, G. R. & Burnstock, G. Dedifferentiation, redifferentiation and bundle formation of smooth muscle cells in tissue culture: the influence of cell number and nerve fibres. *J Embryol Exp Morphol* **32**, 297-323 (1974).
- 16 Chamley-Campbell, J. H. & Campbell, G. R. What controls smooth muscle phenotype? *Atherosclerosis* **40**, 347-357, doi:[https://doi.org/10.1016/0021-9150\(81\)90145-3](https://doi.org/10.1016/0021-9150(81)90145-3) (1981).
- 17 Carmeliet, P. Mechanisms of angiogenesis and arteriogenesis. *Nature Medicine* **6**, 389-395, doi:Doi 10.1038/74651 (2000).
- 18 Hungerford, J. E. & Little, C. D. Developmental biology of the vascular smooth muscle cell: Building a multilayered vessel wall. *Journal of Vascular Research* **36**, 2-27, doi:Doi 10.1159/000025622 (1999).
- 19 Ross, R. Atherosclerosis is an inflammatory disease. *Am Heart J* **138**, S419-S420, doi:Doi 10.1016/S0002-8703(99)70266-8 (1999).
- 20 Caplice, N. M. *et al.* Smooth muscle cells in human coronary atherosclerosis can originate from cells administered at marrow transplantation. *P Natl Acad Sci USA* **100**, 4754-4759, doi:10.1073/pnas.0730743100 (2003).
- 21 Jacobsen, K. *et al.* Diverse cellular architecture of atherosclerotic plaque derives from clonal expansion of a few medial SMCs. *Jci Insight* **2**, doi:10.1172/jci.insight.95890 (2017).
- 22 Speer, M. Y. *et al.* Smooth muscle cells give rise to osteochondrogenic precursors and chondrocytes in calcifying arteries. *Circ Res* **104**, 733-741, doi:10.1161/CIRCRESAHA.108.183053 (2009).
- 23 Feil, S. *et al.* Transdifferentiation of vascular smooth muscle cells to macrophage-like cells during atherogenesis. *Circ Res* **115**, 662-667, doi:10.1161/CIRCRESAHA.115.304634 (2014).

- 24 Shankman, L. S. *et al.* KLF4-dependent phenotypic modulation of smooth muscle cells has a key role in atherosclerotic plaque pathogenesis. *Nat Med* **21**, 628-637, doi:10.1038/nm.3866 (2015).
- 25 Chappell, J. *et al.* Extensive Proliferation of a Subset of Differentiated, yet Plastic, Medial Vascular Smooth Muscle Cells Contributes to Neointimal Formation in Mouse Injury and Atherosclerosis Models. *Circ Res* **119**, 1313-1323, doi:10.1161/CIRCRESAHA.116.309799 (2016).
- 26 Wang, Y. *et al.* Smooth Muscle Cells Contribute the Majority of Foam Cells in ApoE (Apolipoprotein E)-Deficient Mouse Atherosclerosis. *Arterioscler Thromb Vasc Biol*, ATVBAHA119312434, doi:10.1161/ATVBAHA.119.312434 (2019).
- 27 Majesky, M. W. *et al.* Differentiated Smooth Muscle Cells Generate a Subpopulation of Resident Vascular Progenitor Cells in the Adventitia Regulated by Klf4. *Circ Res* **120**, 296-311, doi:10.1161/CIRCRESAHA.116.309322 (2017).
- 28 Long, J. Z. *et al.* A smooth muscle-like origin for beige adipocytes. *Cell Metab* **19**, 810-820, doi:10.1016/j.cmet.2014.03.025 (2014).
- 29 Liu, M. & Gomez, D. Smooth Muscle Cell Phenotypic Diversity. *Arterioscler Thromb Vasc Biol* **39**, 1715-1723, doi:10.1161/ATVBAHA.119.312131 (2019).
- 30 Pan, H. Z. *et al.* Single-Cell Genomics Reveals a Novel Cell State During Smooth Muscle Cell Phenotypic Switching and Potential Therapeutic Targets for Atherosclerosis in Mouse and Human. *Circulation* **142**, 2060-2075, doi:10.1161/Circulationaha.120.048378 (2020).
- 31 Alencar, G. F. *et al.* Stem Cell Pluripotency Genes Klf4 and Oct4 Regulate Complex SMC Phenotypic Changes Critical in Late-Stage Atherosclerotic Lesion Pathogenesis. *Circulation* **142**, 2045-2059, doi:10.1161/CIRCULATIONAHA.120.046672 (2020).
- 32 Wirka, R. C. *et al.* Atheroprotective roles of smooth muscle cell phenotypic modulation and the TCF21 disease gene as revealed by single-cell analysis. *Nature Medicine* **25**, 1280-+, doi:10.1038/s41591-019-0512-5 (2019).
- 33 Dobnikar, L. *et al.* Disease-relevant transcriptional signatures identified in individual smooth muscle cells from healthy mouse vessels. *Nature Communications* **9**, doi:ARTN 456710.1038/s41467-018-06891-x (2018).
- 34 Espinosa-Diez, C., Mandi, V., Du, M., Liu, M. & Gomez, D. Smooth muscle cells in atherosclerosis: clones but not carbon copies. *JVS Vasc Sci* **2**, 136-148, doi:10.1016/j.jvssci.2021.02.002 (2021).
- 35 Owens, G. K. Regulation of differentiation of vascular smooth muscle cells. *Physiol Rev* **75**, 487-517, doi:10.1152/physrev.1995.75.3.487 (1995).

- 36 Campbell, J. H. & Campbell, G. R. Smooth muscle phenotypic modulation--a personal experience. *Arterioscler Thromb Vasc Biol* **32**, 1784-1789, doi:10.1161/ATVBAHA.111.243212 (2012).
- 37 Chamley-Campbell, J., Campbell, G. R. & Ross, R. The smooth muscle cell in culture. *Physiol Rev* **59**, 1-61, doi:10.1152/physrev.1979.59.1.1 (1979).
- 38 Gomez, D. & Owens, G. K. Smooth muscle cell phenotypic switching in atherosclerosis. *Cardiovasc Res* **95**, 156-164, doi:10.1093/cvr/cvs115 (2012).
- 39 Regan, C. P., Adam, P. J., Madsen, C. S. & Owens, G. K. Molecular mechanisms of decreased smooth muscle differentiation marker expression after vascular injury. *Journal of Clinical Investigation* **106**, 1139-1147, doi:Doi 10.1172/Jci10522 (2000).
- 40 Wamhoff, B. R. *et al.* A G/C element mediates repression of the SM22alpha promoter within phenotypically modulated smooth muscle cells in experimental atherosclerosis. *Circ Res* **95**, 981-988, doi:10.1161/01.RES.0000147961.09840.fb (2004).
- 41 Li, L., Miano, J. M., Cserjesi, P. & Olson, E. N. SM22 alpha, a marker of adult smooth muscle, is expressed in multiple myogenic lineages during embryogenesis. *Circ Res* **78**, 188-195 (1996).
- 42 Kovacic, J. C. *et al.* Endothelial to Mesenchymal Transition in Cardiovascular Disease: JACC State-of-the-Art Review. *J Am Coll Cardiol* **73**, 190-209, doi:10.1016/j.jacc.2018.09.089 (2019).
- 43 Chakraborty, R. *et al.* Promoters to Study Vascular Smooth Muscle. *Arterioscler Thromb Vasc Biol*, ATVBAHA119312449, doi:10.1161/ATVBAHA.119.312449 (2019).
- 44 Allahverdian, S., Chaabane, C., Boukais, K., Francis, G. A. & Bochaton-Piallat, M. L. Smooth muscle cell fate and plasticity in atherosclerosis. *Cardiovasc Res* **114**, 540-550, doi:10.1093/cvr/cvy022 (2018).
- 45 Feil, R. *et al.* Ligand-activated site-specific recombination in mice. *P Natl Acad Sci USA* **93**, 10887-10890, doi:DOI 10.1073/pnas.93.20.10887 (1996).
- 46 Kuhbandner, S. *et al.* Temporally controlled somatic mutagenesis in smooth muscle. *Genesis* **28**, 15-22 (2000).
- 47 Wolfsgruber, W. *et al.* A proatherogenic role for cGMP-dependent protein kinase in vascular smooth muscle cells. *Proc Natl Acad Sci U S A* **100**, 13519-13524, doi:10.1073/pnas.1936024100 (2003).
- 48 Feil, S., Hofmann, F. & Feil, R. SM22alpha modulates vascular smooth muscle cell phenotype during atherogenesis. *Circ Res* **94**, 863-865, doi:10.1161/01.RES.0000126417.38728.F6 (2004).

- 49 Wirth, A. *et al.* G12-G13-LARG-mediated signaling in vascular smooth muscle is required for salt-induced hypertension. *Nat Med* **14**, 64-68, doi:10.1038/nm1666 (2008).
- 50 Nemenoff, R. A. *et al.* SDF-1alpha induction in mature smooth muscle cells by inactivation of PTEN is a critical mediator of exacerbated injury-induced neointima formation. *Arterioscler Thromb Vasc Biol* **31**, 1300-1308, doi:10.1161/ATVBAHA.111.223701 (2011).
- 51 Gomez, D., Shankman, L. S., Nguyen, A. T. & Owens, G. K. Detection of histone modifications at specific gene loci in single cells in histological sections. *Nature Methods* **10**, 171, doi:10.1038/nmeth.2332 (2013).
- 52 Herring, B. P., Hoggatt, A. M., Burlak, C. & Offermanns, S. Previously differentiated medial vascular smooth muscle cells contribute to neointima formation following vascular injury. *Vasc Cell* **6**, 21, doi:10.1186/2045-824X-6-21 (2014).
- 53 Cherepanova, O. A. *et al.* Activation of the pluripotency factor OCT4 in smooth muscle cells is atheroprotective. *Nat Med* **22**, 657-665, doi:10.1038/nm.4109 (2016).
- 54 Gomez, D. *et al.* Interleukin-1 beta has atheroprotective effects in advanced atherosclerotic lesions of mice. *Nature Medicine* **24**, 1418+, doi:10.1038/s41591-018-0124-5 (2018).
- 55 Misra, A. *et al.* Integrin beta3 regulates clonality and fate of smooth muscle-derived atherosclerotic plaque cells. *Nat Commun* **9**, 2073, doi:10.1038/s41467-018-04447-7 (2018).
- 56 Sheikh, A. Q., Misra, A., Rosas, I. O., Adams, R. H. & Greif, D. M. Smooth muscle cell progenitors are primed to muscularize in pulmonary hypertension. *Sci Transl Med* **7**, 308ra159, doi:10.1126/scitranslmed.aaa9712 (2015).
- 57 Benditt, E. P. & Benditt, J. M. Evidence for a monoclonal origin of human atherosclerotic plaques. *Proc Natl Acad Sci U S A* **70**, 1753-1756 (1973).
- 58 Murry, C. E., Gipaya, C. T., Bartosek, T., Benditt, E. P. & Schwartz, S. M. Monoclonality of smooth muscle cells in human atherosclerosis. *Am J Pathol* **151**, 697-705 (1997).
- 59 Pearson, T. A., Dillman, J. M., Solex, K. & Heptinstall, R. H. Clonal markers in the study of the origin and growth of human atherosclerotic lesions. *Circ Res* **43**, 10-18 (1978).
- 60 Pearson, T. A., Dillman, J. M., Solez, K. & Heptinstall, R. H. Clonal characteristics in layers of human atherosclerotic plaques. A study of the selection hypothesis of monoclonality. *Am J Pathol* **93**, 93-102 (1978).
- 61 Schwartz, S. M. & Murry, C. E. Proliferation and the monoclonal origins of atherosclerotic lesions. *Annu Rev Med* **49**, 437-460, doi:10.1146/annurev.med.49.1.437 (1998).
- 62 Chen, G. L. & Prchal, J. T. X-linked clonality testing: interpretation and limitations. *Blood* **110**, 1411-1419, doi:10.1182/blood-2006-09-018655 (2007).

- 63 van den Berg, I. M. *et al.* X chromosome inactivation is initiated in human preimplantation embryos. *Am J Hum Genet* **84**, 771-779, doi:10.1016/j.ajhg.2009.05.003 (2009).
- 64 Gomez, D. & Owens, G. K. Reconciling Smooth Muscle Cell Oligoclonality and Proliferative Capacity in Experimental Atherosclerosis. *Circ Res* **119**, 1262-1264, doi:10.1161/CIRCRESAHA.116.310104 (2016).
- 65 DiRenzo, D., Owens, G. K. & Leeper, N. J. "Attack of the Clones": Commonalities Between Cancer and Atherosclerosis. *Circ Res* **120**, 624-626, doi:10.1161/CIRCRESAHA.116.310091 (2017).
- 66 Schwartz, S. M., Virmani, R. & Majesky, M. W. An update on clonality: what smooth muscle cell type makes up the atherosclerotic plaque? *F1000Res* **7**, doi:10.12688/f1000research.15994.1 (2018).
- 67 Clement, M. *et al.* Vascular Smooth Muscle Cell Plasticity and Autophagy in Dissecting Aortic Aneurysms. *Arterioscler Thromb Vasc Biol*, ATVBAHA118311727, doi:10.1161/ATVBAHA.118.311727 (2019).
- 68 Greif, D. M. *et al.* Radial construction of an arterial wall. *Dev Cell* **23**, 482-493, doi:10.1016/j.devcel.2012.07.009 (2012).
- 69 Clowes, A. W., Reidy, M. A. & Clowes, M. M. Kinetics of cellular proliferation after arterial injury. I. Smooth muscle growth in the absence of endothelium. *Lab Invest* **49**, 327-333 (1983).
- 70 Clowes, A. W. & Schwartz, S. M. Significance of quiescent smooth muscle migration in the injured rat carotid artery. *Circ Res* **56**, 139-145 (1985).
- 71 Thomas, W. A., Florentin, R. A., Reiner, J. M., Lee, W. M. & Lee, K. T. Alterations in population dynamics of arterial smooth muscle cells during atherogenesis. IV. Evidence for a polyclonal origin of hypercholesterolemic diet-induced atherosclerotic lesions in young swine. *Exp Mol Pathol* **24**, 244-260 (1976).
- 72 Fuster, J. J. *et al.* Clonal hematopoiesis associated with TET2 deficiency accelerates atherosclerosis development in mice. *Science* **355**, 842-847, doi:10.1126/science.aag1381 (2017).
- 73 Jaiswal, S. *et al.* Clonal Hematopoiesis and Risk of Atherosclerotic Cardiovascular Disease. *N Engl J Med* **377**, 111-121, doi:10.1056/NEJMoa1701719 (2017).
- 74 Lu, Y. W. *et al.* Endothelial Myocyte Enhancer Factor 2c Inhibits Migration of Smooth Muscle Cells Through Fenestrations in the Internal Elastic Lamina. *Arterioscler Thromb Vasc Biol* **37**, 1380-1390, doi:10.1161/ATVBAHA.117.309180 (2017).
- 75 Newman, A. A. *et al.* Irradiation abolishes smooth muscle investment into vascular lesions in specific vascular beds. *Jci Insight* **3**, doi:10.1172/jci.insight.121017 (2018).

- 76 Stary, H. C. Macrophage foam cells in the coronary artery intima of human infants. *Ann N Y Acad Sci* **454**, 5-8, doi:10.1111/j.1749-6632.1985.tb11839.x (1985).
- 77 Natural history of aortic and coronary atherosclerotic lesions in youth. Findings from the PDAY Study. Pathobiological Determinants of Atherosclerosis in Youth (PDAY) Research Group. *Arterioscler Thromb* **13**, 1291-1298 (1993).
- 78 Majesky, M. W. Developmental basis of vascular smooth muscle diversity. *Arterioscler Thromb Vasc Biol* **27**, 1248-1258, doi:10.1161/ATVBAHA.107.141069 (2007).
- 79 Majesky, M. W. Vascular Development. *Arterioscler Thromb Vasc Biol* **38**, e17-e24, doi:10.1161/ATVBAHA.118.310223 (2018).
- 80 Li, S. *et al.* Innate diversity of adult human arterial smooth muscle cells: cloning of distinct subtypes from the internal thoracic artery. *Circ Res* **89**, 517-525 (2001).
- 81 Hao, H. *et al.* Heterogeneity of smooth muscle cell populations cultured from pig coronary artery. *Arterioscler Thromb Vasc Biol* **22**, 1093-1099 (2002).
- 82 Frid, M. G., Moiseeva, E. P. & Stenmark, K. R. Multiple phenotypically distinct smooth muscle cell populations exist in the adult and developing bovine pulmonary arterial media in vivo. *Circ Res* **75**, 669-681 (1994).
- 83 Shanahan, C. M. & Weissberg, P. L. Smooth muscle cell heterogeneity: patterns of gene expression in vascular smooth muscle cells in vitro and in vivo. *Arterioscler Thromb Vasc Biol* **18**, 333-338 (1998).
- 84 Rensen, S. S., Doevendans, P. A. & van Eys, G. J. Regulation and characteristics of vascular smooth muscle cell phenotypic diversity. *Neth Heart J* **15**, 100-108, doi:10.1007/bf03085963 (2007).
- 85 Wissler, R. W. The arterial medial cell, smooth muscle, or multifunctional mesenchyme? *Circulation* **36**, 1-4 (1967).
- 86 Ross, R. & Klebanoff, S. J. The smooth muscle cell. I. In vivo synthesis of connective tissue proteins. *J Cell Biol* **50**, 159-171, doi:10.1083/jcb.50.1.159 (1971).
- 87 Humphrey, J. D., Dufresne, E. R. & Schwartz, M. A. Mechanotransduction and extracellular matrix homeostasis. *Nat Rev Mol Cell Biol* **15**, 802-812, doi:10.1038/nrm3896 (2014).
- 88 Dobnikar, L. *et al.* Disease-relevant transcriptional signatures identified in individual smooth muscle cells from healthy mouse vessels. *Nat Commun* **9**, 4567, doi:10.1038/s41467-018-06891-x (2018).
- 89 Cochain, C. *et al.* Single-Cell RNA-Seq Reveals the Transcriptional Landscape and Heterogeneity of Aortic Macrophages in Murine Atherosclerosis. *Circ Res* **122**, 1661-1674, doi:10.1161/CIRCRESAHA.117.312509 (2018).

- 90 Winkels, H. *et al.* Atlas of the Immune Cell Repertoire in Mouse Atherosclerosis Defined by Single-Cell RNA-Sequencing and Mass Cytometry. *Circ Res* **122**, 1675-1688, doi:10.1161/CIRCRESAHA.117.312513 (2018).
- 91 Kim, K. *et al.* Transcriptome Analysis Reveals Nonfoamy Rather Than Foamy Plaque Macrophages Are Proinflammatory in Atherosclerotic Murine Models. *Circ Res* **123**, 1127-1142, doi:10.1161/CIRCRESAHA.118.312804 (2018).
- 92 Bidy, B. A. *et al.* Single-cell mapping of lineage and identity in direct reprogramming. *Nature* **564**, 219-224, doi:10.1038/s41586-018-0744-4 (2018).
- 93 Kester, L. & van Oudenaarden, A. Single-Cell Transcriptomics Meets Lineage Tracing. *Cell Stem Cell* **23**, 166-179, doi:10.1016/j.stem.2018.04.014 (2018).
- 94 McArdle, S., Mikulski, Z. & Ley, K. Live cell imaging to understand monocyte, macrophage, and dendritic cell function in atherosclerosis. *J Exp Med* **213**, 1117-1131, doi:10.1084/jem.20151885 (2016).
- 95 van den Brink, S. C. *et al.* Single-cell sequencing reveals dissociation-induced gene expression in tissue subpopulations. *Nat Methods* **14**, 935-936, doi:10.1038/nmeth.4437 (2017).
- 96 Suter, D. M. *et al.* Mammalian genes are transcribed with widely different bursting kinetics. *Science* **332**, 472-474, doi:10.1126/science.1198817 (2011).
- 97 Raj, A. & van Oudenaarden, A. Nature, nurture, or chance: stochastic gene expression and its consequences. *Cell* **135**, 216-226, doi:10.1016/j.cell.2008.09.050 (2008).
- 98 Kim, J. K. & Marioni, J. C. Inferring the kinetics of stochastic gene expression from single-cell RNA-sequencing data. *Genome Biol* **14**, R7, doi:10.1186/gb-2013-14-1-r7 (2013).
- 99 Anastassiadis, K. *et al.* Dre recombinase, like Cre, is a highly efficient site-specific recombinase in *E. coli*, mammalian cells and mice. *Dis Model Mech* **2**, 508-515, doi:10.1242/dmm.003087 (2009).
- 100 Karimova, M., Splith, V., Karpinski, J., Pisabarro, M. T. & Buchholz, F. Discovery of Nigri/nox and Panto/pox site-specific recombinase systems facilitates advanced genome engineering. *Sci Rep* **6**, 30130, doi:10.1038/srep30130 (2016).
- 101 He, L. *et al.* Enhancing the precision of genetic lineage tracing using dual recombinases. *Nat Med* **23**, 1488-1498, doi:10.1038/nm.4437 (2017).
- 102 Liu, K. *et al.* A dual genetic tracing system identifies diverse and dynamic origins of cardiac valve mesenchyme. *Development* **145**, doi:10.1242/dev.167775 (2018).
- 103 Pu, W. *et al.* Genetic Targeting of Organ-Specific Blood Vessels. *Circ Res* **123**, 86-99, doi:10.1161/CIRCRESAHA.118.312981 (2018).

- 104 Wang, D. *et al.* Activation of cardiac gene expression by myocardin, a transcriptional cofactor for serum response factor. *Cell* **105**, 851-862, doi:10.1016/s0092-8674(01)00404-4 (2001).
- 105 Du, K. L. *et al.* Myocardin is a critical serum response factor cofactor in the transcriptional program regulating smooth muscle cell differentiation. *Mol Cell Biol* **23**, 2425-2437, doi:10.1128/Mcb.23.7.2425-2437.2003 (2003).
- 106 Wang, Z. *et al.* Myocardin and ternary complex factors compete for SRF to control smooth muscle gene expression. *Nature* **428**, 185-189, doi:10.1038/nature02382 (2004).
- 107 Long, X. C., Creemers, E. E., Wang, D. Z., Olson, E. N. & Miano, J. M. Myocardin is a bifunctional switch for smooth versus skeletal muscle differentiation. *P Natl Acad Sci USA* **104**, 16570-16575, doi:10.1073/pnas.0708253104 (2007).
- 108 Miralles, F., Posern, G., Zaromytidou, A. I. & Treisman, R. Actin dynamics control SRF activity by regulation of its coactivator MAL. *Cell* **113**, 329-342, doi:10.1016/s0092-8674(03)00278-2 (2003).
- 109 Zaromytidou, A. I., Miralles, F. & Treisman, R. MAL and ternary complex factor use different mechanisms to contact a common surface on the serum response factor DNA-binding domain. *Molecular and Cellular Biology* **26**, 4134-4148, doi:10.1128/Mcb.01902-05 (2006).
- 110 Sun, Q. *et al.* Defining the mammalian CArGome. *Genome Res* **16**, 197-207, doi:10.1101/gr.4108706 (2006).
- 111 Miano, J. M., Kitchen, C. M., Chen, J. Y., Wang, D. Z. & Olson, E. N. Myocardin is expressed in adult aorta and activates a smooth muscle cell differentiation program. *Arterioscl Throm Vas* **22**, A2-A2 (2002).
- 112 Yoshida, T. *et al.* Myocardin is a key regulator of CArG-dependent transcription of multiple smooth muscle marker genes. *Circulation Research* **92**, 856-864, doi:10.1161/01.Res.0000068405.49081.09 (2003).
- 113 Chen, J. Y., Kitchen, C. M., Streb, J. W. & Miano, J. M. Myocardin: A component of a molecular switch for smooth muscle differentiation. *J Mol Cell Cardiol* **34**, 1345-1356, doi:10.1006/jmcc.2002.2086 (2002).
- 114 McDonald, O. G., Wamhoff, B. R., Hoofnagle, M. H. & Owens, G. K. Control of SRF binding to CArG box chromatin regulates smooth muscle gene expression in vivo. *J Clin Invest* **116**, 36-48, doi:10.1172/Jci26505 (2006).
- 115 Li, S. J., Wang, D. Z., Wang, Z. G., Richardson, J. A. & Olson, E. N. The serum response factor coactivator myocardin is required for vascular smooth muscle development. *P Natl Acad Sci USA* **100**, 9366-9370, doi:10.1073/pnas.1233635100 (2003).

- 116 Huang, J. H. *et al.* Myocardin regulates expression of contractile genes in smooth muscle cells and is required for closure of the ductus arteriosus in mice. *J Clin Invest* **118**, 515-525, doi:10.1172/Jc133304 (2008).
- 117 Huang, J. H. *et al.* Myocardin is required for maintenance of vascular and visceral smooth muscle homeostasis during postnatal development. *P Natl Acad Sci USA* **112**, 4447-4452, doi:10.1073/pnas.1420363112 (2015).
- 118 Xu, Z. H., Ji, G. D., Shen, J. B., Wang, X. B. & Li, L. SOX9 and myocardin counteract each other in regulating vascular smooth muscle cell differentiation. *Biochem Bioph Res Co* **422**, 285-290, doi:10.1016/j.bbrc.2012.04.149 (2012).
- 119 Yoshida, T., Gan, Q., Shang, Y. T. & Owens, G. K. Platelet-derived growth factor-BB represses smooth muscle cell marker genes via changes in binding of MKL factors and histone deacetylases to their promoters. *Am J Physiol-Cell Ph* **292**, C886-C895, doi:10.1152/ajpcell.00449.2006 (2007).
- 120 Yoshida, T., Gan, Q. & Owens, G. K. Kruppel-like factor 4, Elk-1, and histone deacetylases cooperatively suppress smooth muscle cell differentiation markers in response to oxidized phospholipids. *Am J Physiol-Cell Ph* **295**, C1175-C1182, doi:10.1152/ajpcell.00288.2008 (2008).
- 121 Nagao, M. *et al.* Coronary Disease-Associated Gene TCF21 Inhibits Smooth Muscle Cell Differentiation by Blocking the Myocardin-Serum Response Factor Pathway. *Circulation Research* **126**, 517-529, doi:10.1161/Circresaha.119.315968 (2020).
- 122 Jiang, J. M. *et al.* A core Klf circuitry regulates self-renewal of embryonic stem cells. *Nature Cell Biology* **10**, 353-U103, doi:10.1038/ncb1698 (2008).
- 123 Takahashi, K. & Yamanaka, S. Induction of pluripotent stem cells from mouse embryonic and adult fibroblast cultures by defined factors. *Cell* **126**, 663-676, doi:DOI 10.1016/j.cell.2006.07.024 (2006).
- 124 Wernig, M. *et al.* In vitro reprogramming of fibroblasts into a pluripotent ES-cell-like state. *Nature* **448**, 318-U312, doi:10.1038/nature05944 (2007).
- 125 Haskins, R. M. *et al.* Klf4 has an unexpected protective role in perivascular cells within the microvasculature. *Am J Physiol-Heart C* **315**, H402-H414, doi:10.1152/ajpheart.00084.2018 (2018).
- 126 Liu, Y. *et al.* Kruppel-like factor 4 abrogates myocardin-induced activation of smooth muscle gene expression. *J Biol Chem* **280**, 9719-9727, doi:10.1074/jbc.M412862200 (2005).
- 127 Cherepanova, O. A. *et al.* Oxidized Phospholipids Induce Type VIII Collagen Expression and Vascular Smooth Muscle Cell Migration. *Circulation Research* **104**, 609-U112, doi:10.1161/Circresaha.108.186064 (2009).

- 128 Yoshida, T., Kaestner, K. H. & Owens, G. K. Conditional deletion of Kruppel-like factor 4 delays downregulation of smooth muscle cell differentiation markers but accelerates neointimal formation following vascular injury. *Circulation Research* **102**, 1548-1557, doi:10.1161/Circresaha.108.176974 (2008).
- 129 Turner, E. C., Huang, C. L., Govindarajan, K. & Caplice, N. M. Identification of a Klf4-dependent upstream repressor region mediating transcriptional regulation of the myocardin gene in human smooth muscle cells. *Biochim Biophys Acta* **1829**, 1191-1201, doi:10.1016/j.bbagr.2013.09.002 (2013).
- 130 Salmon, M., Gomez, D., Greene, E., Shankman, L. & Owens, G. K. Cooperative binding of KLF4, pELK-1, and HDAC2 to a G/C repressor element in the SM22alpha promoter mediates transcriptional silencing during SMC phenotypic switching in vivo. *Circ Res* **111**, 685-696, doi:10.1161/CIRCRESAHA.112.269811 (2012).
- 131 Yoshida, T., Gan, Q. & Owens, G. K. Kruppel-like factor 4, Elk-1, and histone deacetylases cooperatively suppress smooth muscle cell differentiation markers in response to oxidized phospholipids. *Am J Physiol Cell Physiol* **295**, C1175-1182, doi:10.1152/ajpcell.00288.2008 (2008).
- 132 Shankman, L. S. *et al.* KLF4-dependent phenotypic modulation of smooth muscle cells has a key role in atherosclerotic plaque pathogenesis (vol 21, pg 628, 2015). *Nature Medicine* **22**, 217-217 (2016).
- 133 Jaenisch, R. & Bird, A. Epigenetic regulation of gene expression: how the genome integrates intrinsic and environmental signals. *Nature Genetics* **33**, 245-254, doi:10.1038/ng1089 (2003).
- 134 Jenuwein, T. & Allis, C. D. Translating the histone code. *Science* **293**, 1074-1080, doi:DOI 10.1126/science.1063127 (2001).
- 135 Hake, S. B., Xiao, A. & Allis, C. D. Linking the epigenetic 'language' of covalent histone modifications to cancer. *Brit J Cancer* **90**, 761-769, doi:10.1038/sj.bjc.6601575 (2004).
- 136 Bird, A. P. & Wolffe, A. P. Methylation-induced repression--belts, braces, and chromatin. *Cell* **99**, 451-454, doi:10.1016/s0092-8674(00)81532-9 (1999).
- 137 Tahiliani, M. *et al.* Conversion of 5-methylcytosine to 5-hydroxymethylcytosine in mammalian DNA by MLL partner TET1. *Science* **324**, 930-935, doi:10.1126/science.1170116 (2009).
- 138 Bird, A. DNA methylation patterns and epigenetic memory. *Genes Dev* **16**, 6-21, doi:10.1101/gad.947102 (2002).
- 139 Kaikkonen, M. U., Lam, M. T. Y. & Glass, C. K. Non-coding RNAs as regulators of gene expression and epigenetics. *Cardiovascular Research* **90**, 430-440, doi:10.1093/cvr/cvr097 (2011).

- 140 Maguire, E. M. & Xiao, Q. Z. Noncoding RNAs in vascular smooth muscle cell function and neointimal hyperplasia. *Febs Journal* **287**, 5260-5283, doi:10.1111/febs.15357 (2020).
- 141 Henikoff, S., Furuyama, T. & Ahmad, K. Histone variants, nucleosome assembly and epigenetic inheritance. *Trends Genet* **20**, 320-326, doi:10.1016/j.tig.2004.05.004 (2004).
- 142 Yao, F. *et al.* Histone Variant H2A.Z Is Required for the Maintenance of Smooth Muscle Cell Identity as Revealed by Single-Cell Transcriptomics. *Circulation* **138**, 2274-2288, doi:10.1161/Circulationaha.117.033114 (2018).
- 143 Cheung, P., Allis, C. D. & Sassone-Corsi, P. Signaling to chromatin through histone modifications. *Cell* **103**, 263-271, doi:Doi 10.1016/S0092-8674(00)00118-5 (2000).
- 144 Millan-Zambrano, G., Burton, A., Bannister, A. J. & Schneider, R. Histone post-translational modifications - cause and consequence of genome function. *Nature Reviews Genetics*, doi:10.1038/s41576-022-00468-7 (2022).
- 145 Zhao, S., Allis, C. D. & Wang, G. G. The language of chromatin modification in human cancers. *Nat Rev Cancer* **21**, 413-430, doi:10.1038/s41568-021-00357-x (2021).
- 146 Bannister, A. J. & Kouzarides, T. Regulation of chromatin by histone modifications. *Cell Research* **21**, 381-395, doi:10.1038/cr.2011.22 (2011).
- 147 Bernstein, B. E. *et al.* Methylation of histone H3 Lys 4 in coding regions of active genes. *Proc Natl Acad Sci U S A* **99**, 8695-8700, doi:10.1073/pnas.082249499 (2002).
- 148 Heintzman, N. D. *et al.* Distinct and predictive chromatin signatures of transcriptional promoters and enhancers in the human genome. *Nature Genetics* **39**, 311-318, doi:10.1038/ng1966 (2007).
- 149 Bernstein, B. E. *et al.* A bivalent chromatin structure marks key developmental genes in embryonic stem cells. *Cell* **125**, 315-326, doi:10.1016/j.cell.2006.02.041 (2006).
- 150 Rea, S. *et al.* Regulation of chromatin structure by site-specific histone H3 methyltransferases. *Nature* **406**, 593-599, doi:Doi 10.1038/35020506 (2000).
- 151 Feng, Q. *et al.* Methylation of H3-lysine 79 is mediated by a new family of HMTases without a SET domain. *Curr Biol* **12**, 1052-1058, doi:Pii S0960-9822(02)00901-6, Doi 10.1016/S0960-9822(02)00901-6 (2002).
- 152 Shi, Y. *et al.* Histone demethylation mediated by the nuclear amine oxidase homolog LSD1. *Cell* **119**, 941-953 (2004).
- 153 Cloos, P. A. C. *et al.* The putative oncogene GASC1 demethylates tri- and dimethylated lysine 9 on histone H3. *Nature* **442**, 307-311, doi:10.1038/nature04837 (2006).
- 154 Whetstine, J. R. *et al.* Reversal of histone lysine trimethylation by the JMJD2 family of histone demethylases. *Cell* **125**, 467-481, doi:10.1016/j.cell.2006.03.028 (2006).

- 155 Tsukada, Y. *et al.* Histone demethylation by a family of JmjC domain-containing proteins. *Nature* **439**, 811-816, doi:10.1038/nature04433 (2006).
- 156 Manabe, I. & Owens, G. K. Recruitment of serum response factor and hyperacetylation of histones at smooth muscle-specific regulatory regions during differentiation of a novel P19-derived in vitro smooth muscle differentiation system. *Circulation Research* **88**, 1127-1134, doi:DOI 10.1161/hh1101.091339 (2001).
- 157 Shang, Y. T., Yoshida, T., Amendt, B. A., Martin, J. F. & Owens, G. K. Pitx2 is functionally important in the early stages of vascular smooth muscle cell differentiation. *J Cell Biol* **181**, 461-473, doi:DOI 10.1083/jcb.200711145 (2008).
- 158 Qiu, P., Ritchie, R. P., Gong, X. Q., Hamamori, Y. & Li, L. Dynamic changes in chromatin acetylation and the expression of histone acetyltransferases and histone deacetylases regulate the SM22alpha transcription in response to Smad3-mediated TGFbeta1 signaling. *Biochem Biophys Res Commun* **348**, 351-358, doi:10.1016/j.bbrc.2006.07.009 (2006).
- 159 Qiu, P. & Li, L. Histone acetylation and recruitment of serum responsive factor and CREB-binding protein onto SM22 promoter during SM22 gene expression. *Circ Res* **90**, 858-865, doi:10.1161/01.res.0000016504.08608.b9 (2002).
- 160 Cao, D. S. *et al.* Modulation of smooth muscle gene expression by association of histone acetyltransferases and deacetylases with myocardin. *Molecular and Cellular Biology* **25**, 364-376, doi:10.1128/Mcb.25.1.364-376.2005 (2005).
- 161 Liu, R. J. *et al.* Ten-Eleven Translocation-2 (TET2) Is a Master Regulator of Smooth Muscle Cell Plasticity. *Circulation* **128**, 2047-2057, doi:10.1161/Circulationaha.113.002887 (2013).
- 162 Gomez, D., Shankman, L. S., Nguyen, A. T. & Owens, G. K. Detection of histone modifications at specific gene loci in single cells in histological sections. *Nat Methods* **10**, 171-177, doi:10.1038/Nmeth.2332 (2013).
- 163 Shankman, L. S. *et al.* KLF4-dependent phenotypic modulation of smooth muscle cells has a key role in atherosclerotic plaque pathogenesis. *Nat Med* **21**, 628-637, doi:10.1038/nm.3866 (2015).
- 164 Wang, Y. *et al.* Clonally expanding smooth muscle cells promote atherosclerosis by escaping efferocytosis and activating the complement cascade. *P Natl Acad Sci USA* **117**, 15818-15826, doi:10.1073/pnas.2006348117 (2020).
- 165 Wang, Y. *et al.* Smooth Muscle Cells Contribute the Majority of Foam Cells in ApoE (Apolipoprotein E)-Deficient Mouse Atherosclerosis. *Arterioscler Thromb Vasc Biol* **39**, 876-887, doi:10.1161/ATVBAHA.119.312434 (2019).
- 166 Villeneuve, L. M. *et al.* Epigenetic histone H3 lysine 9 methylation in metabolic memory and inflammatory phenotype of vascular smooth muscle cells in diabetes. *P Natl Acad Sci USA* **105**, 9047-9052, doi:10.1073/pnas.0803623105 (2008).

- 167 Harman, J. L. *et al.* Epigenetic Regulation of Vascular Smooth Muscle Cells by Histone H3 Lysine 9 Dimethylation Attenuates Target Gene-Induction by Inflammatory Signaling. *Arterioscl Throm Vas* **39**, 2289-2302, doi:10.1161/Atvbaha.119.312765 (2019).
- 168 Jones, P. A. & Takai, D. The role of DNA methylation in mammalian epigenetics. *Science* **293**, 1068-1070, doi:DOI 10.1126/science.1063852 (2001).
- 169 Okano, M., Bell, D. W., Haber, D. A. & Li, E. DNA methyltransferases Dnmt3a and Dnmt3b are essential for de novo methylation and mammalian development. *Cell* **99**, 247-257, doi:10.1016/s0092-8674(00)81656-6 (1999).
- 170 Leonhardt, H., Page, A. W., Weier, H. U. & Bestor, T. H. A Targeting Sequence Directs DNA Methyltransferase to Sites of DNA-Replication in Mammalian Nuclei. *Cell* **71**, 865-873, doi:Doi 10.1016/0092-8674(92)90561-P (1992).
- 171 Suelves, M., Carrio, E., Nunez-Alvarez, Y. & Peinado, M. A. DNA methylation dynamics in cellular commitment and differentiation. *Brief Funct Genomics* **15**, 443-453, doi:10.1093/bfpg/elw017 (2016).
- 172 Tahiliani, M. *et al.* Conversion of 5-Methylcytosine to 5-Hydroxymethylcytosine in Mammalian DNA by MLL Partner TET1. *Science* **324**, 930-935, doi:10.1126/science.1170116 (2009).
- 173 Yin, X. T. & Xu, Y. H. Structure and Function of TET Enzymes. *DNA Methyltransferases - Role and Function* **945**, 275-302, doi:10.1007/978-3-319-43624-1_12 (2016).
- 174 Long, H. K., Blackledge, N. P. & Klose, R. J. ZF-CxxC domain-containing proteins, CpG islands and the chromatin connection. *Biochem Soc T* **41**, 727-740, doi:10.1042/Bst20130028 (2013).
- 175 Xu, Y. F. *et al.* Tet3 CXXC Domain and Dioxygenase Activity Cooperatively Regulate Key Genes for Xenopus Eye and Neural Development. *Cell* **151**, 1200-1213, doi:10.1016/j.cell.2012.11.014 (2012).
- 176 Xu, Y. F. *et al.* Genome-wide Regulation of 5hmC, 5mC, and Gene Expression by Tet1 Hydroxylase in Mouse Embryonic Stem Cells. *Molecular Cell* **42**, 451-464, doi:10.1016/j.molcel.2011.04.005 (2011).
- 177 Zhang, H. K. *et al.* TET1 is a DNA-binding protein that modulates DNA methylation and gene transcription via hydroxylation of 5-methylcytosine. *Cell Research* **20**, 1390-1393, doi:10.1038/cr.2010.156 (2010).
- 178 Pan, F., Weeks, O., Yang, F. C. & Xu, M. J. The TET2 interactors and their links to hematological malignancies. *Iubmb Life* **67**, 438-445, doi:10.1002/iub.1389 (2015).
- 179 Broome, R. *et al.* TET2 is a component of the estrogen receptor complex and controls 5mC to 5hmC conversion at estrogen receptor cis-regulatory regions. *Cell Rep* **34**, doi:ARTN 10877610.1016/j.celrep.2021.108776 (2021).

- 180 Guallar, D. *et al.* RNA-dependent chromatin targeting of TET2 for endogenous retrovirus control in pluripotent stem cells. *Nature Genetics* **50**, 443-451, doi:10.1038/s41588-018-0060-9 (2018).
- 181 Zhou, L. Y. *et al.* TET2-interacting long noncoding RNA promotes active DNA demethylation of the MMP-9 promoter in diabetic wound healing. *Cell Death & Disease* **10**, doi:ARTN 81310.1038/s41419-019-2047-6 (2019).
- 182 He, Y. F. *et al.* Tet-mediated formation of 5-carboxylcytosine and its excision by TDG in mammalian DNA. *Science* **333**, 1303-1307, doi:10.1126/science.1210944 (2011).
- 183 Ito, S. *et al.* Role of Tet proteins in 5mC to 5hmC conversion, ES-cell self-renewal and inner cell mass specification. *Nature* **466**, 1129-1133, doi:10.1038/nature09303 (2010).
- 184 Ito, S. *et al.* Tet Proteins Can Convert 5-Methylcytosine to 5-Formylcytosine and 5-Carboxylcytosine. *Science* **333**, 1300-1303, doi:10.1126/science.1210597 (2011).
- 185 Maiti, A. & Drohat, A. C. Thymine DNA Glycosylase Can Rapidly Excise 5-Formylcytosine and 5-Carboxylcytosine POTENTIAL IMPLICATIONS FOR ACTIVE DEMETHYLATION OF CpG SITES. *J Biol Chem* **286**, 35334-35338, doi:10.1074/jbc.C111.284620 (2011).
- 186 Hiltunen, M. *et al.* DNA hypomethylation and methyltransferase expression in atherosclerotic lesions. *Vasc Med* **7**, 5-11, doi:DOI 10.1191/1358863x02vm418oa (2002).
- 187 Laukkanen, M. O. *et al.* Local hypomethylation in atherosclerosis found in rabbit ec-sod gene. *Arterioscl Throm Vas* **19**, 2171-2178, doi:Doi 10.1161/01.Atv.19.9.2171 (1999).
- 188 Elia, L. *et al.* UHRF1 epigenetically orchestrates smooth muscle cell plasticity in arterial disease. *J Clin Invest* **128**, 2473-2486, doi:10.1172/JCI96121 (2018).
- 189 Wang, Y. S. *et al.* microRNA-152 Mediates DNMT1-Regulated DNA Methylation in the Estrogen Receptor alpha Gene. *Plos One* **7**, doi:ARTN e3063510.1371/journal.pone.0030635 (2012).
- 190 Ying, A. K. *et al.* Methylation of the estrogen receptor-alpha gene promoter is selectively increased in proliferating human aortic smooth muscle cells. *Cardiovascular Research* **46**, 172-179, doi:Doi 10.1016/S0008-6363(00)00004-3 (2000).
- 191 Azechi, T., Sato, F., Sudo, R. & Wachi, H. 5-aza-2 '-Deoxycytidine, a DNA Methyltransferase Inhibitor, Facilitates the Inorganic Phosphorus-Induced Mineralization of Vascular Smooth Muscle Cells. *Journal of Atherosclerosis and Thrombosis* **21**, 463-476, doi:DOI 10.5551/jat.20818 (2014).
- 192 Zhuang, J. H. *et al.* The Yin-Yang Dynamics of DNA Methylation Is the Key Regulator for Smooth Muscle Cell Phenotype Switch and Vascular Remodeling. *Arterioscl Throm Vas* **37**, 84-97, doi:10.1161/Atvbaha.116.307923 (2017).

- 193 Strand, K. A. *et al.* High Throughput Screen Identifies the DNMT1 (DNA Methyltransferase-1) Inhibitor, 5-Azacytidine, as a Potent Inducer of PTEN (Phosphatase and Tensin Homolog) Central Role for PTEN in 5-Azacytidine Protection Against Pathological Vascular Remodeling. *Arterioscl Throm Vas* **40**, 1854-1869, doi:10.1161/Atvbaha.120.314458 (2020).
- 194 Lian, C. G. *et al.* Loss of 5-Hydroxymethylcytosine Is an Epigenetic Hallmark of Melanoma. *Cell* **150**, 1135-1146, doi:10.1016/j.cell.2012.07.033 (2012).
- 195 Ostriker, A. C. *et al.* TET2 Protects Against Vascular Smooth Muscle Cell Apoptosis and Intimal Thickening in Transplant Vasculopathy. *Circulation* **144**, 455-470, doi:10.1161/Circulationaha.120.050553 (2021).
- 196 Flynt, A. S. & Lai, E. C. Biological principles of microRNA-mediated regulation: shared themes amid diversity. *Nature Reviews Genetics* **9**, 831-842, doi:10.1038/nrg2455 (2008).
- 197 Pan, Y. Q., Balazs, L., Tigyi, G. & Yue, J. M. Conditional deletion of Dicer in vascular smooth muscle cells leads to the developmental delay and embryonic mortality. *Biochem Bioph Res Co* **408**, 369-374, doi:10.1016/j.bbrc.2011.02.119 (2011).
- 198 Albinsson, S. *et al.* MicroRNAs Are Necessary for Vascular Smooth Muscle Growth, Differentiation, and Function. *Arterioscl Throm Vas* **30**, 1118-U1180, doi:10.1161/Atvbaha.109.200873 (2010).
- 199 Cordes, K. R. *et al.* miR-145 and miR-143 regulate smooth muscle cell fate and plasticity. *Nature* **460**, 705-U780, doi:10.1038/nature08195 (2009).
- 200 Ella, L. *et al.* The knockout of miR-143 and-145 alters smooth muscle cell maintenance and vascular homeostasis in mice: correlates with human disease. *Cell Death and Differentiation* **16**, 1590-1598, doi:10.1038/cdd.2009.153 (2009).
- 201 Boettger, T. *et al.* Acquisition of the contractile phenotype by murine arterial smooth muscle cells depends on the Mir143/145 gene cluster. *Journal of Clinical Investigation* **119**, 2634-2647, doi:10.1172/Jci38864 (2009).
- 202 Cheng, Y. H. *et al.* MicroRNA-145, a Novel Smooth Muscle Cell Phenotypic Marker and Modulator, Controls Vascular Neointimal Lesion Formation. *Circulation Research* **105**, 158-U113, doi:10.1161/Circresaha.109.197517 (2009).
- 203 Xin, M. *et al.* MicroRNAs miR-143 and miR-145 modulate cytoskeletal dynamics and responsiveness of smooth muscle cells to injury. *Gene Dev* **23**, 2166-2178, doi:10.1101/gad.1842409 (2009).
- 204 Zhong, W. *et al.* Hypermethylation of the Micro-RNA 145 Promoter Is the Key Regulator for NLRP3 Inflammasome-Induced Activation and Plaque Formation (vol 3, pg 604, 2018). *Jacc-Basic Transl Sc* **5**, 1264-1265, doi:10.1016/j.jacbts.2020.11.003 (2020).

- 205 Du, M. *et al.* miRNA/mRNA co-profiling identifies the miR-200 family as a central regulator of SMC quiescence. *iScience* **25**, 104169, doi:10.1016/j.isci.2022.104169 (2022).
- 206 Pu, Z., Lu, J. B. & Yang, X. H. Emerging Roles of Circular RNAs in Vascular Smooth Muscle Cell Dysfunction. *Frontiers in Genetics* **12**, doi:ARTN 749296 10.3389/fgene.2021.749296 (2022).
- 207 Sun, Y. *et al.* A Novel Regulatory Mechanism of Smooth Muscle alpha-Actin Expression by NRG-1/circACTA2/miR-548f-5p Axis. *Circ Res* **121**, 628-635, doi:10.1161/CIRCRESAHA.117.311441 (2017).
- 208 Ma, Y. *et al.* circACTA2 mediates Ang II-induced VSMC senescence by modulation of the interaction of ILF3 with CDK4 mRNA. *Aging (Albany NY)* **13**, 11610-11628, doi:10.18632/aging.202855 (2021).
- 209 Simion, V., Haemmig, S. & Feinberg, M. W. LncRNAs in vascular biology and disease. *Vasc Pharmacol* **114**, 145-156, doi:10.1016/j.vph.2018.01.003 (2019).
- 210 Ieda, M. *et al.* Direct reprogramming of fibroblasts into functional cardiomyocytes by defined factors. *Cell* **142**, 375-386, doi:10.1016/j.cell.2010.07.002 (2010).
- 211 Stergachis, A. B. *et al.* Developmental fate and cellular maturity encoded in human regulatory DNA landscapes. *Cell* **154**, 888-903, doi:10.1016/j.cell.2013.07.020 (2013).
- 212 Park, S. H. *et al.* Ultrastructure of human embryonic stem cells and spontaneous and retinoic acid-induced differentiating cells. *Ultrastruct Pathol* **28**, 229-238, doi:10.1080/01913120490515595 (2004).
- 213 Hawkins, R. D. *et al.* Distinct Epigenomic Landscapes of Pluripotent and Lineage-Committed Human Cells. *Cell Stem Cell* **6**, 479-491, doi:10.1016/j.stem.2010.03.018 (2010).
- 214 Wen, B., Wu, H., Shinkai, Y., Irizarry, R. A. & Feinberg, A. P. Large histone H3 lysine 9 dimethylated chromatin blocks distinguish differentiated from embryonic stem cells. *Nature Genetics* **41**, 246-250, doi:10.1038/ng.297 (2009).
- 215 Lee, J. H., Hart, S. R. L. & Skalnik, D. G. Histone deacetylase activity is required for embryonic stem cell differentiation. *Genesis* **38**, 32-38, doi:10.1002/gene.10250 (2004).
- 216 Agger, K. *et al.* UTX and JMJD3 are histone H3K27 demethylases involved in HOX gene regulation and development. *Nature* **449**, 731-U710, doi:10.1038/nature06145 (2007).
- 217 Bilodeau, S., Kagey, M. H., Frampton, G. M., Rahl, P. B. & Young, R. A. SetDB1 contributes to repression of genes encoding developmental regulators and maintenance of ES cell state. *Gene Dev* **23**, 2484-2489, doi:10.1101/gad.1837309 (2009).

- 218 Boyer, L. A. *et al.* Polycomb complexes repress developmental regulators in murine embryonic stem cells. *Nature* **441**, 349-353, doi:10.1038/nature04733 (2006).
- 219 Jackson, M. *et al.* Severe global DNA hypomethylation blocks differentiation and induces histone hyperacetylation in embryonic stem cells. *Molecular and Cellular Biology* **24**, 8862-8871, doi:10.1128/Mcb.24.20.8862-8871.2004 (2004).
- 220 Ernst, P. *et al.* Definitive hematopoiesis requires the mixed-lineage leukemia gene. *Developmental Cell* **6**, 437-443, doi:10.1016/S1534-5807(04)00061-9 (2004).
- 221 Lubitz, S., Glaser, S., Schaft, J., Stewart, A. F. & Anastassiadis, K. Increased apoptosis and skewed differentiation in mouse embryonic stem cells lacking the histone methyltransferase Mll2. *Mol Biol Cell* **18**, 2356-2366, doi:10.1091/mbc.E06-11-1060 (2007).
- 222 Jiang, H. *et al.* Role for Dpy-30 in ES Cell-Fate Specification by Regulation of H3K4 Methylation within Bivalent Domains (vol 144, pg 513, 2011). *Cell* **144**, 825-825, doi:10.1016/j.cell.2011.02.036 (2011).
- 223 Adamo, A. *et al.* LSD1 regulates the balance between self-renewal and differentiation in human embryonic stem cells. *Nature Cell Biology* **13**, 652-U265, doi:10.1038/ncb2246 (2011).
- 224 Ang, S. Y. *et al.* KMT2D regulates specific programs in heart development via histone H3 lysine 4 di-methylation. *Development* **143**, 810-821, doi:10.1242/dev.132688 (2016).
- 225 Popova, E. Y. *et al.* Stage and Gene Specific Signatures Defined by Histones H3K4me2 and H3K27me3 Accompany Mammalian Retina Maturation In Vivo. *Plos One* **7**, doi:ARTN e46867
10.1371/journal.pone.0046867 (2012).
- 226 Pekowska, A., Benoukraf, T., Ferrier, P. & Spicuglia, S. A unique H3K4me2 profile marks tissue-specific gene regulation. *Genome Research* **20**, 1493-1502, doi:10.1101/gr.109389.110 (2010).
- 227 Bernstein, B. E. *et al.* Genomic maps and comparative analysis of histone modifications in human and mouse. *Cell* **120**, 169-181, doi:10.1016/j.cell.2005.01.001 (2005).
- 228 Lupien, M. *et al.* FoxA1 translates epigenetic signatures into enhancer-driven lineage-specific transcription. *Cell* **132**, 958-970, doi:10.1016/j.cell.2008.01.018 (2008).
- 229 Zhang, J., Parvin, J. & Huang, K. Redistribution of H3K4me2 on neural tissue specific genes during mouse brain development. *Bmc Genomics* **13**, doi:Artn S510.1186/1471-2164-13-S8-S5 (2012).
- 230 D'Urso, A. *et al.* Set1/COMPASS and Mediator are repurposed to promote epigenetic transcriptional memory. *Elife* **5**, doi:ARTN e1669110.7554/eLife.16691 (2016).

- 231 Wirka, R. C. *et al.* Atheroprotective roles of smooth muscle cell phenotypic modulation and the TCF21 disease gene as revealed by single-cell analysis. *Nat Med* **25**, 1280-1289, doi:10.1038/s41591-019-0512-5 (2019).
- 232 Pan, H. *et al.* Single-Cell Genomics Reveals a Novel Cell State During Smooth Muscle Cell Phenotypic Switching and Potential Therapeutic Targets for Atherosclerosis in Mouse and Human. *Circulation* **142**, 2060-2075, doi:10.1161/CIRCULATIONAHA.120.048378 (2020).
- 233 Chen, P. Y. *et al.* Smooth Muscle Cell Reprogramming in Aortic Aneurysms. *Cell Stem Cell* **26**, 542-557 e511, doi:10.1016/j.stem.2020.02.013 (2020).
- 234 Pedroza, A. J. *et al.* Single-Cell Transcriptomic Profiling of Vascular Smooth Muscle Cell Phenotype Modulation in Marfan Syndrome Aortic Aneurysm. *Arterioscler Thromb Vasc Biol* **40**, 2195-2211, doi:10.1161/ATVBAHA.120.314670 (2020).
- 235 Liu, M. & Gomez, D. Smooth Muscle Cell Phenotypic Diversity. *Arterioscler Thromb Vasc Biol*, ATVBAHA119312131, doi:10.1161/ATVBAHA.119.312131 (2019).
- 236 Sheikh, A. Q., Lighthouse, J. K. & Greif, D. M. Recapitulation of developing artery muscularization in pulmonary hypertension. *Cell Rep* **6**, 809-817, doi:10.1016/j.celrep.2014.01.042 (2014).
- 237 Alexander, M. R. & Owens, G. K. Epigenetic control of smooth muscle cell differentiation and phenotypic switching in vascular development and disease. *Annu Rev Physiol* **74**, 13-40, doi:10.1146/annurev-physiol-012110-142315 (2012).
- 238 Liu, R. *et al.* Ten-eleven translocation-2 (TET2) is a master regulator of smooth muscle cell plasticity. *Circulation* **128**, 2047-2057, doi:10.1161/CIRCULATIONAHA.113.002887 (2013).
- 239 Gomez, D., Swiatlowska, P. & Owens, G. K. Epigenetic Control of Smooth Muscle Cell Identity and Lineage Memory. *Arterioscler Thromb Vasc Biol* **35**, 2508-2516, doi:10.1161/ATVBAHA.115.305044 (2015).
- 240 Jenuwein, T. & Allis, C. D. Translating the histone code. *Science* **293**, 1074-1080, doi:10.1126/science.1063127 (2001).
- 241 Reik, W. Stability and flexibility of epigenetic gene regulation in mammalian development. *Nature* **447**, 425-432, doi:10.1038/nature05918 (2007).
- 242 Zhu, J. *et al.* Genome-wide chromatin state transitions associated with developmental and environmental cues. *Cell* **152**, 642-654, doi:10.1016/j.cell.2012.12.033 (2013).
- 243 Cheedipudi, S., Genolet, O. & Dobrova, G. Epigenetic inheritance of cell fates during embryonic development. *Front Genet* **5**, 19, doi:10.3389/fgene.2014.00019 (2014).

- 244 Zhang, J., Parvin, J. & Huang, K. Redistribution of H3K4me2 on neural tissue specific genes during mouse brain development. *BMC Genomics* **13 Suppl 8**, S5, doi:10.1186/1471-2164-13-S8-S5 (2012).
- 245 Popova, E. Y. *et al.* Stage and gene specific signatures defined by histones H3K4me2 and H3K27me3 accompany mammalian retina maturation in vivo. *PLoS One* **7**, e46867, doi:10.1371/journal.pone.0046867 (2012).
- 246 Pekowska, A., Benoukraf, T., Ferrier, P. & Spicuglia, S. A unique H3K4me2 profile marks tissue-specific gene regulation. *Genome Res* **20**, 1493-1502, doi:10.1101/gr.109389.110 (2010).
- 247 Ang, S. Y. *et al.* KMT2D regulates specific programs in heart development via histone H3 lysine 4 di-methylation. *Development* **143**, 810-821, doi:10.1242/dev.132688 (2016).
- 248 Pipes, G. C., Creemers, E. E. & Olson, E. N. The myocardin family of transcriptional coactivators: versatile regulators of cell growth, migration, and myogenesis. *Genes Dev* **20**, 1545-1556, doi:10.1101/gad.1428006 (2006).
- 249 Lee, M. G., Wynder, C., Cooch, N. & Shiekhatar, R. An essential role for CoREST in nucleosomal histone 3 lysine 4 demethylation. *Nature* **437**, 432-435, doi:10.1038/nature04021 (2005).
- 250 Yao, F. *et al.* Histone Variant H2A.Z Is Required for the Maintenance of Smooth Muscle Cell Identity as Revealed by Single-Cell Transcriptomics. *Circulation* **138**, 2274-2288, doi:10.1161/circulationaha.117.033114 (2018).
- 251 Williams, K., Christensen, J. & Helin, K. DNA methylation: TET proteins-guardians of CpG islands? *EMBO Rep* **13**, 28-35, doi:10.1038/embor.2011.233 (2011).
- 252 Consortium, E. P. An integrated encyclopedia of DNA elements in the human genome. *Nature* **489**, 57-74, doi:10.1038/nature11247 (2012).
- 253 Spin, J. M. *et al.* Transcriptional profiling of in vitro smooth muscle cell differentiation identifies specific patterns of gene and pathway activation. *Physiol Genomics* **19**, 292-302, doi:10.1152/physiolgenomics.00148.2004 (2004).
- 254 Blank, R. S., Swartz, E. A., Thompson, M. M., Olson, E. N. & Owens, G. K. A retinoic acid-induced clonal cell line derived from multipotential P19 embryonal carcinoma cells expresses smooth muscle characteristics. *Circ Res* **76**, 742-749, doi:10.1161/01.res.76.5.742 (1995).
- 255 Shen, M., Quertermous, T., Fischbein, M. P. & Wu, J. C. Generation of Vascular Smooth Muscle Cells From Induced Pluripotent Stem Cells: Methods, Applications, and Considerations. *Circ Res* **128**, 670-686, doi:10.1161/CIRCRESAHA.120.318049 (2021).
- 256 Manabe, I. & Owens, G. K. Recruitment of serum response factor and hyperacetylation of histones at smooth muscle-specific regulatory regions during differentiation of a novel

- P19-derived in vitro smooth muscle differentiation system. *Circ Res* **88**, 1127-1134, doi:10.1161/hh1101.091339 (2001).
- 257 Xin, M. *et al.* MicroRNAs miR-143 and miR-145 modulate cytoskeletal dynamics and responsiveness of smooth muscle cells to injury. *Genes Dev* **23**, 2166-2178, doi:10.1101/gad.1842409 (2009).
- 258 Pidkovka, N. A. *et al.* Oxidized phospholipids induce phenotypic switching of vascular smooth muscle cells in vivo and in vitro. *Circ Res* **101**, 792-801, doi:10.1161/CIRCRESAHA.107.152736 (2007).
- 259 Sims, R. J., 3rd, Nishioka, K. & Reinberg, D. Histone lysine methylation: a signature for chromatin function. *Trends Genet* **19**, 629-639, doi:10.1016/j.tig.2003.09.007 (2003).
- 260 Buratowski, S. & Kim, T. The role of cotranscriptional histone methylations. *Cold Spring Harb Symp Quant Biol* **75**, 95-102, doi:10.1101/sqb.2010.75.036 (2010).
- 261 Schneider, R. *et al.* Histone H3 lysine 4 methylation patterns in higher eukaryotic genes. *Nat Cell Biol* **6**, 73-77, doi:10.1038/ncb1076 (2004).
- 262 Orford, K. *et al.* Differential H3K4 methylation identifies developmentally poised hematopoietic genes. *Dev Cell* **14**, 798-809, doi:10.1016/j.devcel.2008.04.002 (2008).
- 263 Cakouros, D. *et al.* Specific functions of TET1 and TET2 in regulating mesenchymal cell lineage determination. *Epigenetics Chromatin* **12**, 3, doi:10.1186/s13072-018-0247-4 (2019).
- 264 Montagner, S. *et al.* TET2 Regulates Mast Cell Differentiation and Proliferation through Catalytic and Non-catalytic Activities. *Cell Rep* **15**, 1566-1579, doi:10.1016/j.celrep.2016.04.044 (2016).
- 265 Wang, Y., Li, X. & Hu, H. H3K4me2 reliably defines transcription factor binding regions in different cells. *Genomics* **103**, 222-228, doi:10.1016/j.ygeno.2014.02.002 (2014).
- 266 Chen, L. L. *et al.* SNIP1 Recruits TET2 to Regulate c-MYC Target Genes and Cellular DNA Damage Response. *Cell Rep* **25**, 1485-1500 e1484, doi:10.1016/j.celrep.2018.10.028 (2018).
- 267 Sardina, J. L. *et al.* Transcription Factors Drive Tet2-Mediated Enhancer Demethylation to Reprogram Cell Fate. *Cell Stem Cell* **23**, 727-741 e729, doi:10.1016/j.stem.2018.08.016 (2018).
- 268 Yamagata, K. & Kobayashi, A. The cysteine-rich domain of TET2 binds preferentially to mono- and dimethylated histone H3K36. *J Biochem* **161**, 327-330, doi:10.1093/jb/mvx004 (2017).

- 269 Zhong, W. *et al.* Hypermethylation of the Micro-RNA 145 Promoter Is the Key Regulator for NLRP3 Inflammasome-Induced Activation and Plaque Formation. *JACC Basic Transl Sci* **3**, 604-624, doi:10.1016/j.jacbts.2018.06.004 (2018).
- 270 Cordes, K. R. *et al.* miR-145 and miR-143 regulate smooth muscle cell fate and plasticity. *Nature* **460**, 705-710, doi:10.1038/nature08195 (2009).
- 271 D'Urso, A. & Brickner, J. H. Mechanisms of epigenetic memory. *Trends Genet* **30**, 230-236, doi:10.1016/j.tig.2014.04.004 (2014).
- 272 Brickner, D. G. *et al.* H2A.Z-mediated localization of genes at the nuclear periphery confers epigenetic memory of previous transcriptional state. *Plos Biol* **5**, e81, doi:10.1371/journal.pbio.0050081 (2007).
- 273 Kim, M. & Costello, J. DNA methylation: an epigenetic mark of cellular memory. *Exp Mol Med* **49**, e322, doi:10.1038/emm.2017.10 (2017).
- 274 de Almeida, D. C. *et al.* Epigenetic Classification of Human Mesenchymal Stromal Cells. *Stem Cell Reports* **6**, 168-175, doi:10.1016/j.stemcr.2016.01.003 (2016).
- 275 Hyun, K., Jeon, J., Park, K. & Kim, J. Writing, erasing and reading histone lysine methylations. *Exp Mol Med* **49**, e324, doi:10.1038/emm.2017.11 (2017).
- 276 Kim, K. *et al.* Epigenetic memory in induced pluripotent stem cells. *Nature* **467**, 285-290, doi:10.1038/nature09342 (2010).
- 277 Ostriker, A. C. *et al.* TET2 Protects Against VSMC Apoptosis and Intimal Thickening in Transplant Vasculopathy. *Circulation*, doi:10.1161/CIRCULATIONAHA.120.050553 (2021).
- 278 Vengrenyuk, Y. *et al.* Cholesterol loading reprograms the microRNA-143/145-myocardin axis to convert aortic smooth muscle cells to a dysfunctional macrophage-like phenotype. *Arterioscler Thromb Vasc Biol* **35**, 535-546, doi:10.1161/ATVBAHA.114.304029 (2015).
- 279 Miao, F. *et al.* Genome-wide analysis of histone lysine methylation variations caused by diabetic conditions in human monocytes. *J Biol Chem* **282**, 13854-13863, doi:10.1074/jbc.M609446200 (2007).
- 280 Jufvas, A. *et al.* Global differences in specific histone H3 methylation are associated with overweight and type 2 diabetes. *Clin Epigenetics* **5**, 15, doi:10.1186/1868-7083-5-15 (2013).
- 281 Zhang, W., Song, M., Qu, J. & Liu, G. H. Epigenetic Modifications in Cardiovascular Aging and Diseases. *Circ Res* **123**, 773-786, doi:10.1161/CIRCRESAHA.118.312497 (2018).

- 282 Cheung, P. *et al.* Single-Cell Chromatin Modification Profiling Reveals Increased Epigenetic Variations with Aging. *Cell* **173**, 1385-1397 e1314, doi:10.1016/j.cell.2018.03.079 (2018).
- 283 Miano, J. M. Myocardin in biology and disease. *J Biomed Res* **29**, 3-19, doi:10.7555/JBR.29.20140151 (2015).
- 284 Guo, D. C. *et al.* Mutations in smooth muscle alpha-actin (ACTA2) lead to thoracic aortic aneurysms and dissections. *Nat Genet* **39**, 1488-1493, doi:10.1038/ng.2007.6 (2007).
- 285 Zhu, L. *et al.* Mutations in myosin heavy chain 11 cause a syndrome associating thoracic aortic aneurysm/aortic dissection and patent ductus arteriosus. *Nat Genet* **38**, 343-349, doi:10.1038/ng1721 (2006).
- 286 Wirth, A. *et al.* G(12)-G(13)-LARG-mediated signaling in vascular smooth muscle is required for salt-induced hypertension (vol 14, pg 64, 2008). *Nat Med* **14**, 222-222, doi:DOI 10.1038/nm0208-222 (2008).
- 287 Srinivas, S. *et al.* Cre reporter strains produced by targeted insertion of EYFP and ECFP into the ROSA26 locus. *BMC Dev Biol* **1**, 4, doi:10.1186/1471-213x-1-4 (2001).
- 288 Dahl, J. A. & Collas, P. A rapid micro chromatin immunoprecipitation assay (microChIP). *Nat Protoc* **3**, 1032-1045, doi:10.1038/nprot.2008.68 (2008).
- 289 Kaya-Okur, H. S., Janssens, D. H., Henikoff, J. G., Ahmad, K. & Henikoff, S. Efficient low-cost chromatin profiling with CUT&Tag. *Nature Protocols* **15**, 3264-3283, doi:10.1038/s41596-020-0373-x (2020).
- 290 Langmead, B. & Salzberg, S. L. Fast gapped-read alignment with Bowtie 2. *Nature Methods* **9**, 357-U354, doi:10.1038/Nmeth.1923 (2012).
- 291 Ramirez, F. *et al.* deepTools2: a next generation web server for deep-sequencing data analysis. *Nucleic Acids Research* **44**, W160-W165, doi:10.1093/nar/gkw257 (2016).
- 292 Robinson, J. T. *et al.* Integrative genomics viewer. *Nature Biotechnology* **29**, 24-26, doi:10.1038/nbt.1754 (2011).
- 293 Feng, J. X., Liu, T., Qin, B., Zhang, Y. & Liu, X. S. Identifying ChIP-seq enrichment using MACS. *Nature Protocols* **7**, 1728-1740, doi:10.1038/nprot.2012.101 (2012).
- 294 Yu, G. C., Wang, L. G. & He, Q. Y. ChIPseeker: an R/Bioconductor package for ChIP peak annotation, comparison and visualization. *Bioinformatics* **31**, 2382-2383, doi:10.1093/bioinformatics/btv145 (2015).
- 295 Ross-Innes, C. S. *et al.* Differential oestrogen receptor binding is associated with clinical outcome in breast cancer. *Nature* **481**, 389-U177, doi:10.1038/nature10730 (2012).

- 296 Yu, G. C., Wang, L. G., Han, Y. Y. & He, Q. Y. clusterProfiler: an R Package for Comparing Biological Themes Among Gene Clusters. *Omic* **16**, 284-287, doi:10.1089/omi.2011.0118 (2012).
- 297 Wang, L., Yao, F. & Yu, P. Histone Variant H2A.Z Defines Cell Identity in Smooth Muscle Cells as Revealed by Single-Cell Transcriptomics. *Circulation Research* **123**, doi:10.1161/res.123.suppl_1.236 (2018).
- 298 Jalili, V. *et al.* The Galaxy platform for accessible, reproducible and collaborative biomedical analyses: 2020 update. *Nucleic Acids Res* **48**, W395-W402, doi:10.1093/nar/gkaa434 (2020).
- 299 Davis, C. A. *et al.* The Encyclopedia of DNA elements (ENCODE): data portal update. *Nucleic Acids Research* **46**, D794-D801, doi:10.1093/nar/gkx1081 (2018).
- 300 Kupersmidt, I. *et al.* Ontology-based meta-analysis of global collections of high-throughput public data. *PLoS One* **5**, doi:10.1371/journal.pone.0013066 (2010).
- 301 Ashburner, M. *et al.* Gene ontology: tool for the unification of biology. The Gene Ontology Consortium. *Nat Genet* **25**, 25-29, doi:10.1038/75556 (2000).
- 302 The Gene Ontology, C. The Gene Ontology Resource: 20 years and still GOing strong. *Nucleic Acids Res* **47**, D330-D338, doi:10.1093/nar/gky1055 (2019).
- 303 Agarwal, V., Bell, G. W., Nam, J. W. & Bartel, D. P. Predicting effective microRNA target sites in mammalian mRNAs. *Elife* **4**, doi:10.7554/eLife.05005 (2015).
- 304 Espinosa-Diez, C. *et al.* Targeting of Gamma-Glutamyl-Cysteine Ligase by miR-433 Reduces Glutathione Biosynthesis and Promotes TGF-beta-Dependent Fibrogenesis. *Antioxid Redox Signal* **23**, 1092-1105, doi:10.1089/ars.2014.6025 (2015).
- 305 Espinosa-Diez, C. *et al.* MicroRNA regulation of the MRN complex impacts DNA damage, cellular senescence, and angiogenic signaling. *Cell Death Dis* **9**, 632, doi:10.1038/s41419-018-0690-y (2018).
- 306 Rong, J. X., Shapiro, M., Trogan, E. & Fisher, E. A. Transdifferentiation of mouse aortic smooth muscle cells to a macrophage-like state after cholesterol loading. *Proc Natl Acad Sci U S A* **100**, 13531-13536, doi:10.1073/pnas.1735526100 (2003).
- 307 Hendrix, J. A. *et al.* 5' CArG degeneracy in smooth muscle alpha-actin is required for injury-induced gene suppression in vivo. *J Clin Invest* **115**, 418-427, doi:10.1172/JCI22648 (2005).
- 308 Criqui, M. H. *et al.* Lower Extremity Peripheral Artery Disease: Contemporary Epidemiology, Management Gaps, and Future Directions: A Scientific Statement From the American Heart Association. *Circulation* **144**, e171-e191, doi:10.1161/CIR.0000000000001005 (2021).

- 309 Kullo, I. J. & Rooke, T. W. CLINICAL PRACTICE. Peripheral Artery Disease. *N Engl J Med* **374**, 861-871, doi:10.1056/NEJMcpl507631 (2016).
- 310 Djerf, H. *et al.* Absence of Long-Term Benefit of Revascularization in Patients With Intermittent Claudication Five-Year Results From the IRONIC Randomized Controlled Trial. *Circ-Cardiovasc Inte* **13**, doi:ARTN e008450 10.1161/CIRCINTERVENTIONS.119.008450 (2020).
- 311 Iyer, S. R. & Annex, B. H. Therapeutic Angiogenesis for Peripheral Artery Disease: Lessons Learned in Translational Science. *JACC Basic Transl Sci* **2**, 503-512, doi:10.1016/j.jacbts.2017.07.012 (2017).
- 312 Cooke, J. P. & Meng, S. Vascular Regeneration in Peripheral Artery Disease. *Arterioscl Throm Vas* **40**, 1627-1634, doi:10.1161/Atvbaha.120.312862 (2020).
- 313 Annex, B. H. & Cooke, J. P. New Directions in Therapeutic Angiogenesis and Arteriogenesis in Peripheral Arterial Disease. *Circ Res* **128**, 1944-1957, doi:10.1161/CIRCRESAHA.121.318266 (2021).
- 314 Sheikh, A. Q., Misra, A., Rosas, I. O., Adams, R. H. & Greif, D. M. Smooth muscle cell progenitors are primed to muscularize in pulmonary hypertension. *Science Translational Medicine* **7**, doi:ARTN 308ra15910.1126/scitranslmed.aaa9712 (2015).
- 315 Wolf, C. *et al.* Vascular remodeling and altered protein expression during growth of coronary collateral arteries. *J Mol Cell Cardiol* **30**, 2291-2305, doi:DOI 10.1006/jmcc.1998.0790 (1998).
- 316 Scholz, D. *et al.* Ultrastructure and molecular histology of rabbit hind-limb collateral artery growth (arteriogenesis). *Virchows Arch* **436**, 257-270, doi:DOI 10.1007/s004280050039 (2000).
- 317 Hess, D. L. *et al.* Perivascular cell-specific knockout of the stem cell pluripotency gene Oct4 inhibits angiogenesis. *Nature Communications* **10**, doi:ARTN 967, 10.1038/s41467-019-08811-z (2019).
- 318 Alexander, M. R. & Owens, G. K. Epigenetic Control of Smooth Muscle Cell Differentiation and Phenotypic Switching in Vascular Development and Disease. *Annual Review of Physiology, Vol 74* **74**, 13-40, doi:10.1146/annurev-physiol-012110-142315 (2012).
- 319 Bastiaansen, A. J. N. M. *et al.* Lysine Acetyltransferase PCAF Is a Key Regulator of Arteriogenesis. *Arterioscl Throm Vas* **33**, 1902-1910, doi:10.1161/Atvbaha.113.301579 (2013).
- 320 Kaluza, D. *et al.* Histone Deacetylase 9 Promotes Angiogenesis by Targeting the Antiangiogenic MicroRNA-17-92 Cluster in Endothelial Cells. *Arterioscl Throm Vas* **33**, 533+, doi:10.1161/Atvbaha.112.300415 (2013).

- 321 Liu, M. J. *et al.* H3K4 di-methylation governs smooth muscle lineage identity and promotes vascular homeostasis by restraining plasticity. *Developmental Cell* **56**, 2765-+, doi:10.1016/j.devcel.2021.09.001 (2021).
- 322 Baeten, J. T. & Lilly, B. Notch Signaling in Vascular Smooth Muscle Cells. *Adv Pharmacol* **78**, 351-382, doi:10.1016/bs.apha.2016.07.002 (2017).
- 323 Meng, S. *et al.* Reservoir of Fibroblasts Promotes Recovery From Limb Ischemia. *Circulation* **142**, 1647-1662, doi:10.1161/Circulationaha.120.046872 (2020).
- 324 Liu, H., Zhang, W. B., Kennard, S., Caldwell, R. B. & Lilly, B. Notch3 Is Critical for Proper Angiogenesis and Mural Cell Investment. *Circulation Research* **107**, 860-+, doi:10.1161/Circresaha.110.218271 (2010).
- 325 Scheppke, L. *et al.* Notch promotes vascular maturation by inducing integrin-mediated smooth muscle cell adhesion to the endothelial basement membrane. *Blood* **119**, 2149-2158, doi:10.1182/blood-2011-04-348706 (2012).
- 326 Benedito, R. *et al.* The Notch Ligands Dll4 and Jagged1 Have Opposing Effects on Angiogenesis. *Cell* **137**, 1124-1135, doi:10.1016/j.cell.2009.03.025 (2009).
- 327 Cristofaro, B. *et al.* Dll4-Notch signaling determines the formation of native arterial collateral networks and arterial function in mouse ischemia models. *Development* **140**, 1720-1729, doi:10.1242/dev.092304 (2013).
- 328 Sakata, Y. *et al.* Transcription factor CHF1/Hey2 regulates neointimal formation in vivo and vascular smooth muscle proliferation and migration in vitro. *Arterioscl Throm Vas* **24**, 2069-2074, doi:10.1161/01.ATV.0000143936.77094.a4 (2004).
- 329 Brodsky, N. F. *et al.* The transcription factor Hey and nuclear lamins specify and maintain cell identity. *Elife* **8**, doi:ARTN e4474510.7554/eLife.44745 (2019).
- 330 Limbourg, A. *et al.* Evaluation of postnatal arteriogenesis and angiogenesis in a mouse model of hind-limb ischemia. *Nat Protoc* **4**, 1737-1746, doi:10.1038/nprot.2009.185 (2009).
- 331 Kaur, G., Ahn, J., Hankenson, K. D. & Ashley, J. W. Stimulation of Notch Signaling in Mouse Osteoclast Precursors. *Jove-J Vis Exp*, doi:ARTN e5523410.3791/55234 (2017).
- 332 Robinson, J. T. *et al.* Integrative genomics viewer. *Nat Biotechnol* **29**, 24-26, doi:10.1038/nbt.1754 (2011).
- 333 Kearns, N. A. *et al.* Functional annotation of native enhancers with a Cas9-histone demethylase fusion. *Nat Methods* **12**, 401-403, doi:10.1038/nmeth.3325 (2015).
- 334 Li, Y. M. *et al.* Single-Cell Transcriptome Analysis Reveals Dynamic Cell Populations and Differential Gene Expression Patterns in Control and Aneurysmal Human Aortic Tissue. *Circulation* **142**, 1374-1388, doi:10.1161/Circulationaha.120.046528 (2020).

- 335 Majesky, M. W. Developmental basis of vascular smooth muscle diversity. *Arterioscl Throm Vas* **27**, 1248-1258, doi:10.1161/Atvbaha.107.141069 (2007).
- 336 Sawada, H. *et al.* Second Heart Field-Derived Cells Contribute to Angiotensin II-Mediated Ascending Aortopathies. *Circulation* **145**, 987-1001, doi:10.1161/CIRCULATIONAHA.121.058173 (2022).
- 337 MacFarlane, E. G. *et al.* Lineage-specific events underlie aortic root aneurysm pathogenesis in Loeys-Dietz syndrome. *J Clin Invest* **129**, 659-675, doi:10.1172/JCI123547 (2019).
- 338 Turner, A. W. *et al.* Single-nucleus chromatin accessibility profiling highlights regulatory mechanisms of coronary artery disease risk. *Nat Genet*, doi:10.1038/s41588-022-01069-0 (2022).
- 339 Ord, T. *et al.* Single-Cell Epigenomics and Functional Fine-Mapping of Atherosclerosis GWAS Loci. *Circulation Research* **129**, 240-258, doi:10.1161/Circresaha.121.318971 (2021).
- 340 Wu, S. J. *et al.* Single-cell CUT&Tag analysis of chromatin modifications in differentiation and tumor progression. *Nature Biotechnology* **39**, 819-824, doi:10.1038/s41587-021-00865-z (2021).
- 341 Janssens, D. H. *et al.* CUT&Tag2for1: a modified method for simultaneous profiling of the accessible and silenced regulome in single cells. *Genome Biology* **23**, doi:ARTN 8110.1186/s13059-022-02642-w (2022).
- 342 Shen, M. C., Quertermous, T., Fischbein, M. P. & Wu, J. C. Generation of Vascular Smooth Muscle Cells From Induced Pluripotent Stem Cells Methods, Applications, and Considerations. *Circulation Research* **128**, 670-686, doi:10.1161/Circresaha.120.318049 (2021).
- 343 Wei, X., Yi, X., Zhu, X. H. & Jiang, D. S. Histone methylation and vascular biology. *Clin Epigenetics* **12**, 30, doi:10.1186/s13148-020-00826-4 (2020).
- 344 Garcia-Guimaraes, M. *et al.* Calcified neoatherosclerosis causing in-stent restenosis: prevalence, predictors, and implications. *Coron Artery Dis* **30**, 1-8, doi:10.1097/MCA.0000000000000669 (2019).
- 345 Cherepanova, O. A. *et al.* Activation of the pluripotency factor OCT4 in smooth muscle cells is atheroprotective. *Nature Medicine* **22**, 657-+, doi:10.1038/nm.4109 (2016).